

**OPTIMUM PROPORTION OF SUPPLEMENTARY  
CEMENTITIOUS MATERIALS TO PRODUCE BLENDED CEMENT  
UNDER TANNERY WASTEWATER**

by  
**SAMIRA MAHMUD**

A thesis submitted to the Department of Civil Engineering,  
Bangladesh University of Engineering and Technology, Dhaka  
in partial fulfillment of the requirement for the degree of  
Master of Science in Civil Engineering (Structural)



**DEPARTMENT OF CIVIL ENGINEERING  
BANGLADESH UNIVERSITY OF ENGINEERING AND TECHNOLOGY  
DHAKA, BANGLADESH**

**September, 2018**

### **Declaration**

It is hereby declared that the studies embodied in this thesis are the results of experiments carried out by the author under the supervision of Dr. Tanvir Manzur, Professor, Department of Civil Engineering, BUET except where specified by reference to other works. Neither the thesis nor any part of it has been submitted elsewhere for any other purpose.

Samira Mahmud

(Samira Mahmud)

Student ID: 0416042310

Date: 17.09.2018

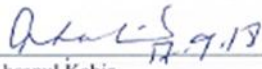
The thesis titled "Optimum Proportion of Supplementary Cementitious Materials to Produce Blended Cement Under Tannery Wastewater", submitted by Samira Mahmud, Roll No: 0416042310, Session: April, 2016 has been accepted as satisfactory in partial fulfillment of the requirement for the degree of Master of Science in Civil Engineering (Structural) on 17th September, 2018.

**BOARD OF EXAMINERS**



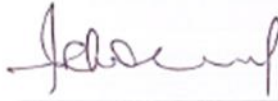
Dr. Tanvir Manzur  
Professor,  
Dept. of Civil Engineering, BUET, Dhaka.

Chairman  
(Supervisor)



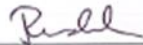
Dr. Ahsanul Kabir  
Professor and Head of the Dept.  
Dept. of Civil Engineering, BUET, Dhaka.

Member  
(Ex-Officio)



Dr. Ishtiaque Ahmed  
Professor,  
Dept. of Civil Engineering, BUET, Dhaka.

Member



Major Dr. Mohammed Russedul Islam  
Assistant Professor,  
Dept. of Civil Engineering,  
Military Institute of Science and Technology (MIST)  
Mirpur, Dhaka.

Member  
(External)

**Dedicated to**  
**My Parents**

## **Acknowledgement**

The author would like to begin by expressing her deepest gratitude to the Almighty ALLAH for allowing the successful completion of the tasks undertaken and accomplishment of the objectives of this study.

The author would like to express her heartfelt appreciation to her thesis supervisor, Dr. Tanvir Manzur, Professor, Department of Civil Engineering, Bangladesh University of Engineering and Technology (BUET), Dhaka. It was a privilege to work under his mentorship. This thesis would not have been a success without his guidance and valuable insights.

The author is grateful to the lab instructors and assistants of Concrete Laboratory for their help and cooperation which made the successful execution of the experiments possible. SEM and XRF were carried out at Department of Glass and Ceramic Engineering (GCE), BUET for which the author is grateful to the corresponding lab personnel. The author would also like to acknowledge Samina Samrose and Saifa Anzum for their help in the experimental programs.

The author would like to take the opportunity of expressing sincere appreciation to Dr. Muhammad Hasanuzzaman, Assistant Professor, Department of Glass and Ceramic Engineering (GCE), BUET, for his support and cooperation with Scanning Electron Microscope (SEM) images.

In the end, the author is ever grateful to her family and friends for their constant support and encouragement throughout this journey to complete the work.

## Abstract

Portland cement concrete is a major construction material worldwide. In Bangladesh, mainly two types of composite cement termed as CEM IIA and CEM IIB are commercially produced. However, different adverse conditions may require different portions of blended components and hence, utilization of single type of blended cement in all instances often fails to provide required durability. In recent years, a rapid growth in leather industry is resulting in construction of a large number of tannery factory buildings and related treatment plants. The tannery wastewater contains several detrimental constituents that severely affect concrete strength and durability. It is therefore, of immense importance that a blended cement be developed that perform satisfactorily under aggressive condition like tannery waste water. This research is aimed at studying the behavior of cement mortars prepared with various types of cement mix combination of fly ash and slag when in contact with aggressive aqueous environment of tannery wastewater. Tannery wastewater samples were simulated in the laboratory following recipe developed from raw wastewater. Several variations of cement mix combinations with fly ash and slag were taken which enabled to study the performance and durability of particular mix in tannery wastewater. Cement mortar specimens were casted and immersed in the laboratory simulated tannery wastewater. The study involved evaluation of compressive strength, expansion, weight loss and monitoring surface deterioration through images. Properties of blended cement mixes were studied through their consistency, setting time and flowability tests. In addition, Scanning Electron Microscope (SEM) images and Energy-dispersive X-ray Spectroscopy (EDS) techniques were used to study the change in microstructure of the cement mortars due to being exposed to the harsh aqueous conditions. The compressive strength results over a period of 180 days revealed that blended cement mixes achieved higher strength, resulted in lower expansion and weight loss than those of Ordinary Portland cement. The loss of compressive strength after 180 days submergence period in simulated tannery wastewater, in only slag mixed cement mortars was about 55% which was significantly less than that of OPC cement mortars 63%. The expansion test results revealed that OPC mortars underwent greater expansion of 0.6% compared to only fly ash blended cement mortars (almost no expansion) over a period of 26 weeks. It was inferred from EDS data that there was greater loss of calcium bearing phases in OPC mortars compared to blended cement mortars, which was coherent with the strength and weight loss results. Considering expansion limit for cement mortar, only fly ash blended cement has been found to exhibit desired performance. Hence, the optimum replacement level for fly ash in cement is recommended to be 30% for producing composite cement to be used in tannery wastewater.

# Table of Contents

Acknowledgement	v
Abstract	vi
Table of Contents	vii
List of Tables	xiii
List of Figures	xiii
List of Abbreviation and Symbols	xviii
<b>Chapter 1: INTRODUCTION</b>	<b>1</b>
1.1 General	1
1.2 Background	1
1.3 Objectives	3
1.4 Scope	3
1.5 Outline of the Thesis	4
<b>Chapter 2: LITERATURE REVIEW</b>	<b>5</b>
2.1 Introduction	5
2.2 Leather Industry in Bangladesh	5
2.3 Tannery Wastewater	6
2.4 Tanning Process	6
2.5 Attack of Major Deteriorating Tannery Wastewater Constituents on Concrete	8
2.5.1 Sulfate Attack on Concrete	8
2.5.1.1 Concrete Behavior in Presence of Sulfate	8
2.5.1.2 Chemistry of Sulfate Attack	9
2.5.1.3 Ettringite Formation and Development	9
2.5.1.4 Morphology of Ettringite Crystals	10

2.5.1.5 Wet-Dry Cycles from Sulfate Exposure	11
2.5.1.6 Crystallization Theories	11
2.5.1.7 Alkali Sulfate Attack on Concrete	12
2.5.1.8 Damages to Concrete due to Sulfate Attack	14
2.5.1.9 Resistance to Sulfate Attack	15
2.5.2 Ammonium Attack on Concrete	16
2.5.2.1 Chemistry of Ammonium Attack on Concrete	16
2.5.2.2 Damage Observed on Structures	18
2.5.2.3 Dissolution of Calcium Hydroxide in Ammonium Nitrate Solution	19
2.5.2.4 Wet-Dry Cycle from Ammonium Exposure	20
2.5.2.5 Crystallization	20
2.5.3 Chloride Attack on Concrete	21
2.5.3.1 Mechanisms of Chloride Ingress into Concrete	21
2.5.3.2 Sodium Chloride Attack on Concrete	22
2.5.4 Sulfide Attack on Concrete	24
2.5.4.1 Chemistry of Sulfide Attack on Concrete	24
2.5.4.2 Formation of H <sub>2</sub> S in Concrete Pipes	25
2.5.4.3 Corrosion of Concrete Pipes due to H <sub>2</sub> S	26
2.6. Sustainable Development and the Cement Industry	27
2.7 CO <sub>2</sub> Emissions from Cement Production	27
2.7.1 Overview of Cement Production	28
2.7.2 Process Description	28
2.8 Fly Ash and Slag as Supplementary Cementitious Materials (SCMs)	29
2.8.1 Fly Ash	30
2.8.1.1 Benefits of Fly Ash to Fresh Concrete	31



2.8.2 Slag	32
2.8.2.1 Binary Cement in Concrete Manufacturing Using GGBS	33
2.9 Setting Time of Fly Ash and Slag Cement	34
2.10 Role of Supplementary Cementitious Materials (SCMs) in Production of Environmentally Sustainable Concrete	35
2.11 Effect of SCMs on Microstructure and Porosity	36
2.12 Resistance to Sulfate Attack by Slag and Fly Ash	37
2.13 Reducing Chloride Corrosion of Reinforcement	37
2.14 Concluding Remarks	38
<b>Chapter 3: MATERIALS AND METHODS</b>	<b>39</b>
3.1 Introduction	39
3.2 Simulation of Tannery Wastewater in Laboratory	39
3.2.1 Synthetic Simulation of Tannery Waste Water	39
3.2.2 Preparation of Stock Solution	39
3.2.3 Preparation of Synthetic Solution using MINEQL+ Software	40
3.3 Cement Mix Combinations	41
3.4 Flow Table Test	42
3.4.1 Preparation of Mortar Bars for Flow Table Test	43
3.4.2 Materials	43
3.4.3 Apparatus	43
3.4.4 Temperature, Humidity	43
3.4.5 Experimental Procedure	44
3.4.6 Measurements of Flow Diameter	44
3.4.7 Calculation	45
3.5 Normal Consistency Test	45
3.5.1 Preparation of Cement Paste for Normal Consistency Test	45

3.5.2	Materials	45
3.5.3	Apparatus	46
3.5.4	Temperature, Humidity	47
3.5.5	Experimental Procedure	47
3.5.6	Determination of Consistency	48
3.5.7	Calculation	48
3.6	Setting Time Test	48
3.6.1	Preparation of Cement Paste for Setting Time Test	49
3.6.2	Materials	49
3.6.3	Apparatus	49
3.6.4	Temperature, Humidity	50
3.6.5	Molding Test Specimen	51
3.6.6	Time of Initial Setting Determination	51
3.6.7	Time of Final Setting Determination	52
3.6.8	Calculation	52
3.7	Compressive Strength Test	52
3.7.1	Apparatus	52
3.7.2	Materials	53
3.7.3	Preparation of Cement Mortar Cubes	53
3.7.4	Hand Tamping	54
3.7.5	Storage of Test Specimens	55
3.7.6	Temperature and Humidity	56
3.7.7	Experimental Procedure	56
3.7.8	Calculation of Compressive Strength	57
3.8	Image Capturing Setup	58
3.9	Scanning Electron Microscope (SEM)	59

3.10 X-ray Fluorescence (XRF)	60
3.11 Energy-dispersive X-ray Spectroscopy (EDS/EDX)	61
3.12 Expansion Test	61
3.12.1 Preparation of Mortar Bars for Expansion Test	62
3.12.1.1 Materials	62
3.12.1.2 Apparatus	62
3.12.1.3 Molding the Test Bars	62
3.12.1.4 Preparation of Molds	63
3.12.1.5 Temperature, Humidity	63
3.12.1.6 Experimental Procedure	63
3.12.1.7 Storage of Test Bars during Exposure to Test Solution	63
3.12.1.8 Measurements of Length Change	63
3.12.1.9 Calculation	64
3.13 Concluding Remarks	65
<b>Chapter 4: RESULTS AND DISCUSSION</b>	<b>66</b>
4.1 Introduction	66
4.2 Cube Designations Representing Different Cement Mix Combinations	66
4.3 X-ray Fluorescence (XRF) Analysis	67
4.4 Properties of Cement and Mortar	68
4.4.1 Normal Consistency of Cement Pastes	68
4.4.2 Setting Time of Cement	69
4.4.3 Flow of mortar	69
4.5 Compressive Strength Results	70
4.5.1 Variation of Mortar Cube Strength with Time for Each Particular Type of Cement Mix	71
4.5.2 Variation of Mortar Cube Strength with Type of Cement Mix for Each	

Particular Testing Period	75
4.5.3 Comparison of Mortar Cubes Strength Having Different Supplementary Materials	77
4.5.4 Variation of Mortar Cube Strength Change (%) with Type of Cement Mix for Each Testing Period	81
4.6 Expansion of Mortar Bars	82
4.6.1 Expansion with Time for Each Particular Cement Mix Type	82
4.7 Weight Loss of Cubes	88
4.7.1 Variation of Weight Loss % with Cement Mix Types for Different Testing Time	88
4.7.2 Variation of Weight Loss % with Time for Different Cement Mix Types	90
4.7.3 Weight Loss Comparison of Mortar Cubes of Different Supplementary Materials	94
4.8 Comparison of Images of Cube Surfaces	96
4.9 SEM Images	99
4.10 Energy-Dispersive X-ray Spectroscopy (EDS) Analysis of Cube Samples	104
4.11 Concluding Remarks	111
<b>Chapter 5: CONCLUSIONS AND SUGGESTIONS</b>	<b>112</b>
5.1 Conclusions	112
5.2 Suggestions for Future Study	114
<b>References</b>	<b>116</b>

## **List of Tables**

Table 2.1: Exposure Categories and Classes	14
Table 2.2: Requirements for establishing suitability of combinations of cementitious materials exposed to water-soluble sulfate	15
Table 3.1: Concentration of the prepared stock solutions	40
Table 3.2 Volume (ml) of different stock solutions to be added for preparation of synthetic tannery wastewater	41
Table 3.3: Cement mix proportions and combinations	42
Table 3.4: Test matrix for cubes and bars	56
Table 4.1: Cement mix proportions and combinations	66
Table 4.2: Mass % of different elements in OPC, Fly Ash and Slag	67

## **List of Figures**

Figure 2.1: Wastes generated from each unit operation of a tannery	7
Figure 2.2: Air void completely filled with ettringite crystals	10
Figure 2.3: Crystallization of gypsum at the aggregate paste interface	13
Figure 2.4: Aggression by sulfates	14
Figure 2.5: Aggression of chloride	23
Figure 2.6: Biogenic Corrosion / Vapor Phase due to Sulfide Attack on Concrete	25
Figure 2.7: Mechanism of Sulfide attack on concrete	26
Figure 3.1: Flow table test	44
Figure 3.2: Schematic diagram of Vicat apparatus	46
Figure 3.3: Vicat apparatus to determine normal consistency of cement	47
Figure 3.4: Vicat apparatus to determine setting time of cement	50
Figure 3.5: Setting time test molds	51

Figure 3.6: Sand, Cement, Water	53
Figure 3.7: Electronic weighing machine	53
Figure 3.8: Mixer machine with bowl and paddle	54
Figure 3.9: Order of tamping in molding of mortar cubes	54
Figure 3.10: Mortar in molds after casting	55
Figure 3.11: Specimens in limewater	55
Figure 3.12: Specimens submerged in simulated tannery wastewater	57
Figure 3.13: Cube in compression testing machine	58
Figure 3.14: Image capturing setup	59
Figure 3.15: Scanning Electron Microscope (SEM)	59
Figure 3.16: Schematic diagram of X-ray fluorescence (XRF)	61
Figure 3.17: Length comparator	64
Figure 4.1: Test results of normal consistency	68
Figure 4.2: Setting time of cubes prepared from different cement mix types	69
Figure 4.3: Flow of mortar prepared from different cement mix types	70
Figure 4.4: Strength of C1 cubes (Normal condition)	73
Figure 4.5: Strength of C1 cubes (Tannery wastewater condition)	73
Figure 4.6: Strength of C2 cubes (Normal condition)	73
Figure 4.7: Strength of C2 cubes (Tannery wastewater condition)	73
Figure 4.8: Strength of C3 cubes (Normal condition)	73
Figure 4.9: Strength of C3 cubes (Tannery wastewater condition)	73
Figure 4.10: Strength of C4 cubes (Normal condition)	74
Figure 4.11: Strength of C4 cubes (Tannery wastewater condition)	74
Figure 4.12: Strength of C5 cubes (Normal condition)	74
Figure 4.13: Strength of C5 cubes (Tannery wastewater condition)	74

Figure 4.14: Strength of C6 cubes (Normal condition)	74
Figure 4.15: Strength of C6 cubes (Tannery wastewater condition)	74
Figure 4.16: Strength of C7 cubes (Normal condition)	75
Figure 4.17: Strength of C7 cubes (Tannery wastewater condition)	75
Figure 4.18: Strength of C8 cubes (Normal condition)	75
Figure 4.19: Strength of C8 cubes (Tannery wastewater condition)	75
Figure 4.20: Strength of cubes after 28 days limewater curing	76
Figure 4.21: Strength of cubes after 90 days in normal and tannery wastewater Condition	76
Figure 4.22: Strength of cubes after 180 days in normal and tannery wastewater Condition	77
Figure 4.23: Strength of mortar cubes kept in normal condition and tannery wastewater condition for 90 days	78
Figure 4.24: Strength of mortar cubes kept in normal condition and tannery wastewater condition for 180 days	78
Figure 4.25: Strength of only fly ash blended cement mortar cubes in tannery wastewater condition	79
Figure 4.26: Strength of only slag blended cement mortar cubes in tannery wastewater Condition	79
Figure 4.27: Strength of both fly ash and slag blended cement mortar cubes in tannery wastewater condition	80
Figure 4.28: Strength change (%) of mortar cubes submerged in tannery wastewater	81
Figure 4.29: Expansion (%) of C1 bars kept in normal condition and tannery wastewater condition	83
Figure 4.30: Expansion (%) of C2 bars kept in normal condition and tannery	

wastewater condition	84
Figure 4.31: Expansion (%) of C3 bars kept in normal condition and tannery wastewater condition	84
Figure 4.32: Expansion (%) of C4 bars kept in normal condition and tannery wastewater condition	85
Figure 4.33: Expansion (%) of C5 bars kept in normal condition and tannery wastewater condition	85
Figure 4.34: Expansion (%) of C6 bars kept in normal condition and tannery wastewater condition	86
Figure 4.35: Expansion (%) of C7 bars kept in normal condition and tannery wastewater condition	86
Figure 4.36: Expansion (%) of C8 bars kept in normal condition and tannery wastewater condition	87
Figure 4.37: Weight loss % of cubes prepared from different cement mix types submerged in tannery wastewater for 90 days	88
Figure 4.38: Weight loss % of cubes prepared from different cement mix types submerged in tannery wastewater for 180 days	89
Figure 4.39: Weight loss % of C1 cubes submerged in tannery wastewater	90
Figure 4.40: Weight loss % of C2 cubes submerged in tannery wastewater	90
Figure 4.41: Weight loss % of C3 cubes submerged in tannery wastewater	91
Figure 4.42: Weight loss % of C4 cubes submerged in tannery wastewater	91
Figure 4.43: Weight loss % of C5 cubes submerged in tannery wastewater	92
Figure 4.44: Weight loss % of C6 cubes submerged in tannery wastewater	92
Figure 4.45: Weight loss % of C7 cubes submerged in tannery wastewater	93
Figure 4.46: Weight loss % of C8 cubes submerged in tannery wastewater	93



Figure 4.47: Weight loss % of only fly ash mixed cement mortar cubes submerged in tannery wastewater	94
Figure 4.48: Weight loss % of only slag mixed cement mortar cubes submerged in tannery wastewater	95
Figure 4.49: Weight loss % of both fly ash and slag mixed cement mortar cubes submerged in tannery wastewater	95
Figure 4.50: Cube surface images before and after submergence in tannery wastewater for 180 days	98
Figure 4.51: SEM image of C1 cubes submerged in tannery wastewater for 180 days (500x zoom)	99
Figure 4.52: SEM image of C1 cubes submerged in tannery wastewater for 180 days (1000x zoom)	100
Figure 4.53: SEM image of C2 cubes submerged in tannery wastewater for 180 days (500x zoom)	101
Figure 4.54: SEM image of C2 cubes submerged in tannery wastewater for 180 days (1000x zoom)	101
Figure 4.55: SEM image of C5 cubes submerged in tannery wastewater for 180 days (500x zoom)	102
Figure 4.56: SEM image of C5 cubes submerged in tannery wastewater for 180 days (1000x zoom)	102
Figure 4.57: SEM image of C6 cubes submerged in tannery wastewater for 180 days (500x zoom)	103
Figure 4.58: SEM image of C6 cubes submerged in tannery wastewater for 180 days (1000x zoom)	103
Figure 4.59: EDS analysis of C1 cube in normal condition	105

Figure 4.60: EDS analysis of C6 cube in normal condition	106
Figure 4.61: EDS analysis of C1 cube in tannery wastewater	107
Figure 4.62: EDS analysis of C2 cube in tannery wastewater	108
Figure 4.63: EDS analysis of C5 cube in tannery wastewater	109
Figure 4.64: EDS analysis of C6 cube in tannery wastewater	110

### **List of Abbreviations and Symbols**

AFm	Alumina, Ferric Oxide, Mono-Sulfate
AFt	Alumina, Ferric Oxide, Tri-Sulfate
ASR	Alkali- Silica Reactivity
ASTM	American Society for Testing And Materials
BS EN	British European Harmonised Standards
C <sub>3</sub> A	Tricalcium Aluminate
C <sub>3</sub> S	Tricalcium Silicates
C <sub>4</sub> AF	Tetracalcium Aluminoferrite
CEM	Calcium Enriched Mixture
CETP	Central Effluent Treatment Plant
C-S-H	Calcium Silicate Hydrate
EDS	Energy-Dispersive X-Ray Spectroscopy
FA	Fly Ash
FP	Fundamental Parameter
GGBS	Ground Granulated Blast Furnace Slag
HPC	High-Performance Concrete
OPC	Ordinary Portland Cement
PC	Portland Cement

PCC	Portland Composite Cement
PREN	Pitting Resistance Equivalent Number
SCM	Supplementary Cementitious Materials
SEM	Scanning Electron Microscopy
XRF	X-Ray Fluorescence

# **Chapter 1**

## **INTRODUCTION**

### **1.1 General**

Concrete structures have gained popularity due to their versatility, durability and several other advantages over other forms of construction. However, when exposed to harsh environmental conditions, concrete structures can deteriorate over time due to chemical reactions of the components of concrete, such as cement hydration products with the environmental agents. The durability of such structures in such cases becomes a matter of concern. The type and composition of materials used in the making of concrete therefore should be decided upon with utmost diligence to ensure durability in the face of such adverse conditions. There is increasing pressure over the construction industry to reduce cement consumption by incorporating supplementary cementitious materials (SCMs) in concrete. Such concrete is also termed as “sustainable concrete”. For the civil engineering community, the concept of sustainable development conveys the use of high-performance materials produced at a reasonable cost and with the lowest possible environmental impact. Assimilating SCMs in cement industry meets both of these requirements.

### **1.2 Background**

Concrete structures are often subjected to aggressive aqueous environments which consist of several chemical agents that can react with concrete to produce adverse effects. Tannery wastewater consists of several chemicals such as sulfates, chlorides, ammonium, sulfide, etc. which, from literature, are known to generate detrimental effects on concrete. The nature and extent of deterioration is dependent on several factors like the composition of the tannery effluent, the concentration of the individual constituents, materials used in construction, etc. Some cementitious materials may be more readily susceptible to damage compared to others. The time period the concrete remains in contact with the water is also a very important factor which will influence the behavior of concrete.

A Central Effluent Treatment Plant (CETP) consisting of reinforced concrete structures, is being constructed to receive wastewater from different tannery industries at Savar, Bangladesh. CETP is an example of structure to be exposed to such deleterious environment (Sagris and Abbott, 2015) and the durability of structures in such cases becomes a matter of concern. If a concrete structure storing or conveying huge volumes of tannery wastewater, fails, the effect would be catastrophic both from environmental and economic perspectives. It is also worthy of mention that further construction of similar structures in future without adequate knowledge and research would be unwise.

Bangladesh, being a developing country with an expanding economy, a substantial amount of construction works can be expected to take place in the near future. This will initiate a boost in the manufacture of cement. It is established that the increased use of supplementary cementitious materials offers the most readily achievable means of reducing greenhouse gas from this industry. The cement production process is known for its high CO<sub>2</sub> emissions, related primarily to the clinkering process. It is estimated that one percent replacement of cement with fly ash represents a 0.7% reduction in energy consumption (Nisbet et al. 2002). The carbon dioxide (CO<sub>2</sub>) produced for the manufacture of one ton of structural concrete (using around 14% cement) is estimated to be 410 kg/m<sup>3</sup> (~180 kg/ton @ density of 2.3 g/cm<sup>3</sup>), which is reduced to 290 kg/m<sup>3</sup> with 30% fly ash replacement of cement (Samarin 1999). Damtoft et al. (2008) estimated that if all the suitable, but unused blast furnace slag and fly ash were to be blended with cement clinker (1:1, w/w), the corresponding reduction in CO<sub>2</sub> from this industry would be around 17%. Worrell et al. (2001) observed the global potential for CO<sub>2</sub> emission reduction through producing blended cement is estimated to be at least 5% of total CO<sub>2</sub> emissions from cement making but can be as high as 20%. Thus, the environmental impact of the cement production process can be reduced significantly by incorporating supplementary cementitious materials.

Locally available composite cement (CEM II) have around 6-35% of supplementary materials in composition of them. Their compositions vary from brand to brand. Therefore, the need for an investigation whether and which supplementary materials in which proportion individually or combined perform better in concrete structures seemed

necessary for future proposition in cement production. With this view in mind, this research has been carried out in the laboratories of Bangladesh University of Engineering and Technology (BUET). The research focused on comparison in strength and durability of cement mortars prepared from different mixing proportions of fly ash and slag with cement and their reactions with tannery wastewater.

### **1.3 Objectives**

The specific objectives of this research are expounded upon as below:

- 1) To simulate synthetic tannery wastewater in laboratory.
- 2) To study the behavior of cement mortar under simulated tannery wastewater by varying proportions of cement constituents and supplementary materials (i.e. fly ash, blast furnace slag).
- 3) To evaluate the effects of adding various proportion of supplementary material on basic cementitious composite properties such as strength, flowability, consistency and setting time.
- 4) To carry out compressive strength test, expansion test and to determine weight loss of mortar cube samples.
- 5) To compare the test results and recommend optimum cement compositions that shows relative better performance and resistance in tannery wastewater.

### **1.4 Scope**

This study was conducted in the context of Bangladesh, using OPC (CEM I) cement and two types of supplementary materials: fly ash and ground granulated blast furnace slag (GGBS) commonly available in the country. The synthetic tannery wastewater simulation was carried out on the basis of previous study on the composition of the samples collected from Hazaribagh area, Dhaka. The study was carried out using cement mortar specimens which were prepared in accordance with ASTM C109 (2013) and ASTM C1012 (2015). The focus of this research was to study the behavior of blended cement mortars and

compare with OPC mortar with respect to strength, expansion, weight loss and surface deterioration. At the end of this study, data acquired from different tests carried on mortars prepared from different proportion of supplementary materials has been analyzed to recommend an optimum replacement proportion which performed better in tannery wastewater.

### **1.5 Outline of the thesis**

The first chapter gives a general introduction and explains the background behind the thesis, gives a brief description of the possible outcomes, identifies the scope of this research and outlines the objectives of this study.

The second chapter gives an extensive literature review on the possible effects of principle constituents of tannery wastewater, causing severe concrete degradation. The degradation mechanisms and the factors affecting the rate and extent of deterioration are discussed. Benefits of using supplementary cementitious materials in partial replacement of cement from both structural and environment conservation perspectives have been discussed.

The third chapter describes in details the methodology adapted for accomplishing the objectives, the materials used, procedure of preparation of the test specimens, the experimental setup for normal consistency, initial and final setting time, flowability, compressive strength and some state of the art techniques of analysis which were used in this thesis such as SEM, EDS and XRF.

The fourth chapter, results and discussions, presents the findings of this research in the form of relevant data, graphs and elaborately explains the trends that these graphs demonstrate. Observations from images are also explained. An attempt is made to compare and contrast the behavior of different cement mix proportions with respect to the experimental results.

In the final chapter, the outcomes of this research are summarized with a conclusion and a few recommendations are proposed in light of the findings of this thesis.

## **Chapter 2**

### **LITERATURE REVIEW**

#### **2.1 Introduction**

This chapter includes the established ideas and knowledge including essential findings, as well as theoretical and methodological contributions to the detrimental effects of different constituents of tannery wastewater on concrete. As the research work aims to focus on the benefits of using supplementary materials as replacement of cement and find an optimum level of replacement, a brief summary of existing research on relevant topic herein has been presented.

#### **2.2 Leather Industry in Bangladesh**

Leather is one of the most important export products of Bangladesh earning foreign exchange. There has been a significant rise in the export of leather footwear due to increasing investment in this sector. The ever-growing leather sector is the country's second largest export earner which has been reported to cross the billion-dollar export mark in 2014 (Al-Muti and Ahmad, 2015). On the contrary, leather tanning has become one of the main causes of environmental and water pollution in the Capital city of Dhaka of 10 million people. The wastewater produced from different tanning processes viz. soaking, liming and unhairing, declaiming and bating, pickling, chrome tanning and retanning is highly polluted with a disagreeable pH, alkalinity, acidity, total solids, total dissolved solids, suspended solid, chemical oxygen demand, biochemical oxygen demand, chlorides and sulfides (Islam et al. 2014).



### **2.3 Tannery Wastewater**

Every year, about 60,000 tons of raw hides and skins are processed which causes an average production of 30–35 m<sup>3</sup> of wastewater per ton of raw hide (Jahan et al. 2014). Nevertheless, depending on the available raw materials, the finishing products and the production processes, production of wastewater varies in wide range of 10–100 m<sup>3</sup> per ton hide (Ates et al. 1997). Hides and skins processing and converting them into leather requires an aqueous medium and hence the wastewater discharged from pits, drums or paddles of tannery mills contains several soluble and insoluble constituents the effluents (Jahan et al. 2014).

### **2.4 Tanning Process**

The main target of tanning process is to transform skins in stable and imputrescible products namely leather and which constitutes of four major groups of sub-processes required to make finished leather: beam house operation, tan yard processes, retanning and finishing (U.S. EPA. 1986, Tunay et al. 1995, Ates et al. 1997). These sub-processes require acids, alkalis, chromium salts, tannins, solvents, sulfides, dyes, auxiliaries, and many others compounds and transform raw or semi-pickled skins into commercial goods. These chemical compounds are not completely absorbed by skins and remain in the effluent (Jahan et al. 2014). The discharge of huge amount of sulfides, lime, and ammonium salts, chlorides, sulfate, and protein in the effluent is caused by the beam house operations like soaking, liming and deliming. This effluent contains high amount of suspended solids, dissolved lime, sodium sulfide, high ammoniacal nitrogen and organic matter. The effluent contains fatty fleshing matter in suspension which comes from unhairing and fleshing. The spent deliming liquors carry significant BOD load and the spent bate liquors on account of presence of soluble skin proteins and ammonium salts containing high organic matter. Pickle liquors are acidic contain high amount of salt (Ramasami et al. 1994).

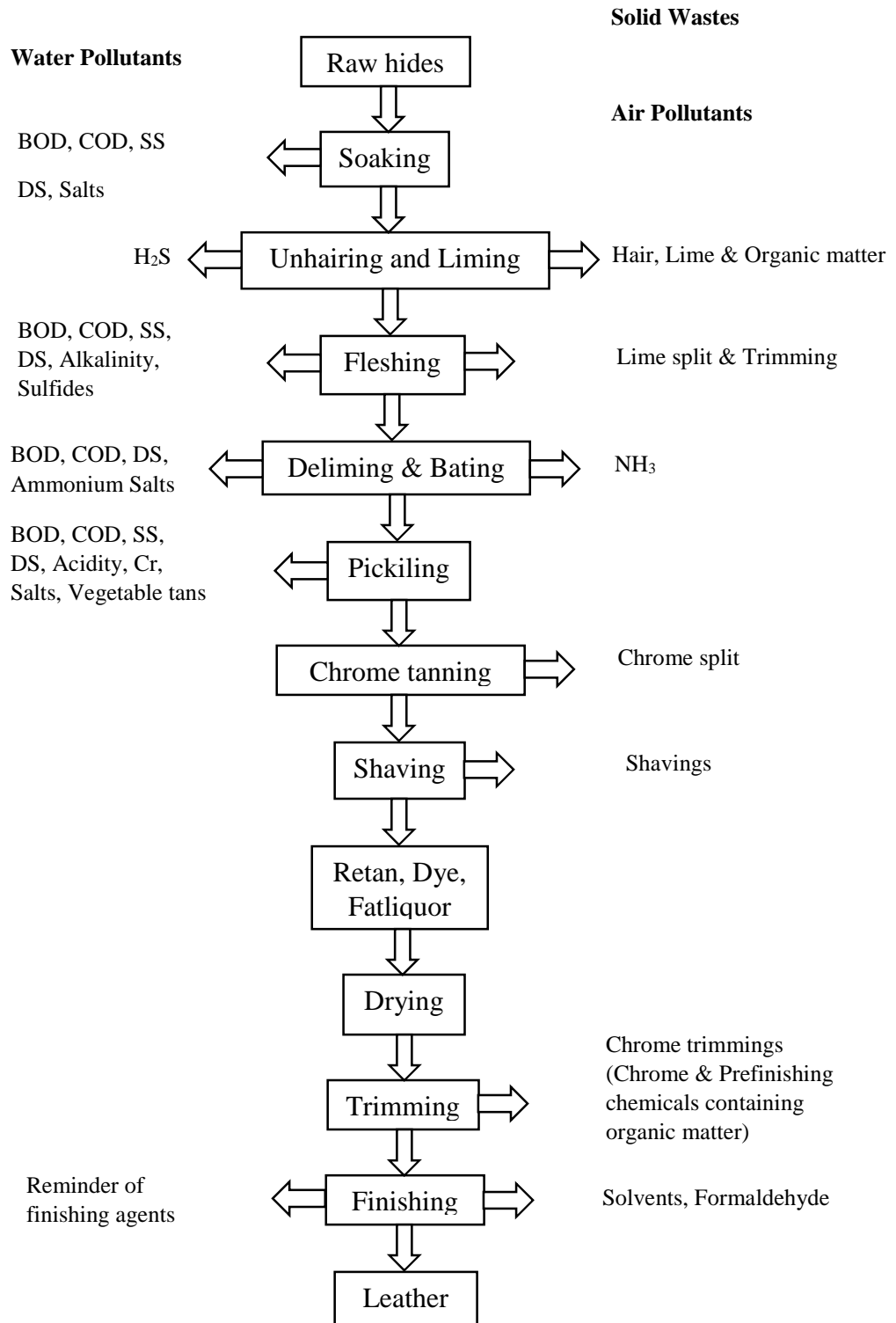


Figure 2.1: Wastes generated from each unit operation of a tannery (Islam et al. 2014)

## **2.5 Attack of Major Deteriorating Tannery Wastewater Constituents on Concrete**

Among all the tannery wastewater constituents, sulfate, ammonium, chloride and sulfide have shown significant detrimental effects on concrete structures (Manzur et al. 2018).

### **2.5.1 Sulfate Attack on Concrete**

Sulfates are a component of tannery effluent, produced from the use of sulfuric acid or products with a high (sodium) sulfate content. Many auxiliary chemicals contain sodium sulfate as a by-product of their manufacture. For example, chrome tanning powders contain high levels of sodium sulfate, so do many synthetic retanning agents (Bosnic et al. 2000). Cements have long been known to undergo deterioration in sulfate rich service environments. The end result of sulfate attack can be excessive expansion, surface area loss, cracking, and loss of strength.

#### **2.5.1.1 Concrete Behavior in Presence of Sulfate**

Solid sulfates do not attack the concrete severely but along with other chemicals they try to enter into porous concrete and react with the hydrated cement products. Sulfate attack on concrete results due to the chemical reaction between the sulfate ion and hydrated calcium aluminate or the calcium hydroxide components of hardened cement paste in the presence of water. The products resulting from these reactions are calcium sulfoaluminate hydrate, commonly referred to as ettringite, and calcium sulfate hydrate, known better as gypsum. These solids have a very much higher volume than the solid reactants and, as a consequence, stresses that may result in breakdown of the paste and ultimately in breakdown of the concrete are produced (Nirmalkumar and Sivakumar, 2008).

To analyse the behavior of concrete in relation with high sulfate content, it is necessary to take into account factors such as the absorption of sulfate from solution, the diffusion of sulfates into the pore structures, and the nature and consequences of the chemical reactions between the sulfate and the hydration products ((Menendez, 1999).

### 2.5.1.2 Chemistry of Sulfate Attack

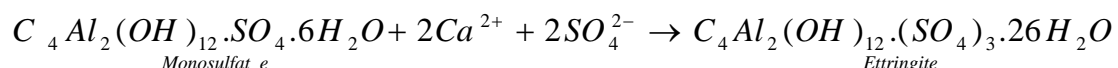
There are three key chemical reactions between sulfate ions and hardened cement pastes (QCL, 1999). These reactions are:

1. Recrystallisation of ettringite: In the presence of the calcium hydroxide formed in cement paste, when the latter comes in contact with sulfate ions, the alumina containing hydrates are converted to the high sulfate form of ettringite. These ettringite crystals grow, expand, or swell by mechanisms, which are still the subject of controversy among researchers.
2. Formation of gypsum: The gypsum formation as a result of cation exchange reactions also causes expansion but is normally linked to loss of mass and strength. CSIRO work proves that gypsum can cause significant local expansion and cracking especially when formed in large masses.
3. Decalcification of the main cementitious phase (C-S-H): This phase is important where the sulfate solution is lower in pH (more acidic) and more gypsum formation leads to both strength loss and expansion. In this case, blended cements with lower initial calcium/silica (C/S) ratios in the C-S-H gel are shown to be less susceptible due to this type of attack.

### 2.5.1.3 Ettringite Formation and Development

Primary ettringite forms normally during hydration of Portland cement through the reaction of sulfate ions which come mainly from gypsum added as a set retarder. However, when ettringite forms in the hardened concrete, significant expansions can be induced which cause damages (Menendez et al. 2012).

In the hydrated cement matrix, the source of alumina is usually monosulfate (AFm) according to the equation:



$C_3A$  or ferrites,  $C_4AF$  which are unreacted, are also potential sources of Aluminium that can react with external sources of sulfates.

Monosulfate will also be present in composite cements containing blast furnace slag, fly ash or natural pozzolana but in the hydrated matrix of these cements, alumina is partly present in phases such as hydrotalcite or hydrogarnet or substituted in the C-S-H. The result is that aluminate isn't available to form an expansive reaction product. (Gollop and Taylor, 1996).

#### 2.5.1.4 Morphology of Ettringite Crystals

The morphology of ettringite crystals often takes the form of needle-like-hexagonal prisms. Usually the morphology of ettringite is long hexagonal crystals but other morphologies are well known such as stout prisms and prisms with hollow re-entrant ends (Menendez, 2010). Ettringite morphology is much influenced by sorption of ions and molecules, such as plasticizers.



Figure 2.2: Air void completely filled with ettringite crystals (Stark and Bollmann, 1999)

### **2.5.1.5 Wet-Dry Cycles from Sulfate Exposure**

It is generally accepted that in the case of wet-dry cycles with exposure to a sulfate solution, the pores fill slowly with salts by precipitation during the dry cycles. During the wet cycles, the pores are refilled generally with lower concentration of salts. Each cycle starts with more fluid ingressing pores. But in successive cycles the remaining volume of pores decreases until the pore is just filled and no more aqueous phase can enter during the wet stage. The pore size distribution, the type of salts, and the environmental conditions (pH, temperatures and duration of the cycles) control the type and extent of deterioration observed. Efflorescence can be observed on the surface of the concrete, or subflorescence could occur below the surface, or both, depending on the environmental conditions. Efflorescence is not aesthetically pleasing and can be easily eliminated by washing the surface, while subflorescence will generate stresses that will deteriorate the structure (Menendez et al. 2012).

### **2.5.1.6 Crystallization Theories**

It is generally agreed (Flatt, 2002) that the main cause of spalling under exposure to sulfate solution and wet-dry cycles is due to crystallization pressure. There are several theories of how crystallization pressure develops. According to Flatt (2002), a crystal will grow in all directions until its surface attains a local weighted mean curvature that is in equilibrium with the concentration of the solution. There exist large repulsive forces between the crystal and the surface of the pore. Due to this, the crystal will stop growing towards the pore surface. Scherer (1999) also showed that large forces are required to overcome the surface tension and hence direct contact between the crystal and the surface of the pore is not possible. A thin film exists between the crystal and pore wall and the concentration of the thin film is not in equilibrium with the radius of the pore. As a result, the tip of crystal grows in the opposite direction of the pore and eventually within the matrix, causes stress.



The alkali ions being relatively small penetrate into the concrete and tend to migrate towards the interior, increasing the alkalinity of the aqueous phase. As a consequence, and under adverse conditions, an alkali-silica reaction occurs with an outward migration of  $\text{OH}^-$  ions.

Like calcium sulfates, the primary action of the alkali sulfates may result in increase in strength because they fill up the pores with newly formed ettringite. However, stress is created as the process is physically expansive. Cracking and spalling occur when the stress exceeds the tensile strength of concrete. A scaly surface is often observed because of the local ettringite formation or crystallization of gypsum or both. Micro cracking also occurs as a result of the decalcification and shrinkage of the C-S-H gel.

Usually gypsum appears as dense crystals formed as parallel columnar growths as shown in the Figure 2.3. The aggregate is shown at the top and bladed columnar gypsum (centre) has filled the annulus between paste (bottom) and aggregate (Menendez, 2010).

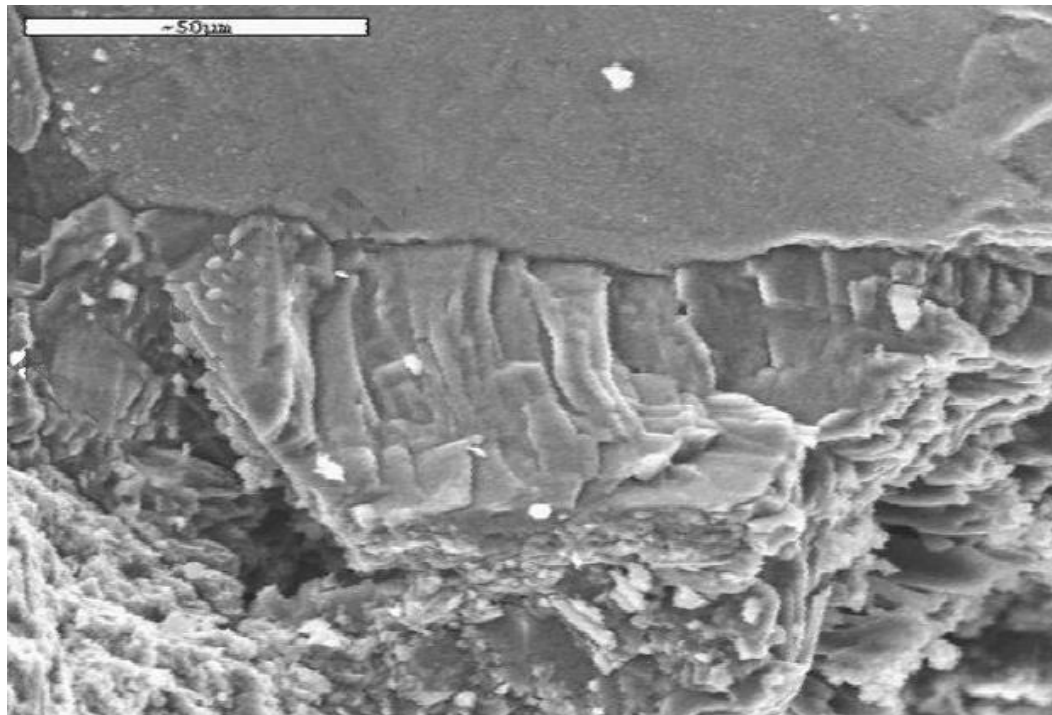


Figure 2.3: Crystallization of gypsum at the aggregate paste interface (Menendez, 1999)



### 2.5.1.8 Damages to Concrete due to Sulfate Attack

The damage to concrete structures resulting from external sulfate attack are related to the following factors (Menendez et al. 2012):

- 1) Transport of ions to the interior of the concrete through the pore system
- 2) Chemical reactions between sulfates and the solid hydration products of cement
- 3) Generation of stress in the interior of the concrete as a result of formation of expansive products
- 4) Mechanical response of the bulk material resulting from these stresses, such as cracking
- 5) Characteristics of concrete components and their proportions.

The ACI building code for structural concrete, includes different class for sulfate exposure according to amount of dissolved sulfate present in water in contact with structure (Table 2.1). Maximum expansion limit for blended cement mortars are also specified in Table 2.2.



Figure 2.4: Aggression by sulfates (Mapei, 2011)

Table 2.1: Exposure Categories and Classes (Table 19.3.1.1 - ACI 318-14, 2014)

Category	Class	Dissolved sulfate ( $\text{SO}_4^{2-}$ ) in water, ppm
Sulfate (S)	S0	$\text{SO}_4^{2-} < 150$
	S1	$150 < \text{SO}_4^{2-} < 1500$
	S2	$1500 < \text{SO}_4^{2-} < 10000$
	S3	$\text{SO}_4^{2-} > 10000$

Table 2.2: Requirements for establishing suitability of combinations of cementitious materials exposed to water-soluble sulfate (Table 26.4.2.2(c) - ACI 318-14, 2014)

Exposure Class	Maximum expansion strain if tested using ASTM C1012		
	At 6 months	At 12 months	At 18 months
S1	0.1%	No requirement	No requirement
S2	0.05%	0.1%	No requirement
S3	No requirement	No requirement	0.1%

### 2.5.1.9 Resistance to Sulfate Attack

Low C<sub>3</sub>A cements are believed to provide resistance against sulfate attack. The products of sulfate attack are not expansive and consequently the matrix is not disrupted, inhibiting further reaction. The un-reactive nature of the hydrated products of low C<sub>3</sub>A cements is attributed to a low level of monosulfate (AFm) and/or the formation of an iron rich form which is slow reacting and is claimed to produce a non-expansive form of ettringite (Odlar, 1984).

Portland composite cements (i.e. CEM II, III, IV and V types according to BS EN 197-1 (2000) provide resistance to sulfate attack which is attributable to the microstructure (Mehta, 1988, Soroushian and Alhozimy, 1982, Stephen, 2000, Hughes, 1985). This arises from the significantly lower permeability of the hydrated matrix.

Additional positives are:

- 1) When the matrix is exposed to concentrated sulfate solutions. reduced level of free calcium hydroxide in the matrix which reduces calcium availability for leaching, for ettringite formation, for gypsum formation,
- 2) Formation of hydrates containing alumina which are non-reactive to sulfate solutions.

The resistance to sulfate attack is often positively influenced by the level of SO<sub>3</sub> in the binder: the higher the level is in the range (1 ~ 4%), the greater is the resistance. This applies to concrete produced from CEM I cements (Frigione et al. 1992) and also

particularly to slag and fly ash containing concretes. The  $\text{SO}_3$  level is lowered by dilution and the hydrated mix becomes more vulnerable to attack by penetrating sulfates in comparison with a binder having an optimized  $\text{SO}_3$  content where the ash and slag are added during the concrete mixing process (Gollop and Taylor, 1996, Kolleck and Lumly, 1990, Prusinski and Carrasquillo, 1995). The improved resistance can be attributed to the increased level of sulfated phases, such as ettringite, formed during initial hydration and remain stable in the presence of an elevated sulfate level.

### **2.5.2 Ammonium Attack on Concrete**

Deliming process produces ammonium nitrate, with comparatively small volumes being produced from liming and unhairing (Bosnicet al.2000). Certain ammonium salts causes most of the damages of concrete.

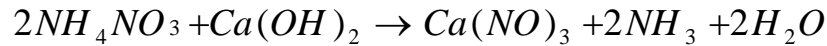
#### **2.5.2.1 Chemistry of Ammonium Attack on Concrete**

In ammonia factories, the signs of swelling, damage and cracks, are generally observed within 3 years after the start of production in the plant (Baxi and Patel, 1998). Chemical attack by ammonium nitrate leads to a very soluble calcium nitrate, a slightly soluble calcium nitro aluminate, and release of ammonia gas. This process mainly induces total leaching of calcium hydroxide and rapid decalcification of C-S-H. The chemical reactions can be categorized into three types which are, in sequence:

- (1) Dissolution: Dissolution of the cementitious compounds which depends on the environment.
- (2) Simple diffusion: Cementitious materials being immersed in ammonium nitrate solutions, calcium ions diffuse to the exterior without any formation of calcium salts in the material, as the solubility of Portlandite increases significantly in these solutions. In this case, the degradation is conducted by a diffusion mechanism and it can be described by Fick's law, relating the degraded thickness to the square root of the immersion time in the aggressive solution.

(3) Crystallization: When concrete is subjected to drying or to wet-dry cycles, salts may crystallize in the partially dry concrete.

Dissolution of cement-based materials through the reaction between ammonium nitrate and calcium hydroxide in the cement paste is initiated by ammonium nitrate. The reaction is expressed in:

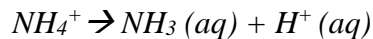


Aluminates can also react with nitrate ions to form a less soluble calcium nitro-aluminate salt,  $3CaO \cdot Al_2O_3 \cdot Ca(NO_3)_2 \cdot 10H_2O$  (Ukrainick et al. 1978). Similarly, in the presence of sulfates, the possibility of formation of a double salt  $CaSO_4 \cdot (NH_4)_2SO_4 \cdot 2H_2O$  has also been mentioned (Mohr, 1925).

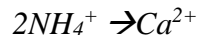
Ammonium salts are hygroscopic and highly soluble in water (24 mol/l at 20 degrees centigrade). They decompose in water according to:



In a basic environment, ammonium ions (weakly acidic) are transformed to aqueous ammonia with the formation of  $H^+$  ions according to the following equation:



Ammonium ions react according to an exchange reaction,

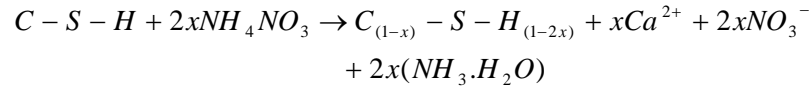


The calcium salt produced (calcium nitrate) is highly soluble and leads to the progressive dissolution of the all calcium bearing cement phases. Moreover in the presence of cementitious material (pH between 12 and 13.5) the equilibrium is strongly moved to the right, i.e aqueous  $NH_3$  and  $H^+$  ions are dominant. This release of  $H^+$  ions decreases the pH and accelerates the successive dissolution of calcium bearing phases. Portlandite, C-S-H, and aluminates AFt ("alumina, ferric oxide, tri-sulfate") and AFm ("alumina, ferric oxide, mono-sulfate") are dissolved according to the following equations:

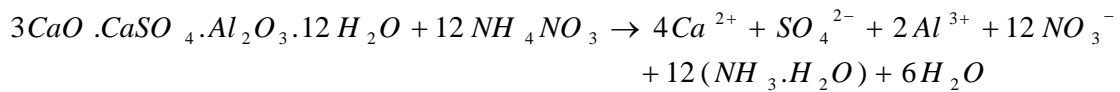
Ca(OH)<sub>2</sub>:



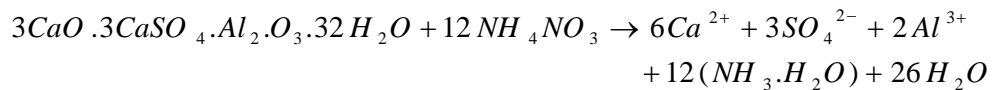
C-S-H:



AFm:



Aft:



### 2.5.2.2 Damage Observed on Structures

Ammonium salts are the most aggressive of the factors that can degrade concrete (Lea, 1965, Biczok, 1972). Damage observed on concrete structures in contact with ammonium nitrate is of two types, depending on the environment:

1. Large increase in porosity with weakening of mechanical properties in concrete continuously immersed in a solution of ammonium nitrate.
2. Notable swelling with occurrence of cracks linked to the formation of expansive crystals in concrete in contact with the air or subjected to wet-dry cycles.

The reaction between ammonium nitrate and concrete was reported as potentially aggressive. Due to the removal of calcium hydroxide, the hardened cement paste will be decalcified causing the pH value to decrease (Biczok, 1972). The reaction produces calcium nitrate and ammonia, both of which are easily water-soluble. Following, an expansive calcium nitroaluminate is formed by reaction between calcium nitrate and hydrated aluminates from the cement paste (Escadeillas, 1993). Lea (1965) reported that

this compound forms “climbing salts” by the transportation of water from humid to dry surface. The concrete is weakened through the leaching of lime in cement paste which eventually leads to cracking on the concrete surface. The deterioration of concrete reduces the effectiveness of concrete as protective cover for steel reinforcement. The steel reinforcement will be corroded, leading to spallation of concrete.

### **2.5.2.3 Dissolution of Calcium Hydroxide in Ammonium Nitrate Solution**

Weight loss or the increase in water porosity causes the state of alteration of cementitious materials (Bajza et al. 1986). These quantities related to the dissolution of hydrates, also vary according to the square root of time, confirming the diffusive nature of the degradation by ammonium nitrate. Gonclaves and Rodrigues (1991) measured mass losses of 8% and 11% in solutions of 0.6mol/l and 6mol/ respectively. Mass losses were reduced with the use of slag (losses of 4% and 7% respectively). These mass losses and increase in porosity are in direct relation with the decalcification of the cement hydrates (Perlot et al. 2006, 2007). The evolution of degradation can also be determined by investigating the loss of strength.

Furthermore, in pure water, the dissolution of calcium hydroxide is lower than that in the ammonium nitrate solution. This causes decalcification and dissolution of other elements of the hardened cement paste and leads to a decrease in the pH-value. As a result, corrosion may occur at accelerated rate in steel reinforcement. With an increase in concentration of the ammonium nitrate solution, the life-time of the concretes decreases significantly, no matter whether it is loaded or unloaded. The life-time and concentration of the solutions have a relation of exponential functions (Schneider and Chen, 2005). Higher the concentration of the solutions, deeper is the penetration of the aggressive ions, after a certain period of immersion. The penetration depths also depend on the initial strengths of the specimens. The simple root law can describe the relation between penetration depth and the immersion time (Schneider and Chen, 2005).

In the case of a paste sample made with an OPC cement which leads to about 20% content of calcium hydroxide, the dissolution of this calcium hydroxide is the essential parameter

governing both decrease in strength and increase in porosity. The loss of strength due to the decalcification of C-S-H is only 6% and can be neglected in relation to the global loss of strength due to the dissolution of  $\text{Ca}(\text{OH})_2$ . In the case of the use of a paste sample with the admixture of silica fume to consume all the calcium hydroxide, the effect of C/S ratio decrease of the C-S-H reduces the strength of about 30%. Then, the effect of the decalcification of C-S-H is not negligible but the residual strength of the material is important and the material could keep its mechanical functions (Carde et al. 1996).

#### **2.5.2.4 Wet-Dry Cycle from Ammonium Exposure**

Rapid decalcification is produced by ammonium nitrate solutions because of the high solubility of its calcium salts. Concrete subjected to drying, swelling is related to the precipitation of salts of calcium nitro-aluminates. Degradation reactions related to ammonium nitrate solutions are fast and severe. Precautions should be taken (high strength concrete, use of pozzolanic additives, low w/c) to enhance the service life of structures placed in such environments.

#### **2.5.2.5 Crystallization**

When concrete is subjected to wet-dry or dry-wet cycles, salts may crystallize in the partially dry concrete. Under these conditions, such crystallization leads to high volume expansion, the formation of cracks and very quickly, total destruction of the material. High alumina content cement can be used as a remedy.

Under the following conditions, crystallization leads to high volume expansion, the formation of cracks and very quickly, total destruction of the material.

- Calcium Nitrate is a soluble material which disintegrates
- Ammonium ion is acidic which decreases the pH value and releases as ammonia gas which creates blister like swelling and concrete spalls.
- Calcium nitro-aluminate salt is less soluble

- Calcium bonding with anything other than aluminate and silicate will weaken the bonds of cement by decreasing effect of calcium with them so formation of calcium sulfate indicates weak bonding and eventually damage occurs

### **2.5.3 Chloride Attack on Concrete**

Chloride is introduced into tannery effluents as sodium chloride on account of the large quantities of common salt used in hide and skin preservation or the pickling process (Bosnic et al.2000).

The degradation of concrete structures subject to environments containing chloride ions, like wastewater treatment plants, poses major problems in economic and environmental terms. The action of these media on reinforced concrete structures causes serious degradation problems after some time which involves very high costs in terms of repair and may in some situations jeopardize the stability of parts of the structure (Ueli et al. 2011, Raupach and Schiessl, 1997, Birbilis and Cherry, 2004).

Chlorides can attack the hydration cement paste phase of concrete, primarily leading to lowering the alkalinity of concrete. Chlorides can alter the product of cement hydration and also cause other forms of concrete deterioration. Calcium Chloride and (to a lesser extent) sodium chloride have been shown to leach calcium hydroxide and cause chemical changes in Portland cement, leading to loss of strength, as well as attacking the steel reinforcement present in most concrete (Wanga et al. 2006).

#### **2.5.3.1 Mechanisms of Chloride Ingress into Concrete**

Numerous mechanisms regulate chloride ingress into concrete which causes degradation (Poulsen and Mejlbro, 2006).

1. Hydrostatic advection or permeation: The process by which external agents are transported into concrete due to hydraulic pressure (pressure differential) working as a driving force is permeability. Having a pressure difference between fluids and concrete, both gases and water penetrate into concrete.



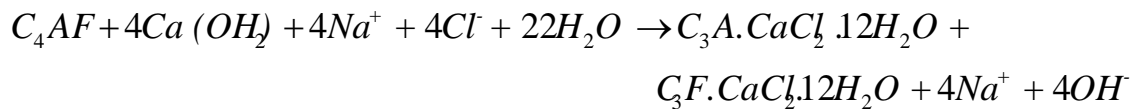
2. Diffusion: It is the process by which external agents are transported into the concrete caused by concentration difference. Normally, diffusion rate is faster in gases than in liquids. Chloride diffusion follows Fick's second law of diffusion which is, the change in chloride content per unit time is equal to the change of flux (the rate of mass transfer) per unit length.
3. Electrical migration: Migration is the process by which ion is transported due to the difference in electrical potential. A natural property of ion is it always moves from zones of high electrical potential to lower electric potential. This phenomenon is significant in the case of chloride transport.
4. Thermal migration: Due to thermal differences, movement of ions occurs. Ions or molecules in a hot environment pass faster than those in a cold environment. If a saturated concrete sample has initial uniform chloride concentration, when one section is heated, chloride ions in the hotter region will move towards the colder regions. Again, water, which is salt saturated, the surface pores of the concrete will migrate rapidly into the cooler parts of the structure under the temperature gradient.

The outcome of all these mechanisms is due to penetration of chlorides into the concrete. But when the concrete is fully saturated, the transport of chlorides is assumed to be governed by diffusion usually. (Poulsen and Mejlbro, 2006)

### **2.5.3.2 Sodium Chloride Attack on Concrete**

As soon as concrete is stored in a chloride solution, chloride ions diffusion occurs into concrete, and the diffusion speed depends on the salt, in which the chloride is a part. In salts, the chloride ions diffuse more quickly than the metal ions. This difference in diffusion speed has the immediate consequence that metal ions penetrate the hardened cement paste less than chloride ions. According to the "mutual diffusion theory", the paste will lose an amount of hydroxide ions,  $\text{OH}^-$  similar to the amount of chloride ions exceeds the equivalent amount of corresponding metal ions. This mechanism explains the entire loss of calcium hydroxide in concrete when concrete is stored in a strong chloride solution (Peterson, 1984).

Distinct nature of the attack can be found when caused by sodium chloride solution, compared with the attacks of magnesium or calcium chloride solutions. In accordance with (Srrolczyk and Heinz, 1968), sodium chloride forms somewhat more of the calcium chloroaluminate hydrate than calcium chloride does. Probably, also for attack of sodium chloride solutions, the tetracalcium aluminate ferrite is attacked rather than the tricalcium aluminate, as the latter compound was consumed in a large extent by the gypsum at the hardening and curing of the concrete. The chemical reaction is:



F stands for  $Fe_2O_3$  (ferric oxide, iron (III) oxide)

This reaction will consume twice as much calcium hydroxide as the corresponding reaction with calcium chloride solution, since calcium must be supplied for the  $CaCl_2$  groups, and not only for the two deficient calcium oxide groups in the  $C_4AF$ .



Figure 2.5: Aggression of chloride (Mapei, 2011)

## 2.5.4 Sulfide Attack on Concrete

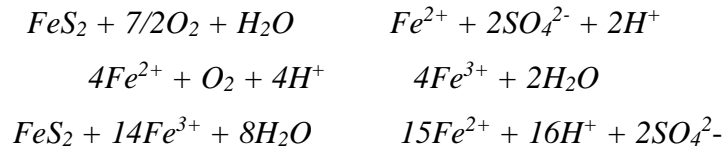
The sulfide content in tannery effluent results from the use of sodium sulfide and sodium hydrosulfide, and the breakdown of hair in the unhairing process (Bosnic et al. 2000). Oxidation of sulfides in aggregates results in additional sulfate being produced that can induce formation of ettringite in the post-hardening stage. The suspect aggregates have particles of pyrite or pyrrhotite, or both, that are slowly oxidized. Liberating sulfate that reacts with the cement components, including any remaining calcium monosulfoaluminate, to form ettringite (Alexander et al. 2012).

Concrete corrosion due to hydrogen sulfide is a major economic problem in sewer networks both because of renovation costs and the costs of preventive measures. Besides this, hydrogen sulfide is both malodorous and toxic.

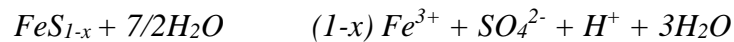
### 2.5.4.1 Chemistry of Sulfide Attack on Concrete

The pyrite and pyrrhotite reactions of oxidation are given below:

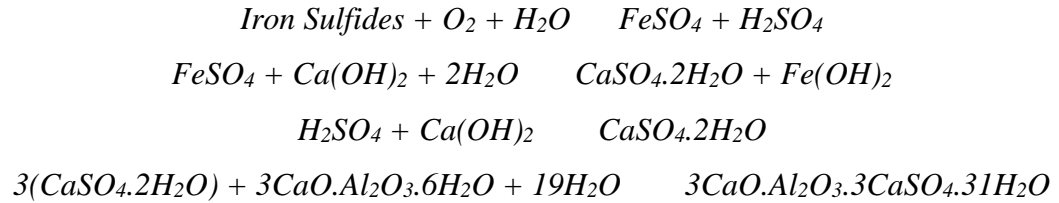
#### Pyrite oxidation



#### Pyrrhotite oxidation



Once the potential for ettringite formation is exceeded, the oxidation products may also continue to form gypsum,  $CaSO_4 \cdot 2H_2O$ . In the presence of alkaline constituents, which are dissolved in the concrete pore solution, ferric ions may also react to produce ferric hydroxides. This process is also associated with expansion, due to the gradual increase in volume of the final products, about 15%. Thus secondary expansion is commenced by formation of expansive products including both ettringite and ferric hydroxide.



Formation of gypsum is also possible in the presence of calcium carbonate, if pH decrease to near neutral, the occurred reaction is:



Figure 2.6: Biogenic Corrosion / Vapor Phase due to Sulfide Attack on Concrete

(Maley, 2006)

#### 2.5.4.2 Formation of H<sub>2</sub>S in Concrete Pipes

When the sulfide containing wastewater from the force main is discharged into a gravity sewer with a free water surface, hydrogen sulfide is emitted to the sewer atmosphere. This means that concrete pipes directly downstream of force mains are potentially in high risk of corroding (Hvitved-Jacobsen, 2002). The emission of hydrogen sulfide to the sewer

atmosphere is dependent on several processes taking place in the wastewater. When the wastewater is discharged into a gravity sewer, oxygen is supplied from the sewer atmosphere and sulfide can be removed by oxidation in the wastewater and in the sewer biofilms. These processes were described in detail by Nielsen et al. (2006). The pH of the wastewater is important for the emission of hydrogen sulfide as hydrogen sulfide is a weak acid with an acid dissociation constant of 7.0 at 25°C and it is only the non-dissociated form of hydrogen sulfide that can be emitted to the sewer atmosphere (Hvitved-Jacobsen, 2002; Yongsiri et al., 2004a, 2004b).

### 2.5.4.3 Corrosion of Concrete Pipes due to H<sub>2</sub>S

When in the sewer atmosphere, hydrogen sulfide is absorbed by the concrete surfaces of the sewer manholes and the sewer pipes where it is oxidized to sulfuric acid. The sulfuric acid lowers the surface pH of the concrete and reacts with the alkaline components of the concrete, forming gypsum, which has little structural strength (Parker, 1945a, 1945b).

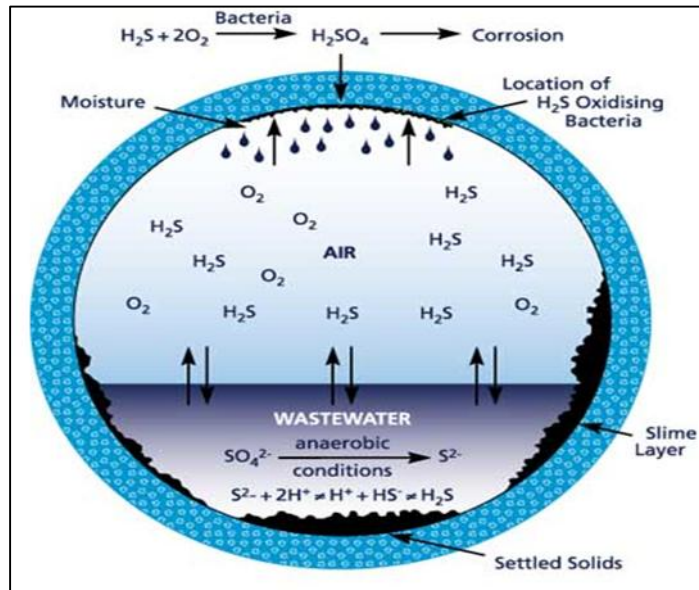


Figure 2.7: Mechanism of Sulfide attack on concrete (Gladstone Regional Council, 2017)

## **2.6. Sustainable Development and the Cement Industry**

Brundtland Commission (Brundtland Commission, 1987) defined “sustainable development” as ‘the development that meets the needs of the present without compromising the ability of future generations to meet their own needs. Due to industrialization and use of fossil fuels in automobiles, extensive emission of greenhouse gases (GHG) has led to global warming, climate changes and other environmental degradations, which has further intensified the need for sustainable development (Struble and Godfrey, 2004). Embodied CO<sub>2</sub> (ECO<sub>2</sub>) is the measure of the amount of CO<sub>2</sub> emissions generated over the duration of a product’s life from the energy needed for the raw material extraction, processing, transportation, assembling, installation, disassembly and deconstruction for any system. The ECO<sub>2</sub> of the construction material is one of the highest. For cement it is 913 kg/ton (United Kingdom Quality Ash Association, 2010).

Being a worldwide demanding constituent ingredient, production of cement becomes vital and as well as a dominant source of global carbon dioxide (CO<sub>2</sub>) emissions, making up approximately 2.4 percent of global CO<sub>2</sub> emissions from industrial and energy sources (Marland et al., 1989). Cement is produced in a large scale, capital rigorous production plants generally situated near limestone quarries or other raw carbonate mineral sources as these sources are the foremost raw materials used in the cement production process. Emission of carbon dioxide is generally a by-product of clinker production, a component of cement used as binder, in which calcium carbonate (CaCO<sub>3</sub>) is calcinated and converted to lime (CaO), the primary component of cement.

## **2.7 CO<sub>2</sub> Emissions from Cement Production**

Cement is a significant construction ingredient produced in virtually all over the world. Carbon dioxide (CO<sub>2</sub>) is a byproduct of a chemical conversion process used in the production of clinker, an intermediate product in cement manufacture, in which limestone (CaCO<sub>3</sub>) is converted to lime (CaO). Moreover, CO<sub>2</sub> is also emitted at the time of cement production by fossil fuel combustion and is responsible for elsewhere. However, the CO<sub>2</sub> from fossil fuels is accounted for in another place in estimation of emission due to fossil

fuels. The Revised 1996 IPCC Guidelines for National Greenhouse Gas Inventories (IPCC Guidelines) provide a general process towards to estimate CO<sub>2</sub> emissions from clinker production, in which the total amount of clinker produced is multiplied by the clinker emission factor.

### **2.7.1 Overview of Cement Production**

Approximately 1 ton of CO<sub>2</sub> is contributed by the production of 1 ton of cement into the atmosphere. As the net cement production all around the world in 2017 is 4.1 billion tons, this would translate to the emission of about 4.1 billion tons of CO<sub>2</sub> into the atmosphere just last year. In developing countries, the need of infrastructures is increasing day by day as well as the demand for concrete and consequently, expected cement, is to increase considerably in the near future (Statista, 2018).

Concrete as construction material has been one of the major inputs for socio-economic development of societies. It is the second largest used material after water and it stands at 2 tons per capita per year. Hence, the global production of concrete would continue to increase with time (Harrison, 2003). There is a general understanding that one ton of cement production leads to almost one ton of CO<sub>2</sub> emission. The supplementary cementitious material (SCM) has been extensively used in the development of high-performance concrete (HPC), which include fly ash, silica fumes, rice husk ashes and ground granulated blast furnace slag (GGBS). The use of SCMs have reduced the consumption of cement in concrete, apart from improvement of the properties of concrete in fresh and hardened form, thereby reducing the emissions of CO<sub>2</sub> in the atmosphere during manufacturing of cement. The extensive emissions of GHGs such as CO<sub>2</sub>, SO<sub>x</sub> and NO<sub>x</sub> have led to many environmental issues like desertification, global warming and climate change (Alaa et al., 2014).

### **2.7.2 Process Description**

Carbon dioxide is released during the production of clinker, a component of cement, in which calcium carbonate (CaCO<sub>3</sub>) is heated in a rotary kiln to induce a series of complex

chemical reactions (IPCC Guidelines). During calcination, CO<sub>2</sub> is released as a by-product occurred in the upper, cooler end of the kiln, or a precalciner, at temperatures of 600-900°C, and results in the conversion of carbonates to oxides. The simplified stoichiometric reaction is as follows:



In the lower end of the kiln, lime (CaO) reacts with silica, aluminum and iron containing materials to produce minerals in the clinker, an intermediate product of cement manufacture, at higher temperature. The clinker is then separated from the kiln to cool, ground to a fine powder, and blended with a small fraction (about 5%) of gypsum in order to produce the most common form of cement known as Portland cement.

## **2.8 Fly Ash and Slag as Supplementary Cementitious Materials (SCMs)**

GGBFS is a dried and finely ground by-product of the blast-furnace iron-making process while fly ash is the fine ash residue collected from the waste of power generating plants. These products both develop cementitious properties when they are activated by the reaction between the cement and water mix. The compounds formed by these reactions not only bind the concrete together, but also help block the pores in the concrete. This improves durability, making it more resistant to chemical attack. Either material can be used as a cement replacement and whether slag and/or fly ash is used depends mainly on the application and local availability. Higher addition rates of either slag or fly ash usually increase initial setting times and reduce very early strength development when compared with straight cement mixes BGC Cement (2017).

Fly ash appears to compensate for some of the workability issues often associated with the use of increased levels of silica fume, whereas the silica fume appears to compensate for the relatively low early strength of fly ash concrete. Advantages of using partial replacement for Portland cement with either fly ash or silica fume in concrete are fairly well established. However, both materials have certain shortfalls and neither could be described as a universal remedy for all concrete problems. Silica fume, while imparting significant contributions to concrete strength and chemical resistance, can create excessive



increases in water demand, extreme maintenance difficulties, and plastic shrinkage problems in concrete if not properly used and can present handling difficulties in the raw state. These factors combined with the increased cost of silica fume evaluated with Portland cement and other pozzolans or slag have been barriers to its wider use in routine “day-to-day” concreting jobs. These are the probable lacking associated with the use of fly ash in concrete.

### **2.8.1 Fly Ash**

Pozzolana from power plant residue such as fly ash are receiving more attention these days. Their uses generally improve the properties of the blended cement concrete, the cost and the reduction of negative environmental effects (Chindaprasirt and Rukzon, 2008). Fly ash improves the properties of concrete or cement paste due to the pozzolanic reaction and its role as a micro-filler. The main implications of the partial replacement of cement by fly ash in cement paste and mortar are micro-structure improvement, pore filling effect and better packing characteristics of the mix. The workability of the blended cement paste and mortar is greatly modified due to the incorporation of finer pozzolana materials such as fly ash, silica fume, etc. This addition depends both on the quality of fly ash and the specific requirements of strength and durability (Kondraivendhan and Bhattacharjee, 2015). When fly ash is added to concrete, the amount of Portland cement is be reduced (Fly ash Facts, 2017).

The hydration products of fly ash reduce the pore size, in this way more durable concrete are obtained (Kocak and Nas, 2014). By the utilization of fly ash, it is not only minimizing the carbon foot print but also sustainable development can be achieved (Wang and Shuang, 2011; Imbabi et al., 2012). It is also observed that the degree of hydration of paste and mortar has been improved by better particle size distribution and finer particle sizes of fly ash (Zhao et al., 2015). If the employed fly ash is finer than the cement, the water demand increases with an increase in fly ash replacement level due to the augmentation of surface area of fly ash particles (Felekoglu et al., 2009).

### **2.8.1.1 Benefits of Fly Ash to Fresh Concrete**

Generally, fly ash benefits fresh concrete by reducing the mixing water requirement and improving the paste flow behavior. The resulting benefits are as follows:

- **Improved workability:** The spherical shaped particles of fly ash act as miniature ball bearings within the concrete mix, thus providing a lubricant effect. This same effect also improves concrete pumpability by reducing frictional losses during the pumping process and work finishability.
- **Decreased water demand:** The replacement of cement by fly ash reduces the water demand for a given slump. When fly ash is used at about 20 percent of the total cementitious, water demand is reduced by approximately 10 percent. Higher fly ash contents will yield higher water reductions. The decreased water demand has little or no effect on drying shrinkage/cracking. Some fly ash is known to reduce drying shrinkage in certain situations.
- **Reduced heat of hydration:** Replacing cement with the same amount of fly ash can reduce the heat of hydration of concrete. This reduction in the heat of hydration does not sacrifice long-term strength gain or durability. The reduced heat of hydration lessens heat rise problems in mass concrete placements.
- **Reduced permeability:** The decrease in water content combined with the production of additional cementitious compounds reduces the pore interconnectivity of concrete, thus decreasing permeability. The reduced permeability results in improved long-term durability and resistance to various forms of deterioration.
- **Improved durability:** The decrease in free lime and the resulting increase in cementitious compounds, combined with the reduction in permeability enhance concrete durability.
- **Sulfate resistance:** Fly ash reacts with available alkali in the concrete, which makes them less available to react with certain silica minerals contained in the aggregates. Fly ash consumes the free lime making it unavailable to react with sulfate. The reduced permeability prevents sulfate penetration into the concrete. Replacement of cement reduces the amount of reactive aluminates available.

- Corrosion resistance: The reduction in permeability increases the resistance to corrosion for fly ash.

### **2.8.2 Slag**

Ground granulated slag is often used in concrete in combination with Portland cement as part of a blended cement. Ground granulated slag reacts with water to produce cementitious properties. Concrete containing ground granulated slag develops strength over a longer period, leading to reduced permeability and better durability. Since the unit volume of Portland cement is reduced, this concrete is less vulnerable to alkali-silica and sulfate attack (Kondraivendhan and Bhattacharjee, 2015). The physical properties of GGBS vary significantly from source to source and region to region as there is no standardized manufacturing process. Hence, its effects on the properties of concrete in fresh and hardened form also change significantly. The curing process also affects the properties of concrete made from ordinary or blended cement incorporating GGBS.

Concrete made with slag cement has higher long-term compressive and flexure strengths compared to Portland cement concrete and it varies for different curing conditions, mix proportions and age of testing. When Portland cement reacts with water, it forms calcium silicate hydrate (C-S-H) and calcium hydroxide  $\text{Ca(OH)}_2$ . C-S-H is a glue that provides strength to the concrete and holds it, while  $\text{Ca(OH)}_2$  is a by-product and does not contribute to the strength of concrete. When slag is used as part of the cementitious constituent in concrete, it reacts with water and  $\text{Ca(OH)}_2$  to form more C-S-H gel and increases the strength (SCA, 2003).

From a structural point of view, GGBS replacement reduces heat of hydration, enhances durability, including higher resistance to sulfate and chloride attack, when compared with normal concrete. On the other hand, it also contributes to environmental protection because it minimizes the use of cement during the production of concrete (Chu, 2007).

### **2.8.2.1 Binary Cement in Concrete Manufacturing Using GGBS**

GGBS is a cementitious material used in concrete. It is a by-product formulated during the manufacture of iron in the blast furnace. GGBS is economically available in large quantities but it requires huge storage facilities. Therefore, it is suitable for various uses in ready-mix concrete, in the production of large quantities of site batched concrete and in precast product manufacturing. Blast furnaces are fed carefully with controlled mixtures of iron-ore, coke and limestone, at a temperature of about 2000°C and then the iron ore is reduced to iron and sinks to the bottom of the furnace. The remaining material that floats on top is the slag and the slag is hurriedly quenched in large volumes of water. This procedure of quenching optimizes the cementitious properties and produces granules like coarse sand particles. After drying the granulated slag, it is ground to a fine powder that is called GGBS, off-white in color having a bulk density of 1200 kg/m<sup>3</sup>. According to Soutsos (2004), at elevated temperature, the early age strength of concrete made with GGBS for equal 28 day compressive strength can be greater than that made with Portland cement only.

Chu (2007) concluded that from a structural point of view, GGBS replacement reduces mainly heat of hydration but enhances durability, including higher resistance to sulfate and chloride attack, when it is compared with normal concrete. On the other hand, it also contributes to environmental protection as it minimizes the use of cement during the production of concrete. Hooton (2000) found that the use of GGBS in concrete enhances durability significantly, if properly proportioned and cured. Further it is effective in improving the resistance to reaction like chloride, sulfate and alkali-silica. Moreover, GGBS concrete minimizes the diffusion of chloride and oxygen and the time to depassivate the steel is increased. Based on the data developed by Hooton (2000), to obtain equivalent performance to a sulfate resisting Portland cement, typically 50% replacement level or less was considered adequate. He also proposed longer curing period for concrete containing GGBS. When slag concrete is placed at lower temperature than 15°C, it should be protected against extreme loss of moisture after initial screening and prior to final finishing and application of curing.

Substitution of GGBS gives lesser heat of hydration, improved durability as well as resistance to sulfate and chloride attack when compared with normal concrete. On the other hand, it also contributes to environmental protection since it ensures the minimization of the use of cement during the production of concrete. A combination of slag cement helps Concrete to have a higher compressive and flexure strength compared to the PC concrete (Samad and Shah, 2017). All these valuable effects of GGBS concrete depends on concrete mix proportions and curing conditions but a maximum replacement level of 50% is recommended for GGBS and the curing temperature of at least 20°C is beneficial. Test has been shown that the slump of the GGBS concrete is unaltered in comparison with PC concrete and is much easier to compact.

The performance of concrete, in terms of its place ability, physical properties, and its durability, can be enhanced by the use of slag-blended cements or separately added ground granulated blast-furnace slag and also has advantages for architectural purposes due to the whiteness it imparts to concrete. Properly proportioned, maintained and cured slag concretes will help to control deleterious alkali–silica reactions, impart sulfate resistance, greatly reduce chloride ingress, and reduce heat of hydration. Other properties like setting times and early age strengths can be controlled through suitable proportioning, while later age properties are typically enhanced (Hooton, 2000).

## **2.9 Setting Time of Fly Ash and Slag Cement**

The initial setting time of the concrete refers to the beginning of hardening of the mixture and the final setting time refers to the sufficient hardness of the concrete mixture (Naik et al., 2001). Studies have reported that with increase in fly ash content within the binder, setting time also increases (Brooks et al., 2000; Carette and Malhotra, 1984). A study shows (Mailvaganam et al., 1983) that setting time of ternary blended concrete made of FA and GGBS shows delayed initial setting time in the range of 60–120 min.

Silica fume is the byproduct of silicon industry and it is a pozzolanic material, which is used to improve the fresh and hardened properties of concrete (Federation internationale de la Precontrainte, 1988; Yazici, 2007). Much research has been conducted on ternary

binder using a combination with FA and SF (Demirboga, 2007; Yazici et al., 2008). A study also (Snelson, 2011) investigated the utilization of fly ash/or ground granulated blast furnace slag (GGBS) with silica fume. Using the GGBS in binder, the setting time can be slightly extended. An extended setting time is an advantage, as it makes concrete remain workable for a longer period of time, therefore resulting in fewer joints and it is extremely useful in warm weather.

## **2.10 Role of Supplementary Cementitious Materials (SCMs) in Production of Environmentally Sustainable Concrete**

In the manufacture of Portland cement, a huge amount of CO<sub>2</sub> is produced which is a great threat for environment. In order to diminish the embodied CO<sub>2</sub> of concrete, Portland cement can be partially replaced with Supplementary Cementitious Materials (SCMs) such as Ground Granulated Blast furnace Slag (GGBS) and Fly Ash (FA). The SCMs have been used widely over the last few decades in the production of concrete as its use offsets the cost of concrete production and reducing the construction cost. Though more vital consideration in the use of SCM, is sustainability dimension of concrete, as with the increasing use of SCM, considerable volume of CO<sub>2</sub> emission are expected to be reduced, thereby mitigating the environmental impact of concrete production. Recent studies show that the average worldwide consumption of concrete is about one ton per year for every living human-being (Samad and Shah, 2017) and due to this extensive use, concrete has a comparatively large environmental footprint. Worldwide, the cement industry accounts for approximately 5% of man-made CO<sub>2</sub> emissions and approximately 40% of this is from burning coal and 60% from the calcination of limestone. (Sustainable Concrete, 2011). The emissions of CO<sub>2</sub> per ton of concrete production for rolling concrete mixes have increased by 7% in 2010 in contrast to 2009 but are lower than the 1990 baseline.

The pozzolanic reactions are slower than the hydration reactions and they start after about five days. So the early age strength of FA concrete is slower than the PC concrete. Fly ash has been used for many years to have improved sulfate resistance, reduction in chloride diffusion, prevention of alkali silica reaction. Fly ash, a cementitious binder, is used to

lower the greenhouse gas emissions, heat generation, enhance durability and extend structure life. In UK, the mix of Fly Ash in concrete manufacture per annum saves about 250,000 tons of CO<sub>2</sub> to the environment (Samad and Shah, 2017). The SCM would continue to be used to minimize the cement use in the production of concrete, with more research on standardizing its requirement, mix design method at global level.

### **2.11 Effect of SCMs on Microstructure and Porosity**

The premature rate of hydration of slag is usually slower than that of Portland cement apart at higher curing temperatures or through very finely ground slag. Basically, the calcium silicate glass in the slag turns into soluble in the alkaline pore solutions provided by the initial reactions of the Portland cement and reacts to form secondary growths of calcium silicate hydrates (C–S–H). In general terms, these calcium silicate hydrates are equivalent to those from the Portland cement, but the ratio of calcium to silica must be inferior, which permits this secondary C–S–H to tie up far more alkalis ( Na<sup>+</sup> and K<sup>+</sup> ) into its crystal structure (this is of important benefit for the control of alkali–aggregate reactions) (Hooton, 2000). As well, more Al<sub>2</sub>O<sub>3</sub> may be incorporated in the C–S–H to have solution for corrosion problem. The MgO is frequently included into a hydrotalcite-like phase. As well, the slag grains can accelerate speed of the hydration of Portland cement by proceeding as nucleation sites for C–S–H to precipitate out of solution and grow onto (Hooton, 2000).

In cement pastes, both the water to cementitious materials ratio (W/CM) (in concrete, it is the water content of the mix) and the degree of hydration govern the volume and connectivity of the capillary pore space. The formation of secondary C–S–H initiates as soon as the slag starts to be dissolved in the alkaline pore solutions, which fills in source of the capillary pore space left by the prior hydration of the Portland cement fraction. The implication is that hydration of the slag can interrupt or make capillary pores discontinuous by providing secondary discrete blockages of C–S–H across pores and additionally, slag has an important role in increasing the bond and decreasing porosity (Hooton, 2000).

## **2.12 Resistance to Sulfate Attack by Slag and Fly Ash**

Slag will dilute the vulnerable  $C_3A$  content of the cement to some extent (not a big issue with silica fume) in addition to reduced penetration of sulfate ions. As well, the  $Ca(OH)_2$  content of the paste will be reduced. Consequently, this will not be available to form gypsum on ettringite crystals (Hooton, 2000). As the amount of  $Al_2O_3$  content of slag rises, it requires to replace the slag to impart sulfate resistance rises as well.

Dunstan first documented that the reduced efficacy of high CaO fly ashes in controlling sulfate attack (1980) and later others (Von Fay and Pierce, 1989 and Tikalsky and Carrasquillo, 1992). The reduced sulfate resistance of mortars or concretes which contains high calcium fly ash has been ascribed to reaction of sulfates with  $C_3A$  or calcium-aluminate glass in the fly ash, or with calcium-aluminate hydrates (e.g., gehlenite). This calcium-aluminate hydrate is produced by hydration of the fly ash (Dunstan, 1980 and Tikalsky and Carrasquillo, 1992). An alternative mechanism put forward by Mehta suggests that it is the ratio of alumina, a reactive ingredient, to sulfate in the cement-fly ash blend that establishes its resistance to sulfate (Mehta, 1986). If this ratio is high, the formation of mono sulfate and calcium-aluminate hydrates is preferential and, on subsequent immersion in sulfate solution, these phases will be converted to ettringite, which results deleterious expansion.

## **2.13 Reducing Chloride Corrosion of Reinforcement**

As diffusion rates of both chlorides and oxygen (required since corrosion products are oxides) are reduced so that the time to depassivation is extended (provided that there is adequate depth of cover and the concrete has been properly maintained, designed, compacted, and cured), it is one of the most beneficial side of slag. Moreover, the slag facilitates to reduce the hydroxyl ion content remained the pore solution and includes higher level of alkalies ( $Na^+$  and  $K^+$ ) into its C-S-H matrix than does Portland cement (Hooton, 2000). Laboratory tests have completely demonstrated that high-volume fly ash concrete can provide a tremendous protection to the reinforcing steel against corrosion (Gu et al. 1998).



## **2.14 Concluding Remarks**

The literature review indicates that the aggressive tannery wastewater constituents have significant detrimental effect on concrete. In contact with tannery wastewater, concrete structure deteriorates. The extent to which damage will happen in different conditions is yet to be examined comprehensively. Supplementary materials like fly ash and slag apt to provide higher strength and sustainability as well as boons for environmental impact.

## **Chapter 3**

### **MATERIALS AND METHODS**

#### **3.1 Introduction**

In this chapter, the methodology employed in carrying out the tests has been discussed. The procedure for synthetic tannery wastewater simulation has been outlined. The materials used, the preparation of test specimens, the tests conducted, the experimental setup, are all discussed in details.

#### **3.2 Simulation of Tannery Wastewater in Laboratory**

Tannery wastewater was simulated in laboratory following recipe and procedures of previous study (Saha and Papry, 2016) where sample was collected from Hazaribagh, Dhaka and its composition revealed the type and amount of typical constituents present in it. The next step was to prepare water sample in the laboratory using information from the chemical analysis so that critical components of collected tannery wastewater samples be present in the simulated water.

##### **3.2.1 Synthetic Simulation of Tannery Waste Water**

The dominant constituents of tannery wastewater that can make concrete susceptible to degradation were identified (Manzur et al. 2018). Total concentration of these anions and cation in tannery wastewater was determined from laboratory testing (Saha and Papry, 2016).

##### **3.2.2 Preparation of Stock Solution**

Previous study revealed that, sodium ( $\text{Na}^+$ ) and nitrate ( $\text{NO}_3^-$ ) ions do not have any detrimental effects on cement concrete (Saha and Papry, 2016). Hence, use of these two

ions to achieve charge balance in the synthetic solution allowed to investigate the effect of other aggressive constituents of tannery wastewater on degradation of cement concrete. Sodium salts of the anions and Ammonium Acetate ( $C_2H_7NO_2$ ) salt were added in distilled water and stirred until the salts were completely dissolved. The amount of salts (gm) added and the volume of stock solution (L) were fixed to achieve the level of concentration as shown in the Table 3.1 below:

Table 3.1: Concentration of the prepared stock solutions

Stock solution	Concentration (mg/L)
NaCl	100,000
NaNO <sub>3</sub>	10,000
Na <sub>2</sub> CO <sub>3</sub>	100
NaHCO <sub>3</sub>	100,000
Na <sub>2</sub> SO <sub>4</sub>	100,000
C <sub>2</sub> H <sub>7</sub> NO <sub>2</sub>	100,000

### 3.2.3 Preparation of Synthetic Solution using MINEQL+ Software

For preparation of 11.31 litres of simulated wastewater, the prepared stock solutions were mixed at a certain mixing ratio (provided in Table 3.2) that was determined on the basis of the water quality of tannery wastewater obtained from MINEQL+ equilibrium water quality modelling software (Schecher and McAvoy, 2001).

Table 3.2 Volume (ml) of different stock solutions to be added for preparation of synthetic tannery wastewater

Sodium Chloride (NaCl)	182.46
Sodium Nitrate (NaNO <sub>3</sub> )	169.52
Sodium Carbonate (Na <sub>2</sub> CO <sub>3</sub> )	62.0165
Sodium Bicarbonate (NaHCO <sub>3</sub> )	1.885
Sodium Sulphate (Na <sub>2</sub> SO <sub>4</sub> )	188.5
Ammonium Acetate (C <sub>2</sub> H <sub>7</sub> NO <sub>2</sub> )	787

From laboratory analysis, pH of the sample tannery wastewater was found to be around 5. The pH of the synthetic solutions could be adjusted by using either nitric acid (HNO<sub>3</sub>) or sodium hydroxide (NaOH). However, while preparing the solutions, pH was found to be greater than 5. Therefore, to keep pH stable at around 5, nitric acid was added to the solution regularly.

### 3.3 Cement Mix Combinations

Several trial mixes have been used with partial substitution of cement with fly ash and slag to achieve the desired blended cement combination to be used as high strength concrete for

structural uses. The addition of the supplementary cementitious materials (SCMs) reduce the cement proportion in concrete, thereby making it relatively sustainable. Total 8 (Eight) types of combinations (provided in Table 3.3) of variation in proportion of Portland Cement (OPC CEM I), Fly Ash and Ground-granulated blast-furnace slag (GGBS) were chosen for this study.

Table 3.3: Cement mix proportions and combinations

<b>Designation</b>	<b>OPC</b>	<b>Fly Ash</b>	<b>Slag</b>
<b>C1</b>	100%	-	-
<b>C2</b>	70%	30%	-
<b>C3</b>	60%	40%	-
<b>C4</b>	70%	-	30%
<b>C5</b>	60%	-	40%
<b>C6</b>	60%	20%	20%
<b>C7</b>	60%	30%	10%
<b>C8</b>	70%	20%	10%

### **3.4 Flow Table Test**

Flow table test was carried out according to ASTM C 1437 (2007) “Standard Test Method for Flow of Hydraulic Cement Mortar” and C 230 (2014).

### **3.4.1 Preparation of Mortar Bars for Flow Table Test**

Mortars were prepared as described in ASTM C 109 (2013), that is, 1 part of cement to 2.75 parts of sand by mass. A water-cement ratio by mass of 0.485 was used.

### **3.4.2 Materials**

- i) Ordinary Portland Cement, OPC (CEM I/ 52.5 N)
- ii) Class F Fly Ash
- iii) Ground-granulated blast-furnace slag (GGBS)
- iv) Graded Standard Sand, as specified in ASTM C 778 (2013)

### **3.4.3 Apparatus**

- i) Flow Table and Flow Mold
- ii) Caliper
- iii) Mixer, Bowl and Paddle; an electrically driven mechanical mixer of the type equipped with paddle and mixing bowl
- iv) Tamper
- v) Trowel having a steel blade 4 to 6 in. [100 to 150 mm] in length, with straight edges
- vi) Straightedge, made of steel, at least 200 mm (8 in.) long and not less than 1.5 mm (0.06 in.) nor more than 3.5 mm (0.14 in.) in thickness. Its edge should not depart from a plane surface by more than 1 mm (0.04-in.)

### **3.4.4 Temperature, Humidity**

The temperature of the molding room and dry materials was maintained between  $23.0 \pm 4.0^\circ\text{C}$ . The relative humidity was maintained to be not less than 50%. The temperature of the mixing water was within the range  $23.0 \pm 2.0^\circ\text{C}$ .

### 3.4.5 Experimental Procedure

The flow table was carefully wiped clean and dry, and the flow mold was placed at the center. A layer of mortar about 25mm (1 in.) in thickness was placed in the mold and 20 times tamped with the tamper. Then the mold was filled with mortar and second layer was tamped. The mortar was cut off to a plane surface flush with the top of the mold by drawing the straightedge or the edge of the trowel with a sawing motion across the top of the mold. Then the mold was lifted away from the mortar just 1min after completing the mixing operation. The table was immediately dropped 25 times in 15s.

### 3.4.6 Measurements of Flow Diameter

The diameter of the mortar was measured along the four lines scribed in the table top, recording each diameter as the number of caliper divisions, estimated to one tenth of a division.



Figure 3.1: Flow table test

### **3.4.7 Calculation**

The flow is the resulting increase in average base diameter of the mortar mass, expressed as a percentage of the original base diameter.

$$Flow = \frac{A}{D} \times 100\%$$

where:

D= The original inside base diameter (D) in millimetres

A = Average of four deformed mortar mass diameter readings in millimetres, minus the original inside base diameter (D) in millimetres.

The flow values for each cement mix combinations was calculated to the nearest 1%.

### **3.5 Normal Consistency Test**

Normal Consistency test was carried out according to ASTM C 187 (1998) “Standard Test Method for Normal Consistency of Hydraulic Cement”. This test method is intended to be used to determine the amount of water required to prepare hydraulic cement pastes for testing.

#### **3.5.1 Preparation of Cement Paste for Normal Consistency Test**

Cement pastes were prepared as described in Test Method ASTM C 305 (2014), that is, 650g of cement with a measured quantity of water.

#### **3.5.2 Materials**

- i) Ordinary Portland Cement, OPC (CEM I/ 52.5 N)
- ii) Class F Fly Ash
- iii) Ground-granulated blast-furnace slag (GGBS)



### 3.5.3 Apparatus

- i) Weighing Device
- ii) Glass Graduates
- iii) Vicat Apparatus
- iv) Tamper
- v) Trowel having a steel blade 4 to 6 in. [100 to 150 mm] in length, with straight edges
- vi) Straightedge, made of steel, at least 200 mm (8 in.) long and not less than 1.5 mm (0.06 in.) nor more than 3.5 mm (0.14 in.) in thickness. Its edge should not depart from a plane surface by more than 1 mm (0.04-in.)

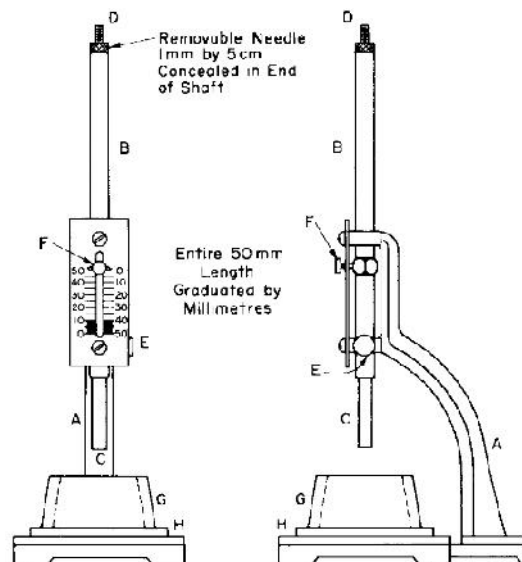


Figure 3.2: Schematic diagram of Vicat apparatus (ASTM C191-13)



Figure 3.3: Vicat apparatus to determine normal consistency of cement

#### **3.5.4 Temperature, Humidity**

The temperature of the air in the vicinity of the mixing slab, the dry cement, molds, and base plates was maintained between 20.0 and 27.5°C (68 and 81.5°F). The temperature of the mixing water did not vary from 23.0°C (73.5°F) by more than  $\pm 2.0^\circ\text{C}$  (3.5°F). The relative humidity of the laboratory shall be not less than 50%.

#### **3.5.5 Experimental Procedure**

The cement paste was quickly formed, into the approximate shape of a ball with gloved hands. Then it was tossed six times through a free path of about 150 mm (6 in.) from one hand to another and inserted into the Vicat ring. The ball was pressed, resting in the palm of one hand, into the larger end of the conical ring, held in the other hand, completely filling

the ring with paste. The ring was placed on its larger end on the base plate and the excess paste at the smaller end at the top of the ring was sliced off by a single oblique stroke of a sharp-edged trowel held at a slight angle with the top of the ring, and the top was smoothed with a few light touches of the pointed end of the trowel.

### **3.5.6 Determination of Consistency**

The paste was centered and confined in the ring, resting on the plate, under the rod. The plunger end of rod was brought in contact with the surface of the paste, and the set-screw was tightened. Then the movable indicator was set to the upper zero mark of the scale, and the rod was released immediately not exceeding 30 s after completion of mixing. The apparatus was free of all vibrations during the test. The paste was of normal consistency when the rod settled to a point  $10 \pm 1$  mm below the original surface in 30 s after being released. Trial pastes were made with varying percentages of water until the normal consistency was obtained. Each trial was made with fresh cement mix.

### **3.5.7 Calculation**

The amount of water required for normal consistency was calculated to the nearest 0.1 % and reported to the nearest 0.5 % of the weight of the dry cement.

## **3.6 Setting Time Test**

Cement, when mixed with water, forms slurry, which gradually becomes less plastic with the passage of time and finally a hard mass is obtained. In this process, a state is reached when the cement paste is sufficiently rigid to withstand a definite amount of pressure. Cement, at this stage to have set and the time required to reach this stage is termed “setting time”.

The term “initial setting time” indicates the beginning of the setting process of cement paste when cement paste starts losing its plasticity. The “final setting time” is the time

elapsed between the moment the water is added to cement and the time when the paste completely lost its plasticity and attained sufficient stability to resist certain definite pressure. This test method conforms to the ASTM standard requirements of specification ASTM C 191 (2013).

### **3.6.1 Preparation of Cement Paste for Setting Time Test**

A paste that was proportioned and mixed to normal consistency, as described in ASTM C187 (1998), was molded and placed in a moist cabinet and allowed to start setting. Periodic penetration tests are performed on this paste by allowing a 1-mm Vicat needle (Figure 3.4) to settle into this paste. The Vicat initial time of setting was calculated as the time elapsed between the initial contact of cement and water and the time when the penetration was at 25 mm. The Vicat final time of setting was calculated as the time when the needle did not sink visibly into the paste.

### **3.6.2 Materials**

- i) Ordinary Portland Cement, OPC (CEM I/ 52.5 N)
- ii) Class F Fly Ash
- iii) Ground-granulated blast-furnace slag (GGBS)

### **3.6.3 Apparatus**

- i) Vicat Apparatus
- ii) Glass Graduates
- iii) Plane non-adsorptive plate,  $100 \pm 5$  mm square of similar planeness, corrosivity, and absorptivity to that of glass
- iv) Mixer, bowl, and paddle
- v) Flat trowel, having a sharpened straight-edged steel blade 100 to 150 mm in length

- vi) Conical ring, made of a rigid non-corroding, non-absorbent material and should have a height  $40 \pm 1$  mm, an inside diameter at the bottom of  $70 \pm 3$  mm, and an inside diameter at the top of  $60 \pm 3$  mm

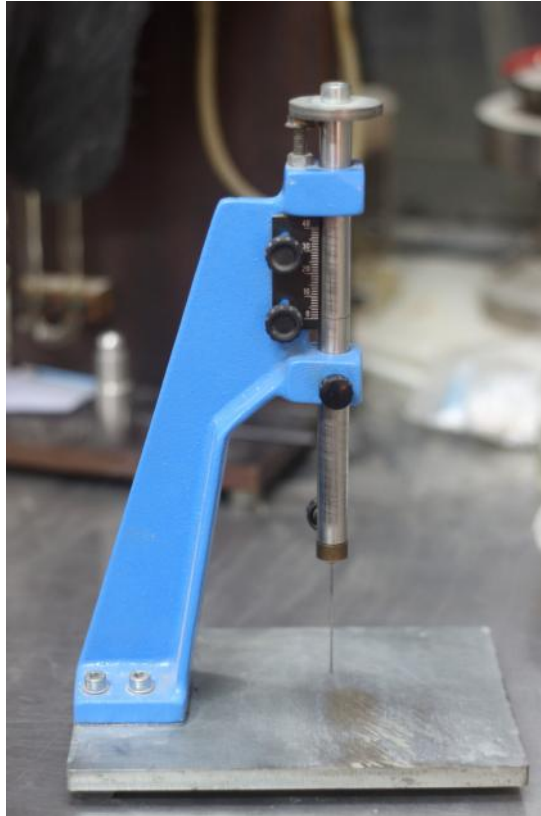


Figure 3.4: Vicat apparatus to determine setting time of cement

### **3.6.4 Temperature, Humidity**

The temperature of the air in the vicinity of the mixing slab, the dry cement, molds, and base plates was maintained at  $23.0 \pm 3.0^{\circ}\text{C}$ . The temperature of the mixing water was maintained at  $23.0 \pm 3.0^{\circ}\text{C}$ . The relative humidity of the mixing room were higher than 50 percent.

### 3.6.5 Molding Test Specimen

The cement paste was quickly formed, into the approximate shape of a ball with gloved hands. Then it was tossed six times through a free path of about 150 mm (6 in.) from one hand to another. The ball was pressed, resting in the palm of one hand, into the larger end of the conical ring, held in the other hand, completely filling the ring with paste. The ring was placed on its larger end onto a non-absorptive plate and the excess paste at the smaller end of the ring was sliced off by a single oblique stroke of a sharp-edged trowel held at a slight angle with the top of the ring, and the top was smoothed with a few light touches of the pointed end of the trowel (Figure 3.5).



Figure 3.5: Setting time test molds

### 3.6.6 Time of Initial Setting Determination

The penetration of the 1-mm needle after every 15 minutes until a penetration of 25 mm or less was obtained is recorded. The penetration test was performed by lowering the needle of the rod until it rests on the surface of the cement paste. The set screw, E was tightened and the indicator was set at the upper end of the scale. The rod was released quickly by releasing the set screw and the needle was allowed to settle for 30 seconds. Then the reading to determine the penetration was taken. Each penetration was made at least 5 mm away from any previous penetration and at least 10 mm away from the inner side of the mold. The time when a penetration of 25 mm was obtained, was recorded. The elapsed

time between the initial contact of cement and water and the penetration of 25 mm was the Vicat initial time of setting.

### **3.6.7 Time of Final Setting Determination**

The Vicat final time of setting was the first penetration measure that did not mark the specimen surface with a complete circular impression. Final set was verified by performing two additional penetration measurements on different areas of the specimen surface within 90s of the first “final set” measurement. The elapsed time between the initial contact of cement and water and the end point determination above was the Vicat final time of setting.

### **3.6.8 Calculation**

The time required for 25mm penetration was recorded as the initial setting time.

The final time of setting was recorded as the elapsed time between the time of the initial contact between cement and water and the time when the needle did not sink visibly into the paste, rounded to the nearest five minutes.

## **3.7 Compressive Strength Test**

This test was conducted in accordance with ASTM C109, ‘The Standard Test Method for Compressive Strength of Hydraulic Cement Mortars Using 2-in. or [50-mm] Cube Specimens’.

### **3.7.1 Apparatus**

- i) Weighing Device
- ii) Glass Graduates of suitable capacities
- iii) Specimen Molds for the 2-in. or [50-mm] cube specimens

- iv) Mixer, Bowl and Paddle; an electrically driven mechanical mixer of the type equipped with paddle and mixing bowl
- v) Tamper
- vi) Trowel having a steel blade 4 to 6 in. [100 to 150 mm] in length, with straight edges.
- vii) Compression Testing Machine

### 3.7.2 Materials

- i) Ordinary Portland Cement, OPC (CEM I/ 52.5 N)
- ii) Class F Fly Ash
- iii) Ground-granulated blast-furnace slag (GGBS)
- iv) Graded Standard Sand: natural silica sand conforming to the requirements for graded standard sand in ASTM Specification C 778 (2013)

### 3.7.3 Preparation of Cement Mortar Cubes

The cement mortar cube specimens were prepared as per ASTM C 109 (2013). The mortar used consisted of 1 part cement and 2.75 parts of sand proportioned by mass. Two-inch test cubes were compacted by tamping in two layers. The cubes were cured one day in the molds and stripped and immersed in lime water until tested.



Figure 3.6: Sand, Cement, Water



Figure 3.7: Electronic weighing machine

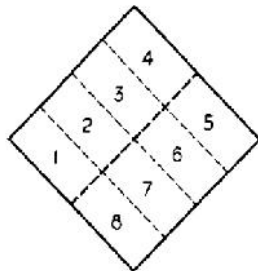




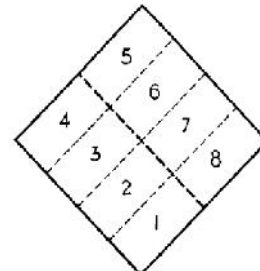
Figure 3.8: Mixer machine with bowl and paddle

### 3.7.4 Hand Tamping

The molding of the specimens was started within a total elapsed time of not more than 2min and 30s after completion of the original mixing of the mortar batch. A layer of mortar about 1in. or [25mm] (approximately one half of the depth of the mold) was placed in all of the cube compartments. The mortar in each cube compartment was tamped 32 times in about 10s in 4 rounds. The 4 rounds of tamping (32 strokes) of the mortar was completed in one cube (as per Figure 3.9) before going to the next. Each round should be at right angles to the other and consist of eight adjacent strokes over the surface of the specimen.



Rounds 1 and 3



Rounds 2 and 4

Figure 3.9: Order of tamping in molding of mortar cubes



Figure 3.10: Mortar in molds after casting

### 3.7.5 Storage of Test Specimens

Immediately upon completion of molding, the test specimens were kept covered with damp cloth for 24 hours. After 24 hours, the specimens were removed from the molds and submerged in saturated lime water for 28 days in storage tanks constructed of non-corroding materials (Figure 3.11). The storage water was kept clean by changing as required.



Figure 3.11: Specimens in limewater

### 3.7.6 Temperature and Humidity

The temperature of the air in the vicinity of the mixing slab, the dry materials, molds, base plates, and mixing bowl, was maintained between  $[23.0\pm 3.0^{\circ}\text{C}]$ . The relative humidity of the laboratory was maintained to be not less than 50%.

### 3.7.7 Experimental Procedure

The cement mortar cubes were taken out of lime water after 28 days and dried in the oven for 3 hours at  $110^{\circ}\text{C}$ . Then, images of an exposed surface were taken for each cube using an image capturing setup and DSLR camera (Manzur et al., 2016). After that, the weight of each cube was measured (initial weight) using a weighing device. Large container was filled with simulated tannery wastewater sample. Next, the cubes were kept in two condition, a) normal air condition and b) submerged in simulated tannery wastewater sample in containers (Figure 3.12). Three cubes for each types of cement mix and conditions were prepared.

Table 3.4: Test matrix for cubes and bars

<b>Day 0 (Initial)</b>	<b>Day 90</b>		<b>Day 180</b>	
Cured in Limewater for 28 days	Kept in Normal Condition	Submerged in Simulated Tannery Wastewater	Kept in Normal Condition	Submerged in Simulated Tannery Wastewater



Figure 3.12: Specimens submerged in simulated tannery wastewater

The 0 day strength and weight values refer to the strength and weight measured after 28 days of curing in lime water. The same process was followed for data collection for each test day. After completion of a designated submergence period, the mortar cubes were removed from the container and dried in the oven for 3-4 hours at 110<sup>0</sup>C. Then pictures of the mortar samples were taken using an image capturing setup and DSLR camera. Then the weight of each of cube was taken following compressive strength test carried out on the cubes. Some of the crushed samples were salvaged for SEM image and EDS analysis.

### 3.7.8 Calculation of Compressive Strength

The total maximum load indicated by the testing machine (Figure 3.13) was recorded, and the compressive strength was calculated as follows:

$$f_m = P/A$$

where:

$f_m$  = Compressive strength in MPa

$P$  = Total maximum calibrated load in [N], and

$A$  = Area of loaded surface [mm<sup>2</sup>]

The compressive strength of all acceptable test specimens made from the same sample and tested at the same period were averaged and reported to the nearest 0.1 MPa. For a particular test condition, the load which was considered in calculation was the average load of the three corresponding cubes.



Figure 3.13: Cube in compression testing machine

### **3.8 Image Capturing Setup**

The image capturing setup (Figure 3.14) consisted of a black cylindrical object made of nylon. An LED source was fitted to the upper end which emitted LED light when connected to a power supply. The specimen was placed inside the cylinder such that it was at the bottom end of the cylinder. Image was captured from the light source end. The position of camera was fixed and a fixed focal length lens was used to maintain the same distance for every cube surface. Images were taken to compare the conditions of cube before and after submergence in tannery wastewater for different testing days.



Figure 3.14: Image capturing setup

### 3.9 Scanning Electron Microscope (SEM)

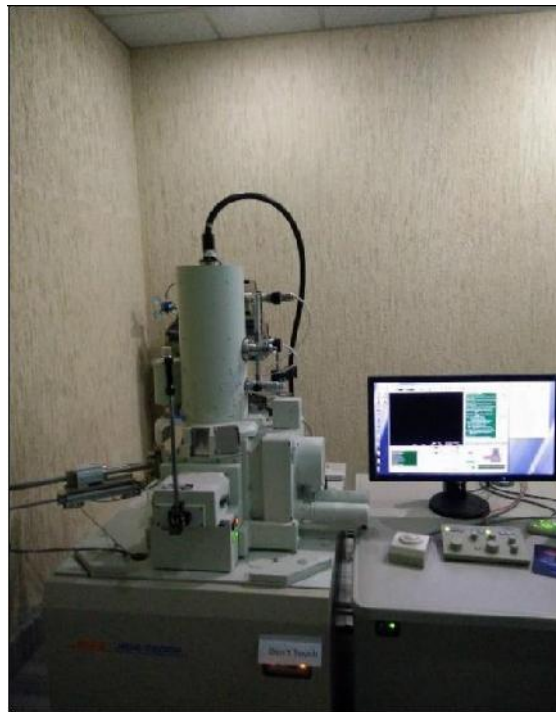


Figure 3.15: Scanning Electron Microscope (SEM)

Scanning electron microscope (SEM) was used to examine the microstructure of the mortar cubes. The mortar cubes were broken and fragments having approximately 10mm height and 12mm diagonal length were selected as samples for imaging. As the setup involves vacuum condition and high energy beam of electrons, the samples for SEM were prepared accordingly. A Jeol JSM-7600F Schottky Field Emission Scanning Electron Microscopy (FE-SEM) was used (Figure 3.15). The accelerating voltage was kept at 5.00kV while the working distance was held at 8-10mm at various magnifications (100x, 500x & 1000x).

Application of an ultrathin coating of electrically conducting material is required as cement mortar is non-conductive. Hence, a platinum coating was applied all over the specimen. Sample fragment was placed onto an aluminum stub with silver conductive paint and inserted in the machine.

### **3.11 X-ray Fluorescence (XRF)**

X-ray fluorescence (XRF) was conducted to obtain the composition of oxides in cement, fly ash and slag. It is a powerful quantitative and qualitative analytical tool for elemental analysis of materials. The basic concept for all XRF spectrometers is a source, a sample, and a detection system as shown in Figure 3.16 (X-Ray Fluorescence (XRF), 2017). In most cases for XRF, the source is an X-ray tube. The elements in the sample are excited and characteristic radiation emitted from them diffract into different directions through an analyzing crystal or monochromater. While the sample position is fixed, the angles of the crystal and detector are changed in compliance with Bragg's law so that a particular wavelength can be measured. A detector measures the fluorescence radiation emitted from the sample.

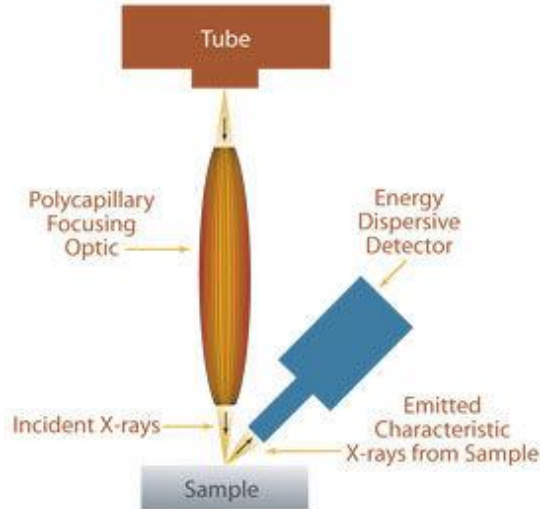


Figure 3.16: Schematic diagram of X-ray fluorescence (XRF)

### 3.11 Energy-dispersive X-ray Spectroscopy (EDS/EDX)

Energy-dispersive X-ray spectroscopy was used for the elemental analysis of mortars. The same instrument for obtaining SEM microphotographs was also employed for EDS.

EDS results were obtained immediately after the SEM photographs were taken. The sample which was placed on the instrument was confronted with electron beam to excite the atoms. X-rays of characteristic wavelength were emitted which were detected by the spectrometer. Identification of the elements was accomplished by matching the X-ray energy peaks obtained with those of known wavelengths for the corresponding elements.

### 3.12 Expansion Test

The expansion test was carried out in accordance with ASTM C 1012 (2004) and C 490 (2011).



### **3.12.1 Preparation of Mortar Bars for Expansion Test**

Mortars were prepared as described in Test Method C 109 (2013), that is, 1 part cement to 2.75 parts of sand by mass.

#### **3.12.1.1 Materials**

- i) Ordinary Portland Cement, OPC (CEM I/ 52.5 N)
- ii) Fly Ash
- iii) Ground-granulated blast-furnace slag (GGBS)
- iv) Graded Standard Sand, as specified in Specification C 778 (2013)

#### **3.12.1.2 Apparatus**

- i) Weighing Device
- ii) Glass Graduates of suitable capacities
- iii) Specimen Molds of size 25 by 25 by 285mm.
- iv) Stainless Steel Gage Studs, as specified in Specification C 490.
- v) Mixer, Bowl and Paddle; an electrically driven mechanical mixer of the type equipped with paddle and mixing bowl
- vi) Tamper
- vii) Trowel having a steel blade 4 to 6 in. [100 to 150 mm] in length, with straight edges.
- viii) Length Comparator

#### **3.12.1.3 Molding the Test Bars**

The test bars were molded in accordance with ASTM C 157 (2008).

#### **3.12.1.4 Preparation of Molds**

The interior surfaces of the mold were covered with grease. After this operation, the gauge studs were set, taking care to keep them clean, and free of oil, grease, and foreign matter.

#### **3.12.1.5 Temperature, Humidity**

The temperature of the molding room and dry materials was maintained between  $23.0 \pm 4^\circ\text{C}$ . The relative humidity was maintained to be not less than 50%. The temperature of the mixing water was within the range  $23 \pm 2.0^\circ\text{C}$ .

#### **3.12.1.6 Experimental Procedure**

After  $23 \pm 1/2$  hours of casting, the test specimens were removed from the molds and submerged in lime water for 28 days. After 28 days they were withdrawn from lime water and the length of each bar (initial length) was measured using length comparator. The test specimens were thereby kept in two condition, a) normal air condition and b) submerged in simulated tannery wastewater sample. Two bars each cement mix types were prepared for each conditions and their changes in length were measured at several time intervals over a period of 26 weeks (6 months).

#### **3.12.1.7 Storage of Test Bars during Exposure to Test Solution**

The container of the bars in simulated tannery wastewater was covered to prevent evaporation from the inside, or dilution with water from the outside.

#### **3.12.1.8 Measurements of Length Change**

At 1, 2, 3, 4, 8, 13, 15, 18 and 26 weeks, after the bars were placed in normal air condition and submerged in simulated tannery wastewater sample, they were tested for length change

using the length comparator (Figure 3.17) in accordance with Specification ASTM C 490 (2011).

The specimens were rotated slowly in the measuring instrument while the comparator reading was being taken. The minimum reading of the dial was taken if the rotation caused a change in the dial reading. The specimens were placed in the instrument with the same end up each time a comparator reading was taken.



Figure 3.17: Length comparator

### 3.12.1.9 Calculation

The length change at any time period was calculated as follows:

$$DL = \frac{Lx - Li}{Lg} \times 100\%$$

where:

DL = Change in length at x age, %,

Lx = Comparator reading of specimen at x age - reference bar comparator reading at x age

$L_i$  = Initial comparator reading of specimen - reference bar comparator reading, at the same time

$L_g$  =N gage length, or 250 mm (10 in.)

The length change values for each bar were calculated to the nearest 0.001% and averages were reported to the nearest 0.01 %.

### **3.13 Concluding Remarks**

This chapter described how tannery wastewater was simulated in the laboratory and mortars were prepared. The description of the experimental setup and data collection procedure was elaborated. Test procedures of determining the basic properties of cement with fly ash and slag proportions such as normal consistency, flowability, initial and final setting time were discussed. Mortars were assessed for their compressive strength, expansion and weight loss to explore the effect of supplementary materials in the mix. The microstructure also shed some light on the behavior of mortars examining their properties by scanning electron microscopy (SEM) imaging and Energy-Dispersive X-ray Spectroscopy (EDS) Analysis data. The next chapter presents the data encountered in the form of graphs and an attempt is made to explain the trends of these data.

## Chapter 4

### RESULTS AND DISCUSSION

#### 4.1 Introduction

In this chapter, results of various tests performed in the study for comparing the effect of different tannery wastewater constituents on mortar cubes and bars prepared from different variation of cement, fly ash and slag combinations are presented. Compressive strength of mortar cubes, expansion of mortar bars and weight loss of mortar cubes under different conditions are discussed in details. Images taken of the cubes surface after submergence in simulated tannery wastewater are presented and compared with the control samples. Finally, SEM images and EDS analysis are shown and results are co-related with findings. The obtained results are presented in the form of graphs, images and tables.

#### 4.2 Cube Designations Representing Different Cement Mix Combinations

Table 4.1 shows the designation of eight different types of mix proportions used to prepare mortar cubes along with their replacement proportions.

Table 4.1: Cement mix proportions and combinations

<b>Designation</b>	<b>OPC</b>	<b>Fly Ash</b>	<b>Slag</b>
<b>C1</b>	100%	-	-
<b>C2</b>	70%	30%	-
<b>C3</b>	60%	40%	-
<b>C4</b>	70%	-	30%
<b>C5</b>	60%	-	40%
<b>C6</b>	60%	20%	20%
<b>C7</b>	60%	30%	10%
<b>C8</b>	70%	20%	10%

### 4.3 X-ray Fluorescence (XRF) Analysis

Composition of cement, fly ash and slag used in the study were determined (Table 4.2) by XRF analysis which was conducted in Department of Glass & Ceramic Engineering, BUET. X-ray fluorescence (XRF) analysis gives relative amount of elements in the cement which is converted to the weight fraction of each element in oxide form. The fundamental parameter (FP) method, which uses the calculated theoretical intensities and the measured intensities to determine the composition of a sample, was used in this study to perform quantitative analysis of OPC, fly ash and slag samples.

Table 4.2: Mass % of different elements in OPC, Fly Ash and Slag

Analyte	OPC	Fly Ash	Slag
CaO	66.22%	1.35%	49.16%
SiO <sub>2</sub>	18.11%	64.50%	32.28%
Al <sub>2</sub> O <sub>3</sub>	2.81%	22.37%	8.16%
Fe <sub>2</sub> O <sub>3</sub>	3.85%	5.81%	0.79%
MgO	2.16%	0.52%	6.01%
SO <sub>3</sub>	4.51%	0.12%	2.19%
Na <sub>2</sub> O	0.20%	0.06%	0.19%
K <sub>2</sub> O	1.23%	1.59%	0.40%
TiO <sub>2</sub>	0.36%	2.77%	0.76%
P <sub>2</sub> O <sub>5</sub>	0.14%	0.68%	0.03%
MnO	0.10%	0.05%	-
Cr <sub>2</sub> O <sub>3</sub>	0.08%	0.06%	0.02%
SrO	0.20%	0.03%	-
ZnO	0.01%	0.02%	-
Cl	0.02%	-	-
NiO	-	-	0.01%
ZrO <sub>2</sub>	-	0.05%	-
CuO	-	0.015%	-
Rb <sub>2</sub> O	-	0.01%	-
Y <sub>2</sub> O <sub>3</sub>	-	0.01%	-

#### 4.4 Properties of Cement and Mortar

A number of tests were conducted on cement paste and cement mortar prepared with the eight mix combinations taken for this research.

##### 4.4.1 Normal Consistency of Cement Pastes

Consistency of cement paste remained constant (25%) for OPC cement C1, OPC and fly ash combinations C2 and C3 and OPC, fly ash and slag combinations of C6, C7 and C8. The values of consistency increased with increasing percentage of slag with OPC (C4 and C5) as seen in Figure 4.1. The normal consistency increased to values of 25.5% and 26% in case of C4 and C5 where slag was present in 30% and 40% proportion with OPC in the blended cement mix. As slag is finer, addition of this enhanced the requirement of water as compared to fly ash addition owing to the high surface area and high levels of water demand of slag.

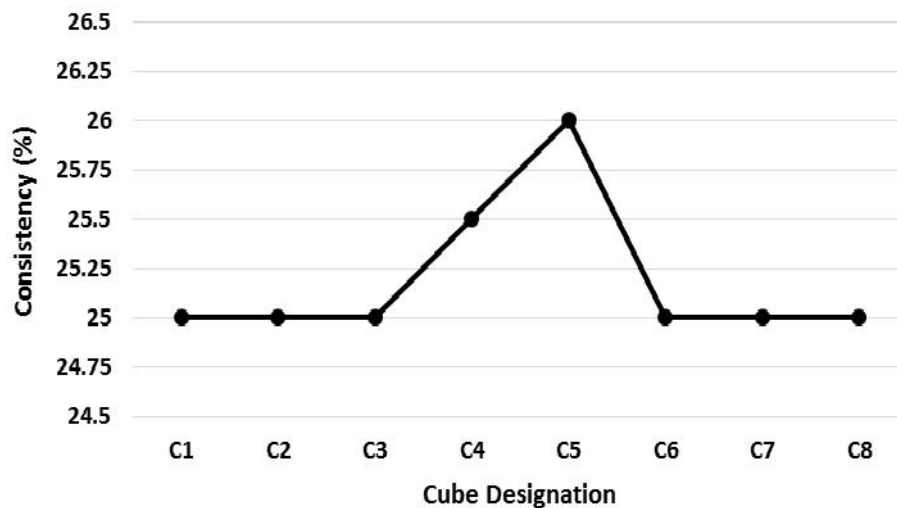


Figure 4.2: Test results of normal consistency

#### 4.4.2 Setting Time of Cement

Both initial and final setting times were affected by addition of fly ash and slag and in both cases the behavior followed similar pattern (Figure 4.2). Studies have reported that with increase in fly ash and slag content within the binder, setting time also increases (Brooks et al., 2000, Carette and Malhotra, 1984 and BGC Cement, 2017). The rate of increase was higher in slag blended cement than fly ash mixed cement. Highest values of initial setting time was 210 minutes in C3 and final setting time was observed highest in C6 (350 minutes). This is because the effect of GGBS is more pronounced at high level replacement in binders (Dave et al. 2016). When carefully examined, it is evident that reducing slag percentage in cement mix, decreased both initial and final setting time which is why C6 show higher setting time than C7 and C8.

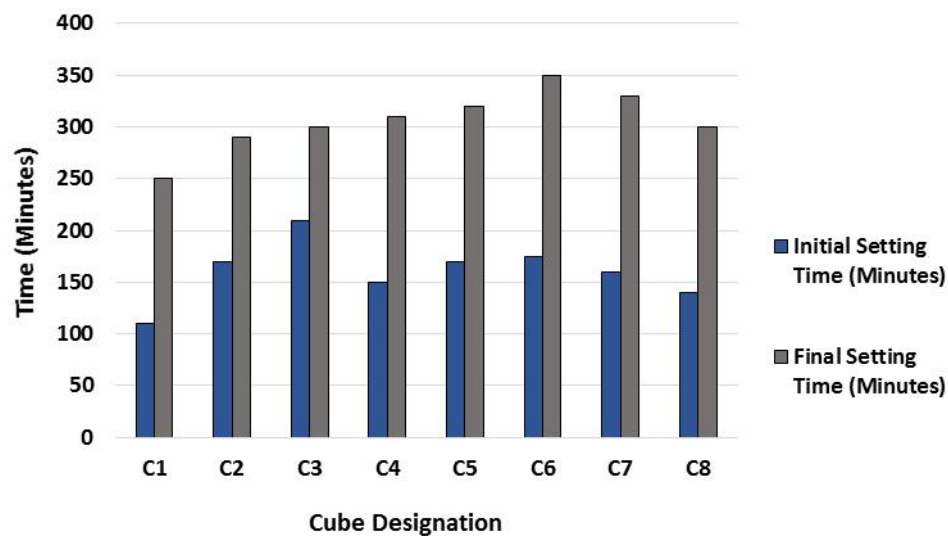


Figure 4.2: Setting time of cubes prepared from different cement mix types

#### 4.4.3 Flow of Mortar

Flow table test was performed to assess the workability parameters of cement mortar. The use of slag and fly ash as supplementary materials had immense effect on flowability of cement mortar. With increasing amount of fly ash and slag, flowability increased from 27% (C2) to 28% (C3) and from 26% (C4) to 27% (C5), respectively. Among combination of



both fly ash and slag blended cement mix, C7 showed 28% and C6 and C8 showed 27% value of flowability as shown in Figure 4.3.

Fly ash benefits mortar and concrete by reducing the mixing water requirement and improving the paste flow behavior. The spherical shaped particles of fly ash act as miniature ball bearings within the mix, thus providing a lubricant effect (Fly ash Facts, 2017).

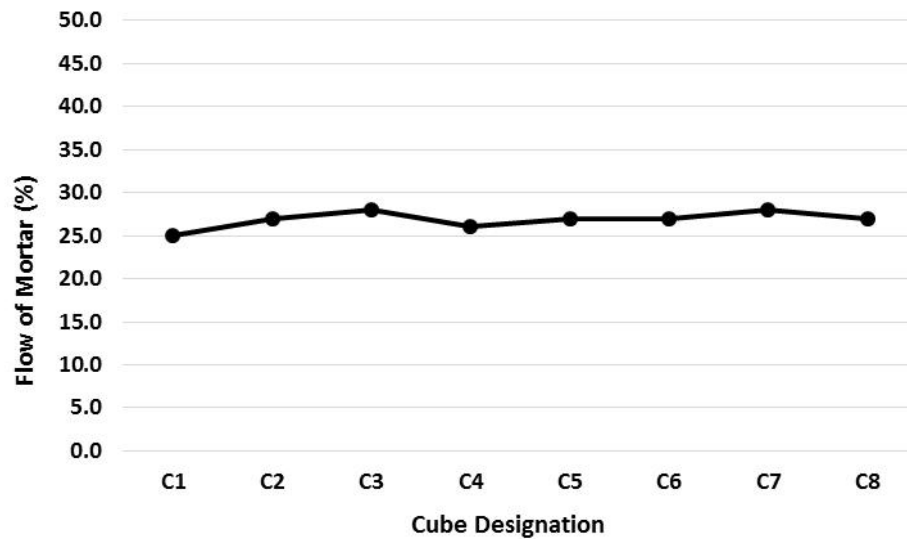


Figure 4.3: Flow of mortar prepared from different cement mix types

#### 4.5 Compressive Strength Results

Compressive strength of mortar cubes prepared from different cement mix combinations at different testing days are demonstrated in graphs and discussed. Figures 4.4 to 4.28 show the compressive strengths of mortar cubes prepared with different cement mix proportions in normal condition and tannery wastewater condition over a period of 180 days. A gain in strength is depicted as positive, while a loss is shown as negative.

#### **4.5.1 Variation of Mortar Cube Strength with Time for Each Particular Type of Cement Mix**

The initial strength of C1 cubes after being submerged for 28 days in limewater was 38.63MPa. Referring to Figure 4.4, the trend line for the graph of strength of C1 in normal condition is upward sloping, depicting increase in strength to 45.26 MPa over the 180 day period. On the other hand, the strength of C1 in tannery wastewater decreased abruptly over the 180 days time period, reaching a value of 26.72 MPa (Figure 4.5) from the initial value of 38.63 MPa at 90 days and finally, dropped to a value of 16.71 MPa on day 180.

As Figures 4.6and 4.8 show, the graphs of C2 and C3 cubes kept in normal condition show gradual increase in strength to values up to 43.36MPa and 42.64MPa, respectively after 180 days. Referring to Figures 4.7and 4.9, the strength of C2and C3 in tannery wastewater show an overall negative trend, that is, the strength diminished over the test period. After 180 days, the strength was found to have fallen to 16.66 MPa and 16.01 MPa from initial values of 36.44 MPa and 33.26 MPa for C2 and C3 in tannery wastewater, respectively which are slightly lower than strength value of 16.71 MPa of C1 in tannery wastewater in 180 days. This implies that presence of fly ash has no significant effect on strength of cement composites under tannery waste water.

For C4 and C5 kept in normal condition, the increase in strength was more as compared to that for C1 kept in normal condition. As Figure 4.10and 4.12 show, the initial strength values of C4 and C5 were 41.57 MPa and 43.74 MPa whereas strength values 48.6 MPa and 50.32 were found respectively on day 180 which were higher than value of 45.26 MPa of C1 kept in normal condition after 180 days.

For C4 and C5 in tannery wastewater, the decrease in strength were less compared to that for C1 in tannery wastewater. According to Soutsos (2004), the early age strength of concrete made with GGBS for equal 28 day compressive strength can be greater than that made with Portland cement only. As Figure 4.11and 4.13 show, the initial strength (strength after 28 days limewater curing) values of C4 and C5 were 41.58 MPa and 43.74 MPa, respectively whereas C1 cubes made with Portland cement showed 38.63 MPa of strength at 28 days. Eventually, strength values of 20.47 MPa and 22.57 MPa were found respectively for C4 and C5, on day 180 which were quite higher than the value of 16.71

MPa of C1 in tannery wastewater after 180 days. Therefore, it can be remarked that better result in strength is observed with increase in slag replacement in cement mortar.

Comparing among the three cement mix types where both fly ash and slag have been combined with cement, in C6 where both supplementary materials had equal proportions in the mix, strength after 180 days in normal condition was 45.92 MPa in Figure 4.14. However, when the fly ash proportion increased in C7, Figure 4.16 shows reduced strength of 44.93 MPa in 180 days. Furthermore, as Figure 4.18 shows, when slag proportion reduced in C8, a value of 45.09 MPa was found on day 180. Strength graphs present same trend for C6, C7 and C8 in tannery wastewater. In C6, strength in 180 days was 17.36 MPa in Figure 4.12. In Figure 4.17, C7 shows reduced strength of 16.06 MPa in 180 days when the fly ash proportion increased. Figure 4.19 shows, in C8, a value of 17.07 MPa was found on day 180 when slag proportion reduced. Therefore, it can be noted that the strength had fallen considerably with increase in fly ash and decrease in slag proportions in cement mix.

The reduction in strength in C2 and C3 in tannery wastewater were higher compared to that in C1 in tannery wastewater. Hence, combination of only fly ash with cement has not been very much beneficial. On the other hand, the gain in strength in C4 and C5 in tannery wastewater were greater with increase in slag proportion. In combining both supplementary materials, C6 with equal slag and fly ash proportion significantly reduced the extent of strength loss of mortar cubes than C7 and C8.

It can be inferred from the strength results that less fly ash and more slag proportions either individually or combined showed better performance with respect to compressive strength values in both normal and tannery wastewater condition. These phenomena owe to the facts that slag has higher reactivity and lead to better and relative rapid hydration. On the other hand, fly ash delivers late hydration.

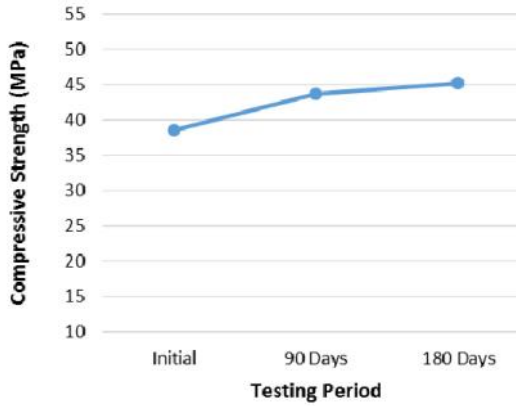


Figure 4.4: Strength of C1 cubes (Normal condition)

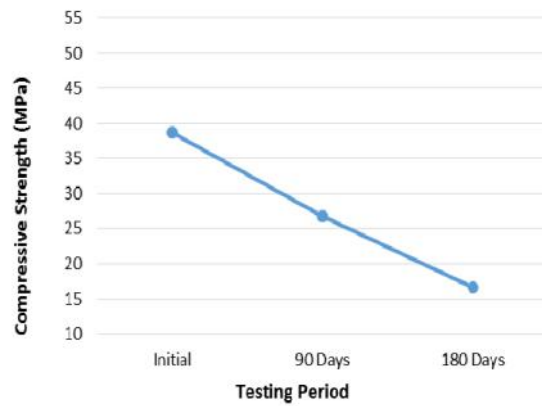


Figure 4.5: Strength of C1 cubes (Tannery wastewater condition)

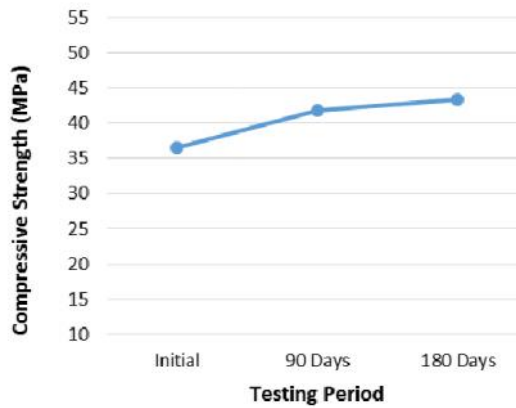


Figure 4.6: Strength of C2 cubes (Normal condition)

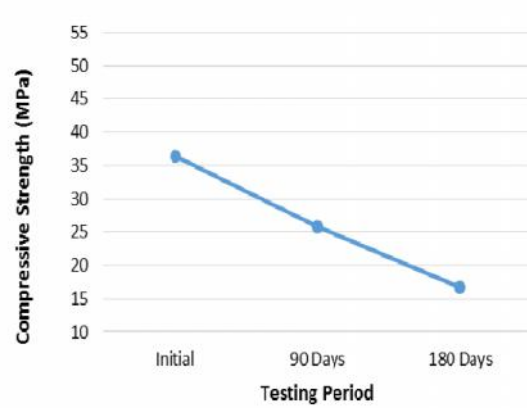


Figure 4.7: Strength of C2 cubes (Tannery wastewater condition)

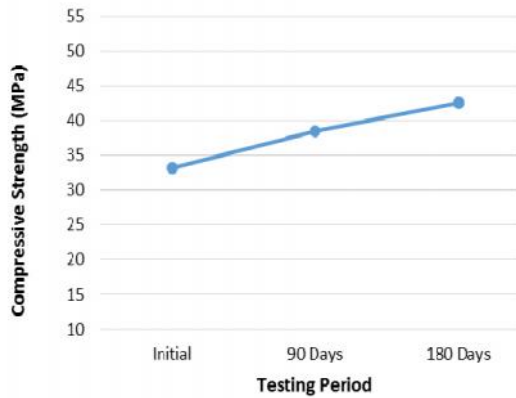


Figure 4.8: Strength of C3 cubes (Normal condition)

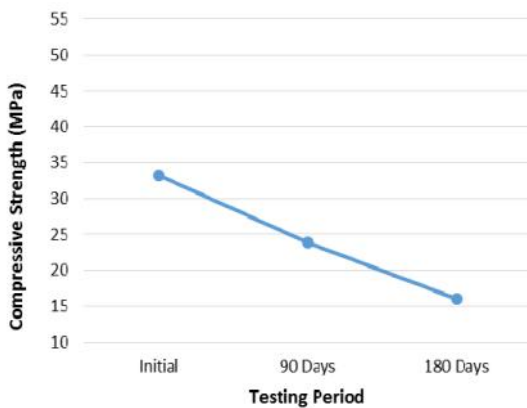


Figure 4.9: Strength of C3 cubes (Tannery wastewater condition)

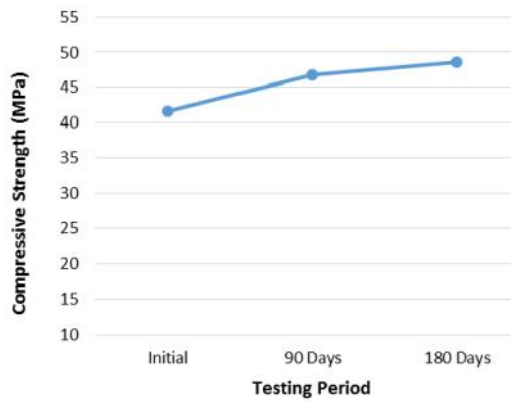


Figure 4.10: Strength of C4 cubes (Normal condition)

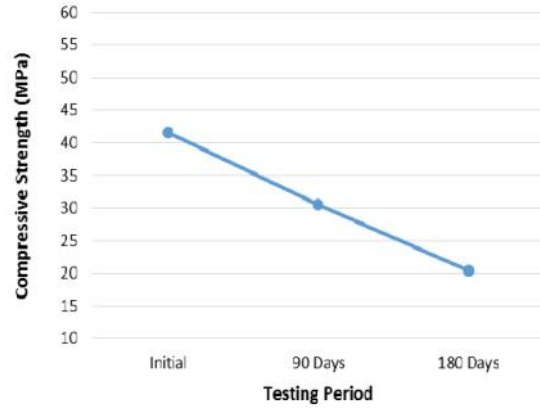


Figure 4.11: Strength of C4 cubes (Tannery wastewater condition)

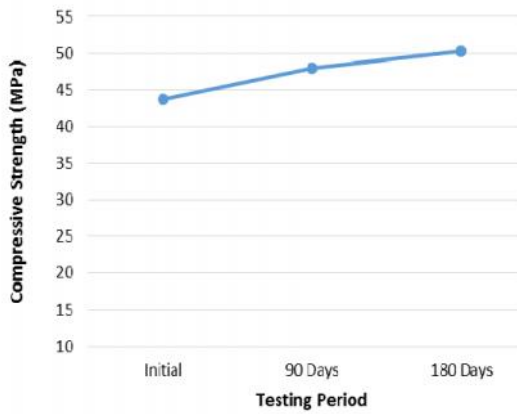


Figure 4.12: Strength of C5 cubes (Normal condition)

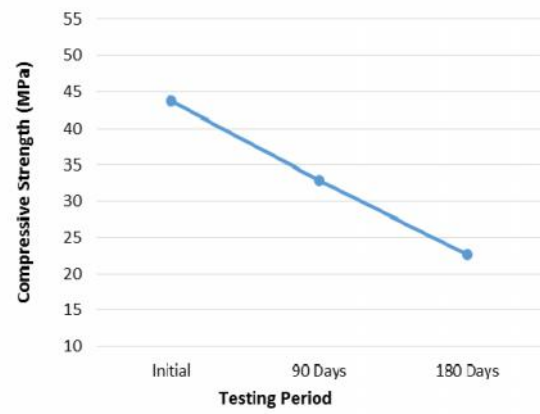


Figure 4.13: Strength of C5 cubes (Tannery wastewater condition)

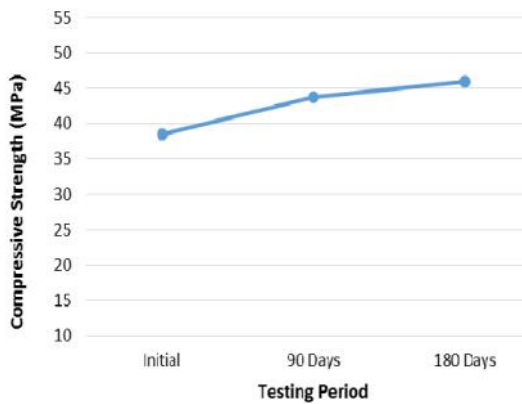


Figure 4.14: Strength of C6 cubes (Normal condition)

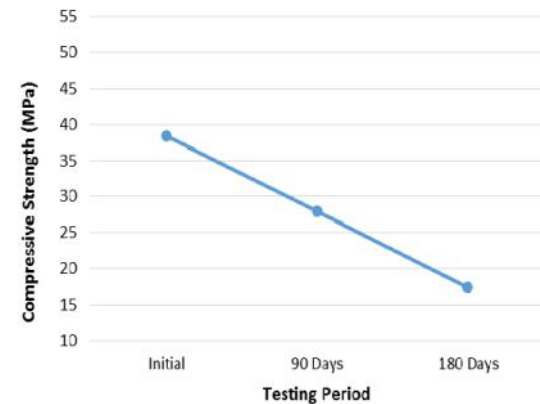


Figure 4.15: Strength of C6 cubes (Tannery wastewater condition)

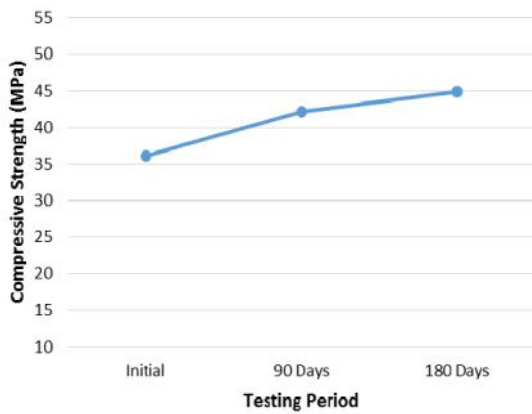


Figure 4.16: Strength of C7 cubes (Normal condition)

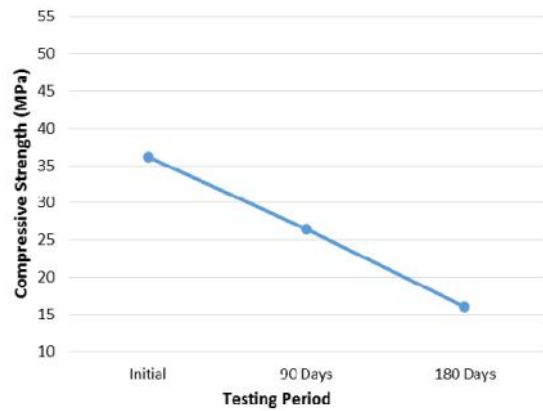


Figure 4.17: Strength of C7 cubes (Tannery wastewater condition)

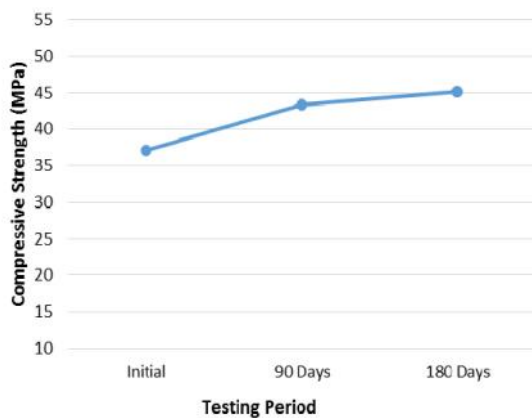


Figure 4.18: Strength of C8 cubes (Normal condition)

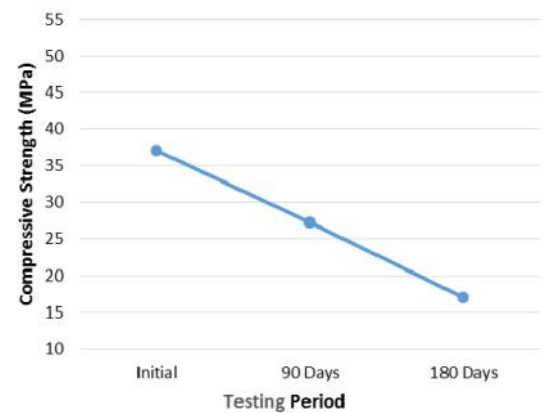


Figure 4.19: Strength of C8 cubes (Tannery wastewater condition)

#### 4.5.2 Variation of Mortar Cube Strength with Type of Cement Mix for Each Particular Testing Period

As it can be observed from Figures- 4.20, 4.21 and 4.22, slag mixed cement (without any fly ash), C4 and C5 cubes showed maximum strength values in all conditions e.g. 28 days limewater curing, normal condition and tannery wastewater condition. After 180 days submergence period in tannery wastewater, the maximum values of strength are observed

as 20.47 MPa for C4 cubes and 22.57 MPa for C5 cubes where C1 (OPC) cubes showed relative lower strength of 16.71MPa. The blended combinations of fly ash and slag exhibited 180 days strength values of 17.36, 16.06, and 17.07 MPa, respectively for C6, C7 and C8 cubes. Samples with only fly ash addition e.g. C2 and C3 cubes, showed relatively reduced strength values of 16.66 MPa and 16.01 MPa as compared to other blended combination samples.

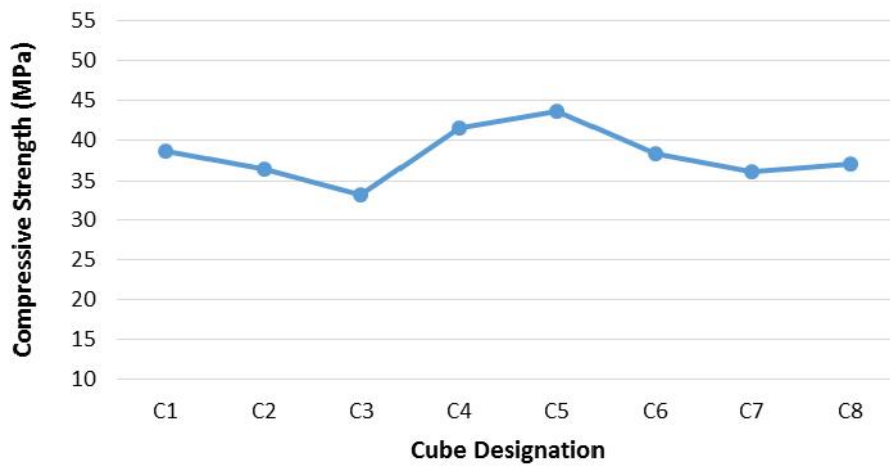


Figure 4.20: Strength of cubes after 28 days limewater curing

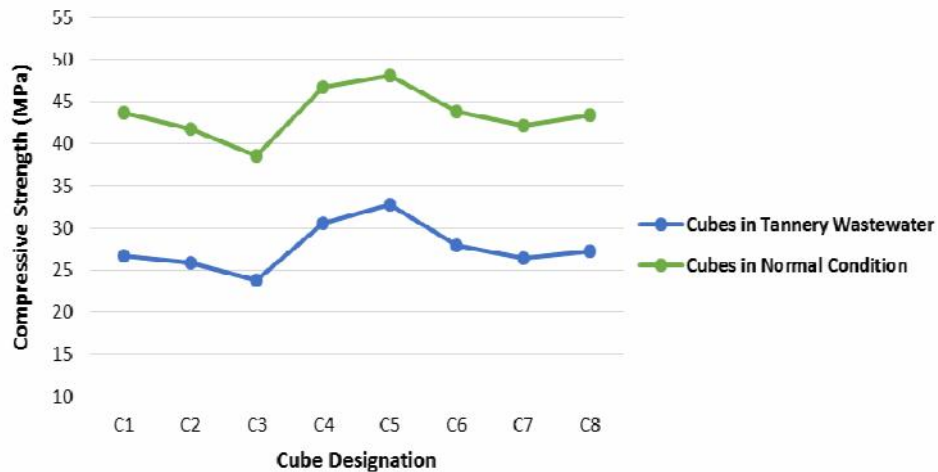


Figure 4.21: Strength of cubes after 90 days in normal and tannery wastewater condition

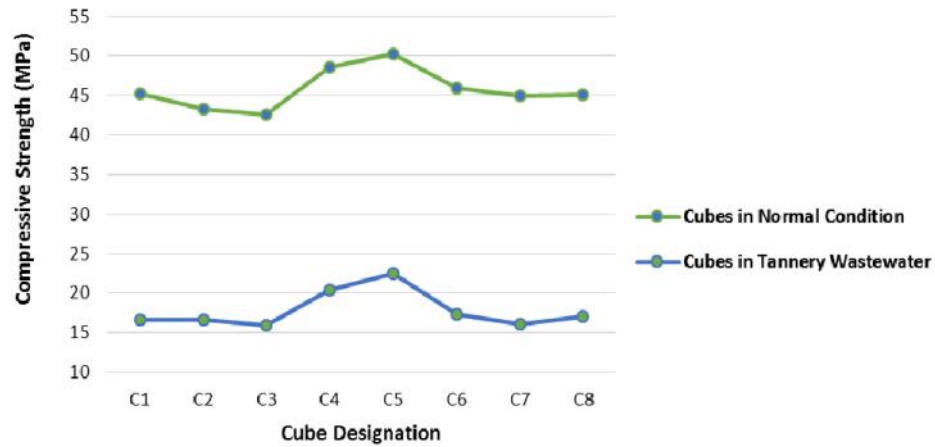


Figure 4.22: Strength of cubes after 180 days in normal and tannery wastewater condition

#### 4.5.3 Comparison of Mortar Cubes Strength Having Different Supplementary Materials

As it can be observed from Figures 4.23 and 4.24, the cubes went through loss of strength in tannery wastewater over 180 days test period. Cube strength values reduced when fly ash replacement level increased to 40% (C3) from 30% (C3) as evident from Figure 4.25. On the other hand, considerable increase in strength was observed when slag replacement level increased in similar amount (Figure 4.26).

When both fly ash and slag were present in cement mix (Figure 4.27), C6 which had both the supplementary materials in equal amount of 20% proportions present, showed higher strength value than C7 (30% fly ash and 10% slag) and C8 (20% fly ash and 10% slag).



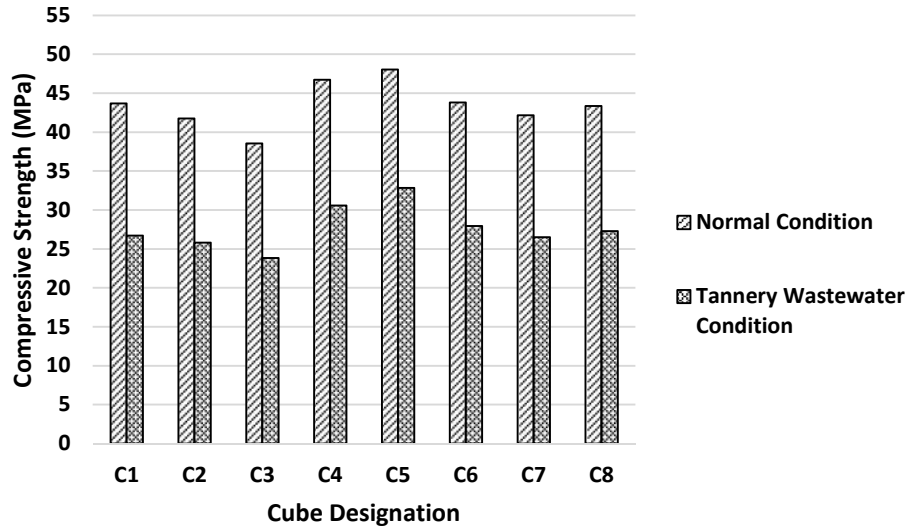


Figure 4.23: Strength of mortar cubes kept in normal condition and tannery wastewater condition for 90 days

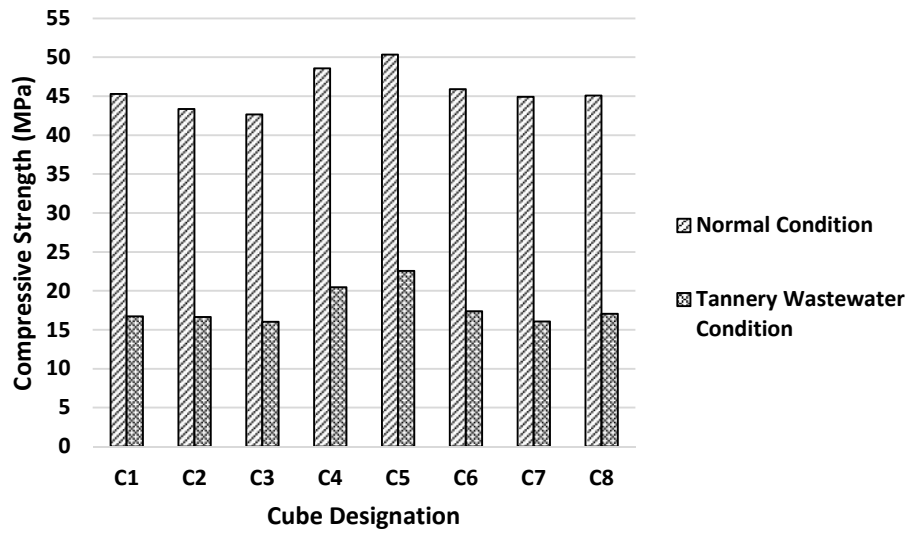


Figure 4.24: Strength of mortar cubes kept in normal condition and tannery wastewater condition for 180 days

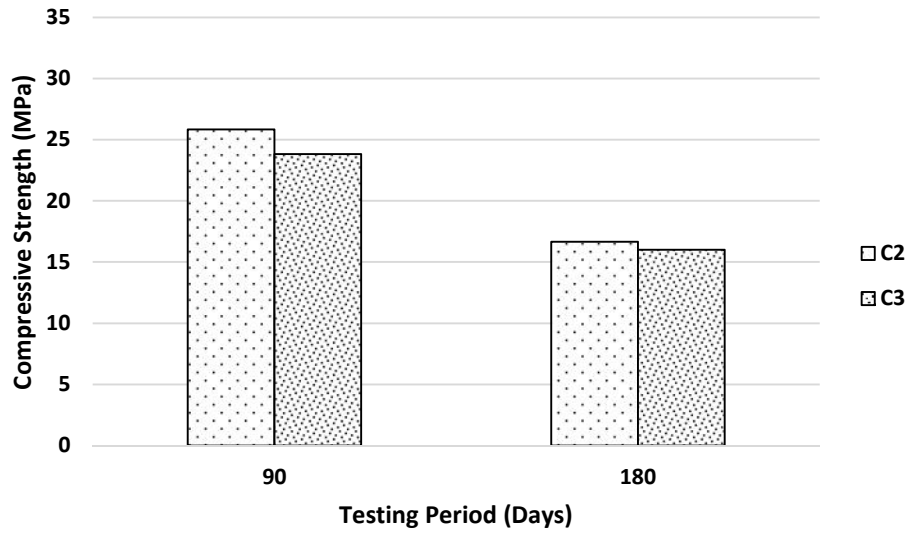


Figure 4.25: Strength of only fly ash blended cement mortar cubes in tannery wastewater condition

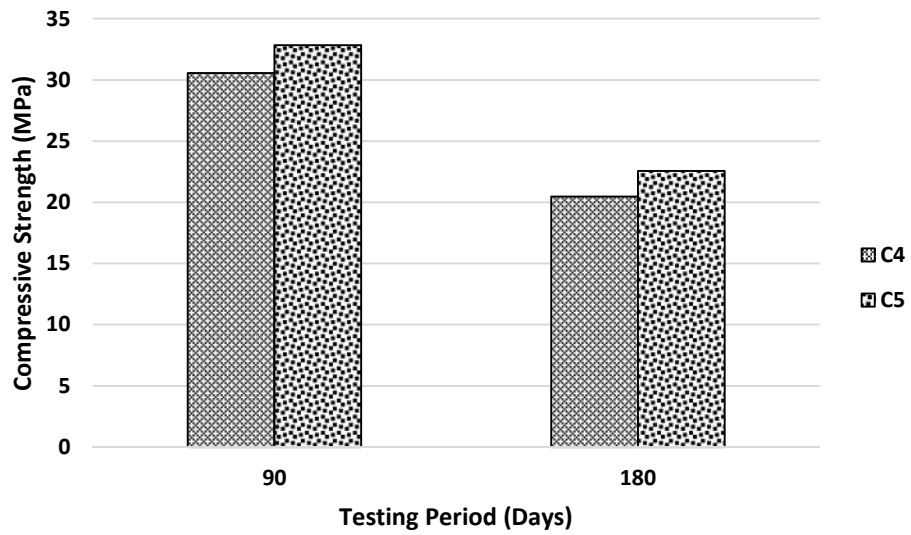


Figure 4.26: Strength of only slag blended cement mortar cubes in tannery wastewater condition

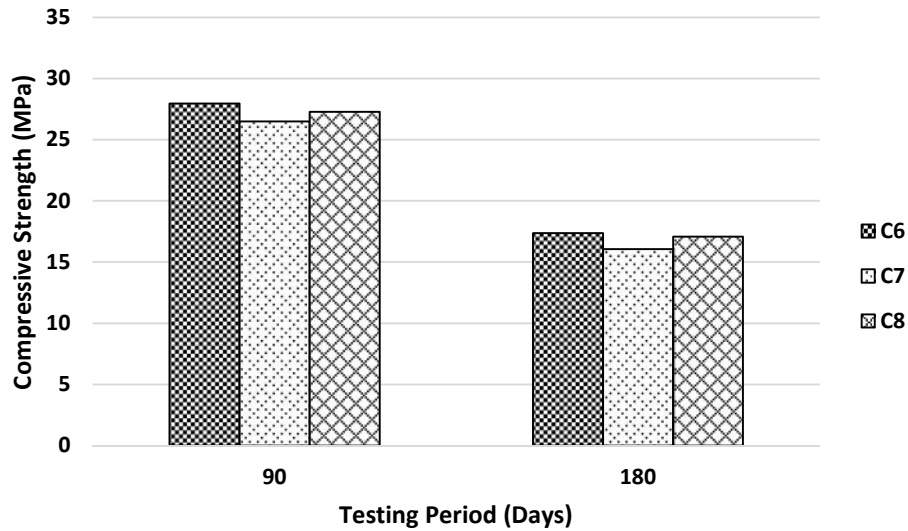


Figure 4.27: Strength of both fly ash and slag blended cement mortar cubes in tannery wastewater condition

It is observed that the strength reduced gradually with respect to increase in fly ash replacement. As explained by (Kondraivendhan and Bhattacharjee, 2015), this reduction in compressive strength is due to the effective water to cement ratio which increases with an increase in fly ash replacement level. Moreover, the pozzolanic reaction being a slow reaction; requires more time to react completely to attain higher strength than Portland cement.

It can also be inferred from the strength results that slag proportions either individually or combined with fly ash exhibited better performance in terms of compressive strength. This may be due to the fact that slag has higher reactivity and consequently showed lower strength loss. For fly ash, it requires time to gain strength and therefore, tannery wastewater appears to be in action before full hydration could be achieved. This is to be investigated further with higher number of test samples and longer testing period as well as studying their properties.

#### 4.5.4 Variation of Mortar Cube Strength Change (%) with Type of Cement Mix for Each Testing Period

The strength change (in percent of initial strength after 28 days limewater curing) graph exhibits downward value (Figure 4.28) for cubes submerged under tannery wastewater. However, different samples show different rate of reduction in strength which can be used as the basis for identifying better performing blended cement. Slag mixed samples in all instances exhibited better performance than OPC samples under tannery wastewater condition. Cubes prepared from combinations of cement and slag (C4 and C5) have lost less strength as compared to OPC (C1) cubes under tannery wastewater. It is observed that OPC samples (C1) under tannery waste water showed 63.08% less strength than that of OPC samples subjected to normal curing condition. Overall, the presence of fly ash and slag improved cube strength to a great extent compared to OPC strength under tannery wastewater. In tannery wastewater for 180 days, among the cubes prepared from all seven combinations of fly ash and slag, C5 samples showed the least decrease in strength (55.15%).

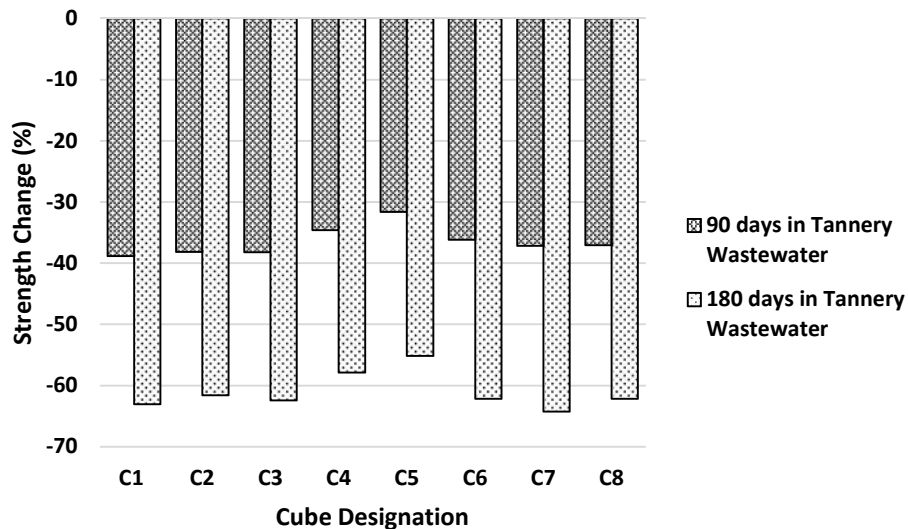


Figure 4.28: Strength change (%) of mortar cubes submerged in tannery wastewater

## **4.6 Expansion of Mortar Bars**

This section provides an interpretation of the graphical results obtained employing the expansion test data. Figures 4.29 through 4.36 show expansion with time for each particular blended cement type for clarity of understanding. The readings were taken after 28 days lime water curing of the mortar bars which is denoted as 0 submergence period.

### **4.6.1 Expansion with Time for Each Particular Cement Mix Type**

Figure 4.29 shows the expansion of OPC mortar bars kept in normal condition and submerged in tannery wastewater. In the first thirteen weeks, the magnitudes of expansion in both condition bars were very close. On the 13<sup>th</sup> week, the expansion in bars in normal condition was 0.032% and that in tannery wastewater condition was 0.046%. After this, the rate of expansion in tannery wastewater bars seemed to escalate remarkably, reaching values of 0.4485% and 0.644% on weeks 18 and 26, respectively. The expansion in normal condition bars was found to remain almost constant from week 18 to week 26.

The expansion in fly ash blended cement (C2 and C3) bars under both normal and tannery wastewater condition over 26 weeks show very negligible values as shown in Figures 4.30 and 4.31. On the other hand, expansion in slag blended cement (C4 and C5) bars in tannery wastewater seem to increase slowly up to 13 weeks, then suddenly jump to higher rate of increase in 15 weeks that continues till 26 weeks. C4 bars showed 0.43% and C5 bars showed 0.47% expansion in tannery wastewater (Figure 4.32) where they showed almost no expansion (0.01% and 0.06%, respectively) in normal condition as shown in Figure 4.33.

The change in expansion graph for C6 cubes in tannery wastewater condition in Figure 4.34 is upward throughout 26 weeks reaching a value of 0.22%. Bars kept in normal condition which were prepared with same cement mix combination of equal proportion (20%) of fly ash and slag with Portland cement, showed no expansion in 26 weeks.

In the case of C7 bars in tannery wastewater, very little or no expansion up to the 13<sup>th</sup> week was observed. The values then increased and expansion of 0.115% and 0.129% occurred by the end of 18<sup>th</sup> and 26<sup>th</sup> weeks, respectively. C7 bars kept in normal condition shows overall constant negligible values in 26 weeks.

For C8 bar in tannery wastewater in Figure 4.36, trend of expansion graph changes from upward to downward then again upward and show 0.166% values after the 26<sup>th</sup> week. Under normal condition, C8 bars show negligible values all through 26 weeks.

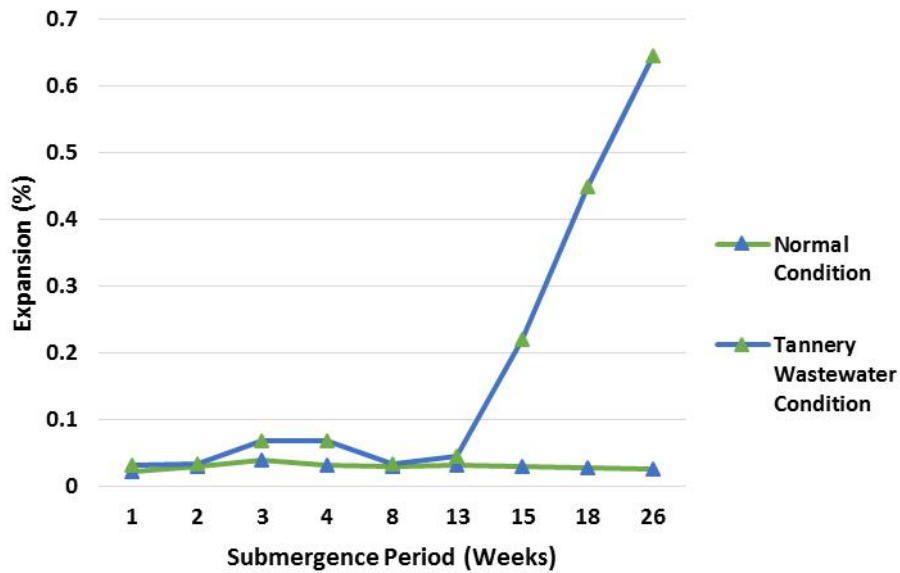


Figure 4.29: Expansion (%) of C1 bars kept in normal condition and tannery wastewater condition

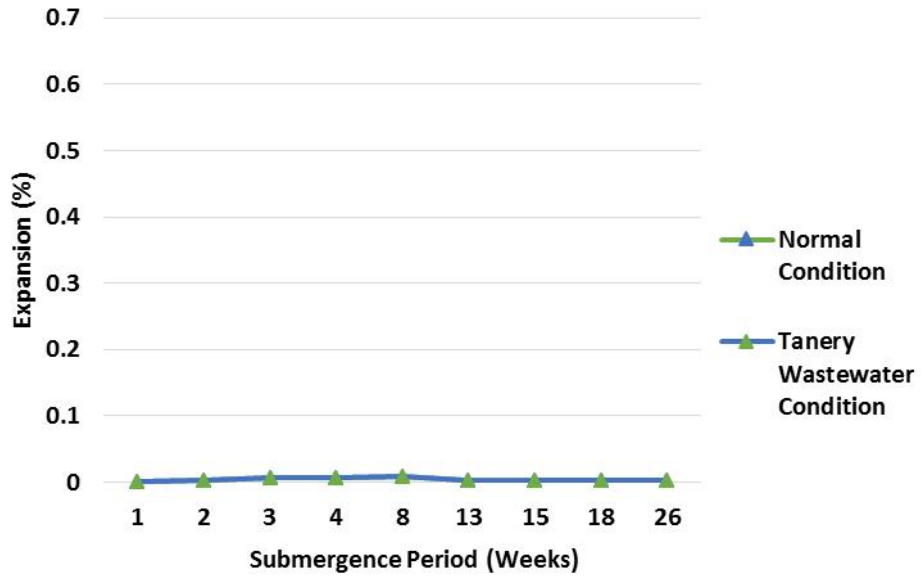


Figure 4.30: Expansion (%) of C2 bars kept in normal condition and tannery wastewater condition

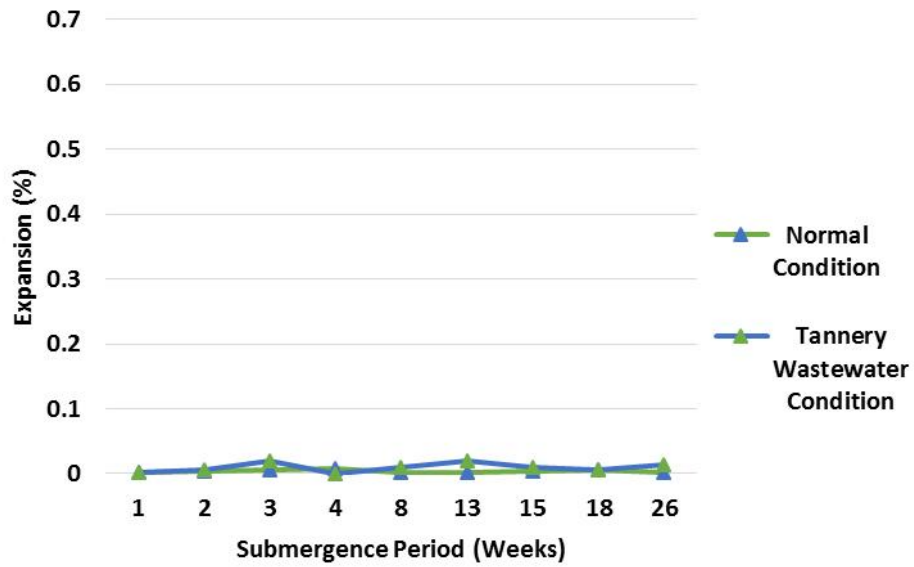


Figure 4.31: Expansion (%) of C3 bars kept in normal condition and tannery wastewater condition

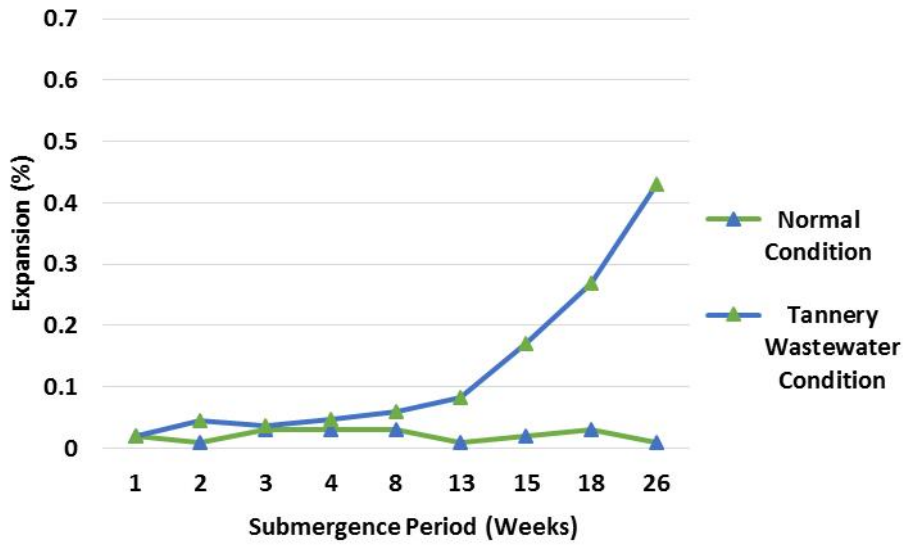


Figure 4.32: Expansion (%) of C4 bars kept in normal condition and tannery wastewater condition

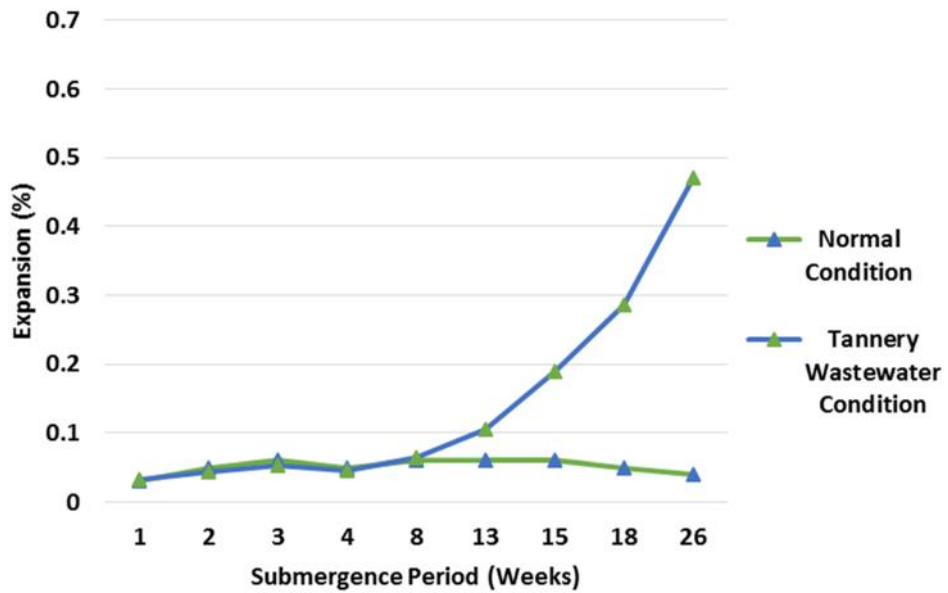


Figure 4.33: Expansion (%) of C5 bars kept in normal condition and tannery wastewater condition



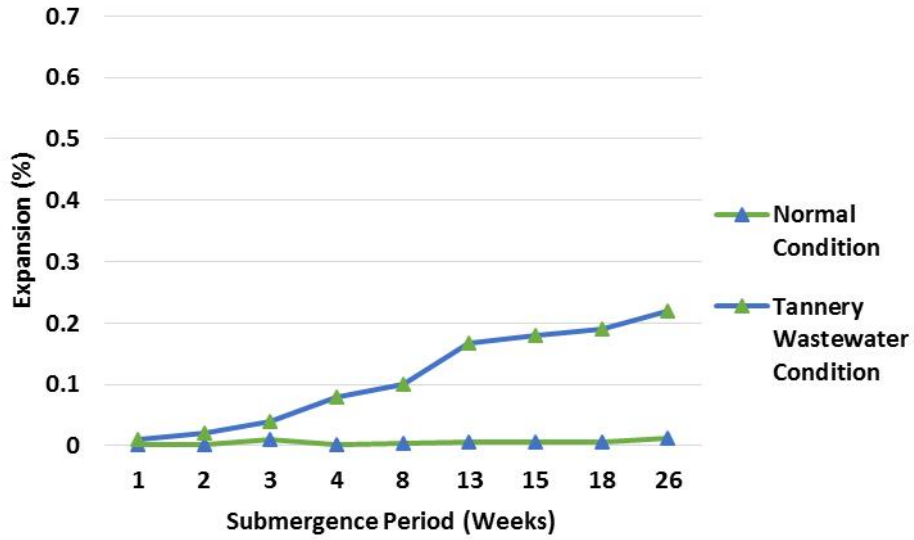


Figure 4.34: Expansion (%) of C6 bars kept in normal condition and tannery wastewater condition

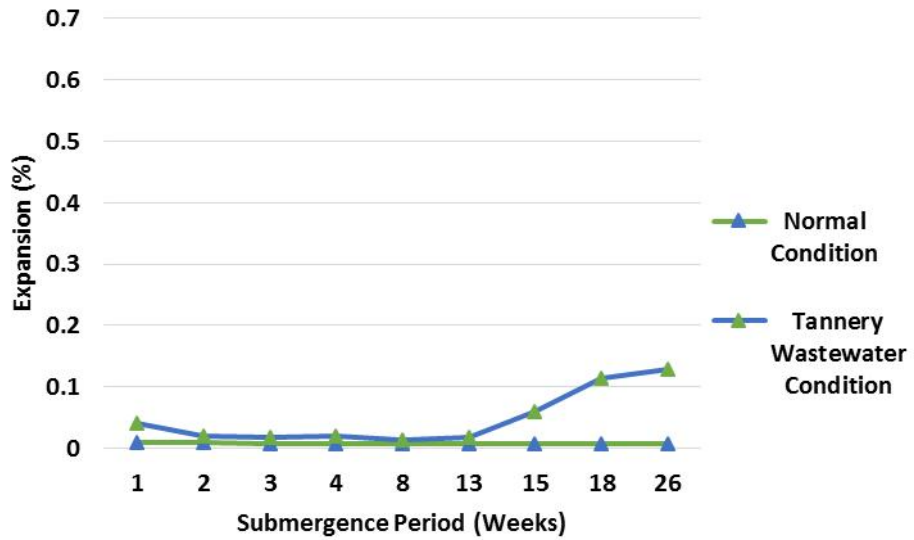


Figure 4.35: Expansion (%) of C7 bars kept in normal condition and tannery wastewater condition

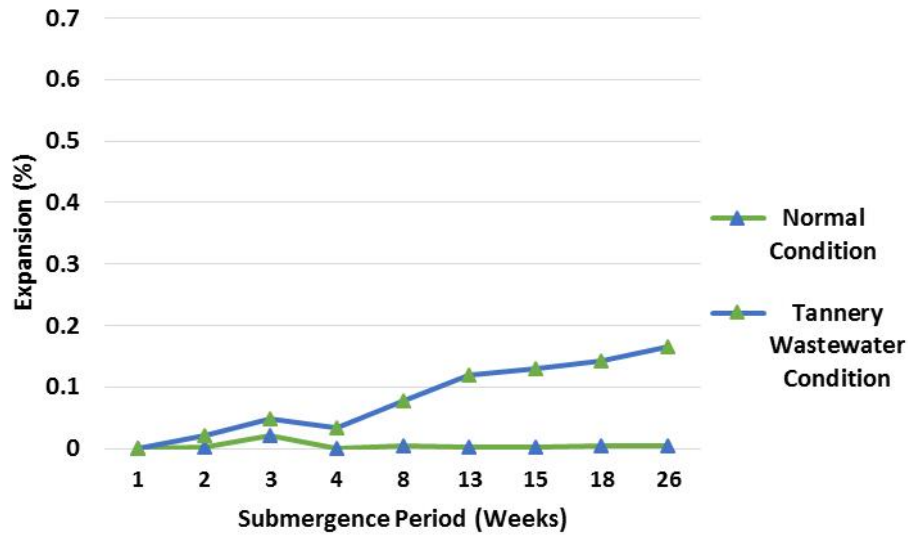


Figure 4.36: Expansion (%) of C8 bars kept in normal condition and tannery wastewater condition

With addition of fly ash, decrease in water content combined with the production of additional cementitious compounds due to late hydration caused by pozzalonic effect of fly ash, reduces the pore interconnectivity of concrete, thus decreasing permeability. The reduced permeability results in improved long-term durability and resistance to expansion (Fly Ash Facts, 2017).

As per ASTM C1012 and ACI 318, the expansion limit is 0.10% (Table 2.2) after 6, 12 and 18 months for moderate (S1), severe (S2) and very severe (S3) sulfate exposure conditions, respectively. The sulfate content in ASTM C1012 test solution is 50,000 mg/L. However, the sulfate content in tannery wastewater is 1,00,000 mg/L which is two times greater than test solution's sulfate content. In addition, several other deteriorating chemicals are present in tannery wastewater. In this study, expansion results were observed for 6 months of exposure. It was found that expansion values were significantly below the permissible value of 0.10% (below 0.02% to be exact) for only fly ash blended cement (C2 & C3). Hence, it is anticipated that fly ash blended cement would not exceed the limit of 0.1% at 18 months for S3 class. However, the slag blended cement mortar shows expansion values of 0.47% which is greater than 0.10% expansion limit. The slag blended cement

mortar needs to be tested following ASTM C1012 test conditions to investigate their performance in order to compare with performance under tannery waste water. Such study is important to understand whether a different expansion limit is required for tannery waste water exposure condition or not.

#### 4.7 Weight Loss of Cubes

Weight of cubes was taken before and after submergence in simulated tannery wastewater and weight loss percentage was calculated by comparing the change of weight with initial weight values.

##### 4.7.1 Variation of Weight Loss % with Cement Mix Types for Different Testing Time

From Figures 4.37 and 4.38, it is observed that among fly ash blended cement mix, C3 showed higher weight loss and among slag blended mix, C4 showed higher weight loss values. However, C1 cubes showed the maximum weight loss. Weight change is relatively very less in blended cement mix if compared to C1.

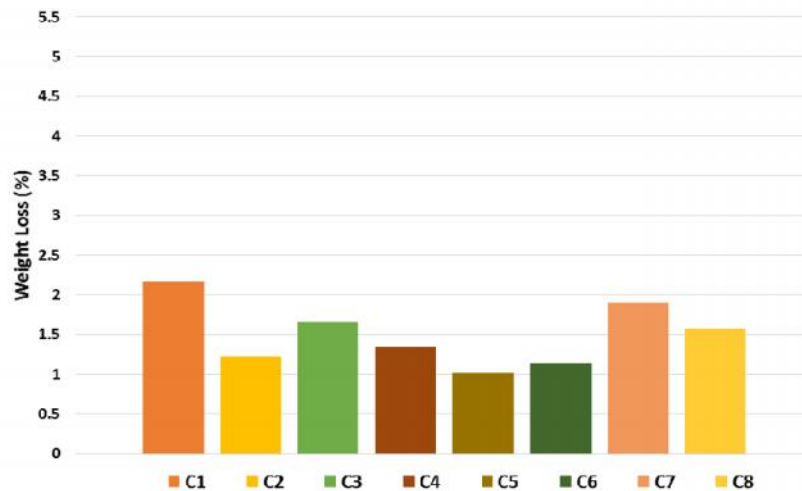


Figure 4.37: Weight loss % of cubes prepared from different cement mix types submerged in tannery wastewater for 90 days

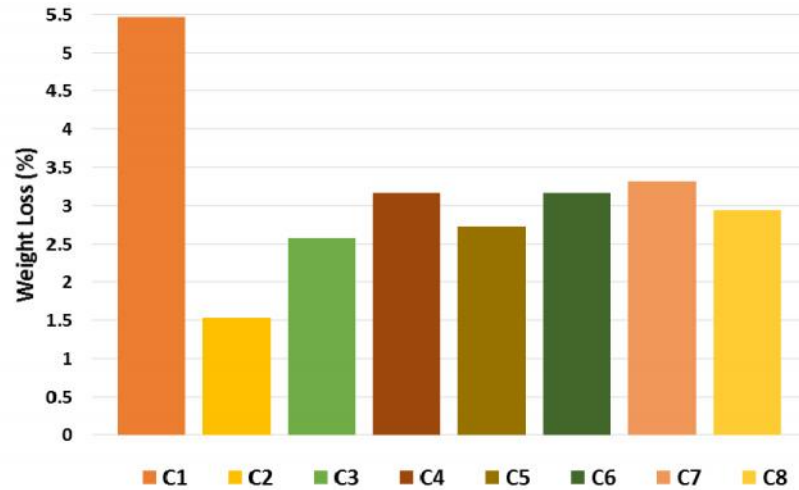


Figure 4.38: Weight loss % of cubes prepared from different cement mix types submerged in tannery wastewater for 180 days

For cubes submerged in tannery wastewater, the result of sulfate attack is excessive expansion, surface area loss, cracking, and loss of strength due to formation of ettringite and gypsum. Initially the voids in cubes get filled with ettringite and gypsum formation. As these crystals have significantly higher volume, developed stresses result in breakdown of the paste and ultimately in breakdown of the composite (Menendez et al. 2012). Attack by ammonium nitrate leads to a very soluble calcium nitrate, a slightly soluble calcium nitro aluminate, and release of ammonia gas which induces total leaching of calcium hydroxide and rapid decalcification of C-S-H (Menendez et al. 2012). Oxidation of sulfides in aggregates results in additional sulfate being produced that can induce formation of ettringite in the post-hardening stage (Alexander et al. 2012). Hence, strength loss as well as weight loss is observed.

#### 4.7.2 Variation of Weight Loss % with Time for Different Cement Mix Types

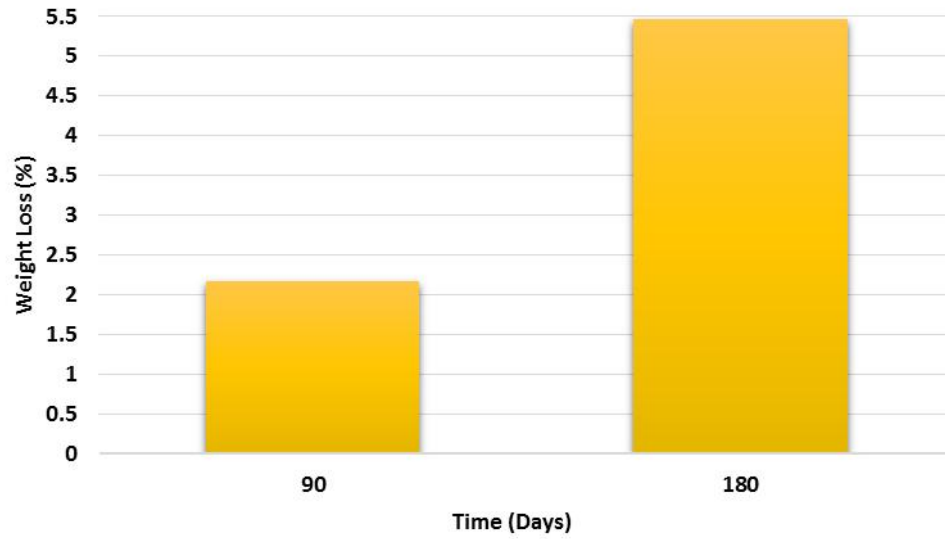


Figure 4.39: Weight loss % of C1 cubes submerged in tannery wastewater

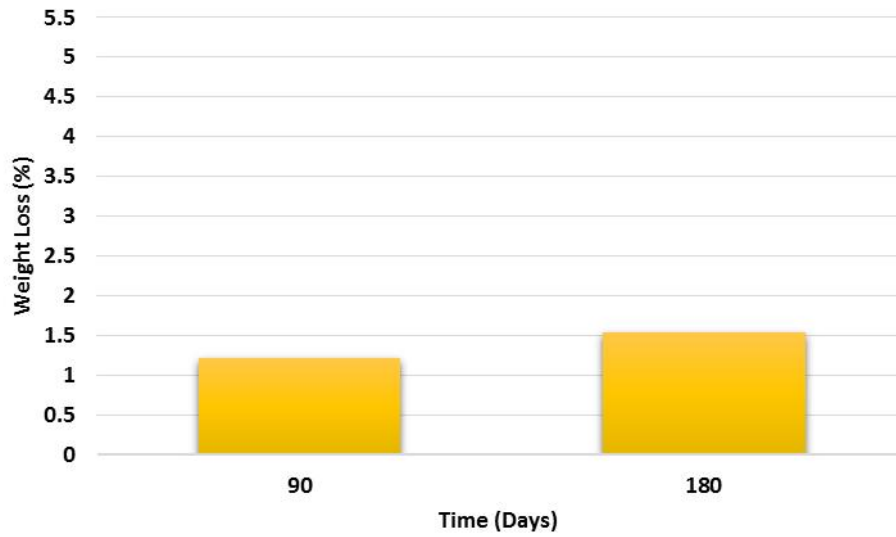


Figure 4.40: Weight loss % of C2 cubes submerged in tannery wastewater

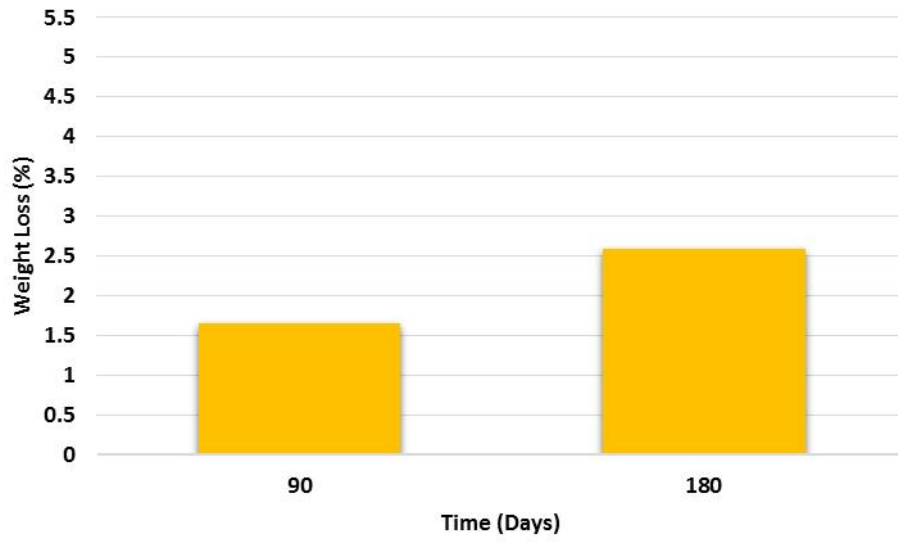


Figure 4.41: Weight loss % of C3 cubes submerged in tannery wastewater

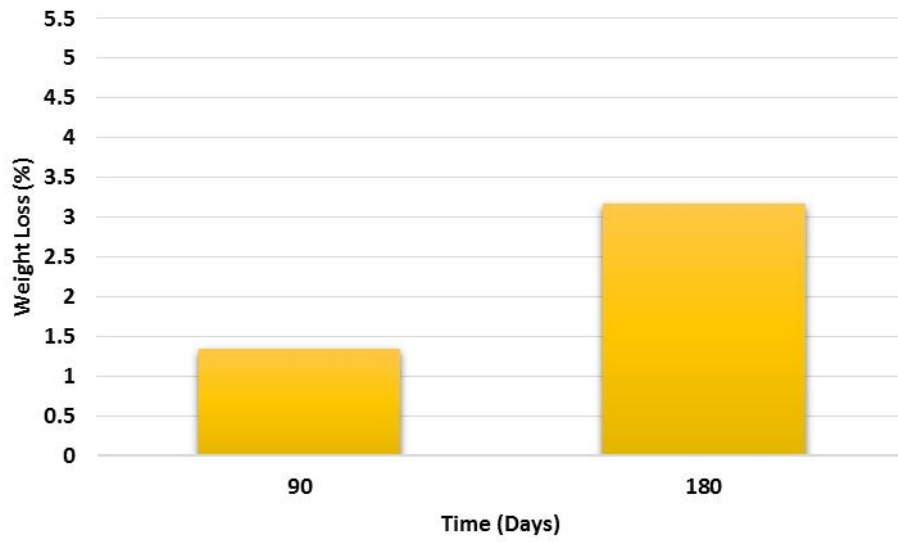


Figure 4.42: Weight loss % of C4 cubes submerged in tannery wastewater

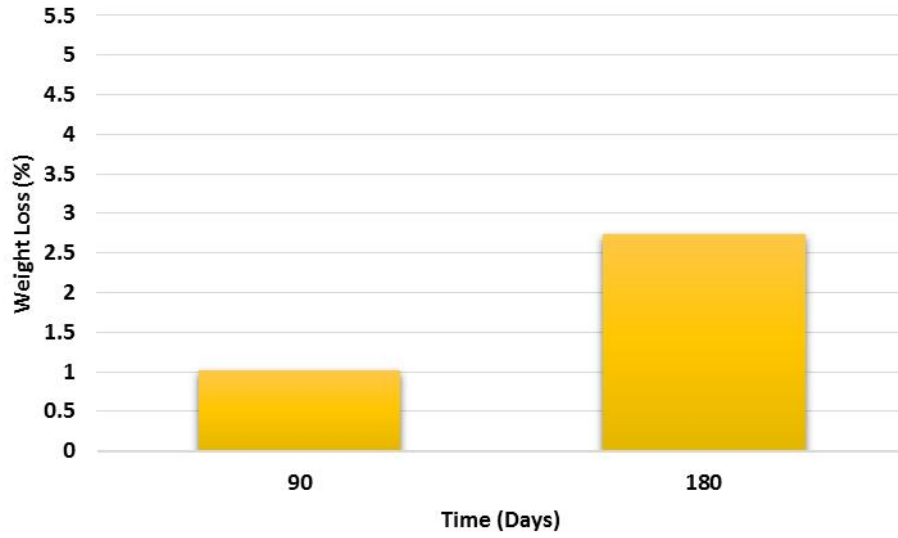


Figure 4.43: Weight loss % of C5 cubes submerged in tannery wastewater

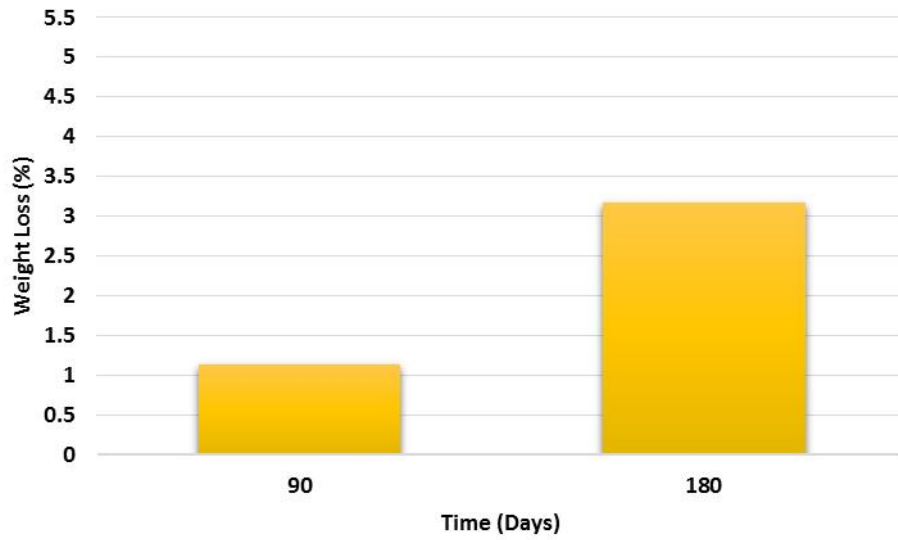


Figure 4.44: Weight loss % of C6 cubes submerged in tannery wastewater

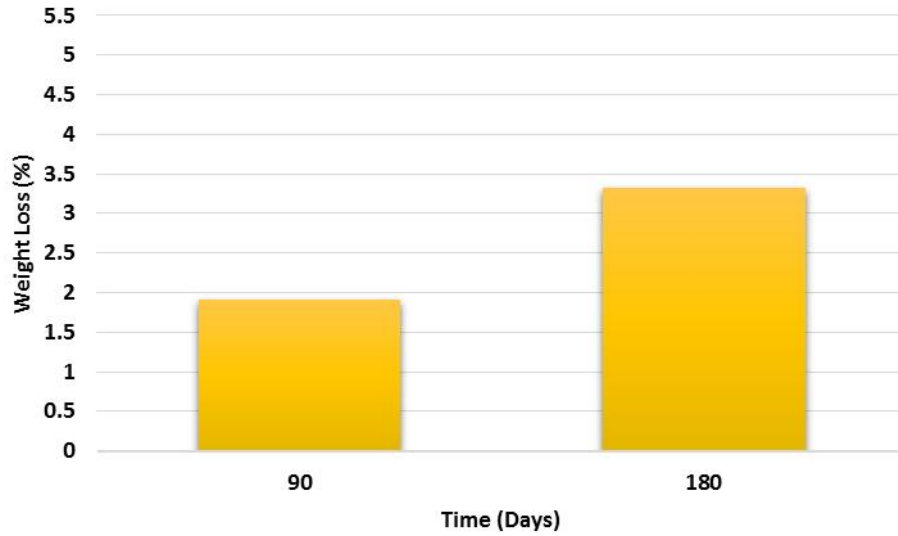


Figure 4.45: Weight loss % of C7 cubes submerged in tannery wastewater

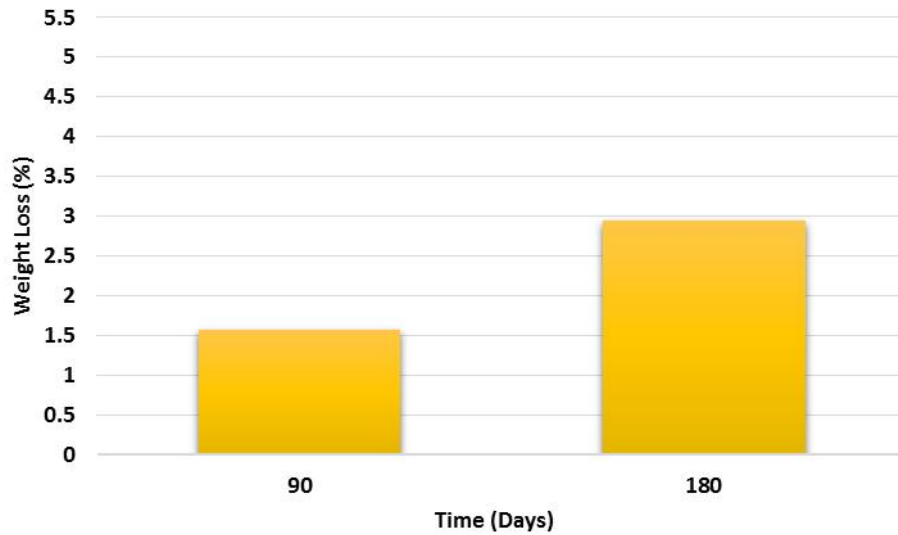


Figure 4.46: Weight loss % of C8 cubes submerged in tannery wastewater

Fly ash blended composites, C2 and C3 cubes showed 1.53% and 2.58% weight loss values (Figures 4.40 and 4.41) after submergence in tannery wastewater for 180 days. Weight loss of slag blended combinations, C4 and C5 cubes showed higher values of weight loss of 3.17% and 2.73%, respectively (Figures 4.42 and 4.43). In the fly ash and slag mixed combinations, C6 showed 3.17%, C7 showed 3.32% and C8 showed 2.94% of weight loss



values after 180 days of submergence in tannery wastewater (Figures 4.44 to 4.46). It is indisputable from these figures that weight change in the blended cement are relatively less if compared to only OPC composites in Figure 4.39. It is due to the presence of fly ash and slag which increase strength in concrete by providing more CaO and SiO<sub>2</sub> that form stable form of C-S-H.

### 4.7.3 Weight Loss Comparison of Mortar Cubes of Different Supplementary Materials

Overall slag blended mortar cubes lost more weight than fly ash blended ones. However, increasing slag replacement level resulted in less weight loss while more weight loss was observed when fly ash replacement level increased to 40% from 30% (Figures 4.47 & 4.48). When both fly ash and slag were present in cement mix (as shown in Figure 4.49), C8 mix which had 20% fly ash and 10% slag proportions showed lower weight loss value than that of C6 (20% fly ash and 20% slag) and C7 (30% fly ash and 10% slag).

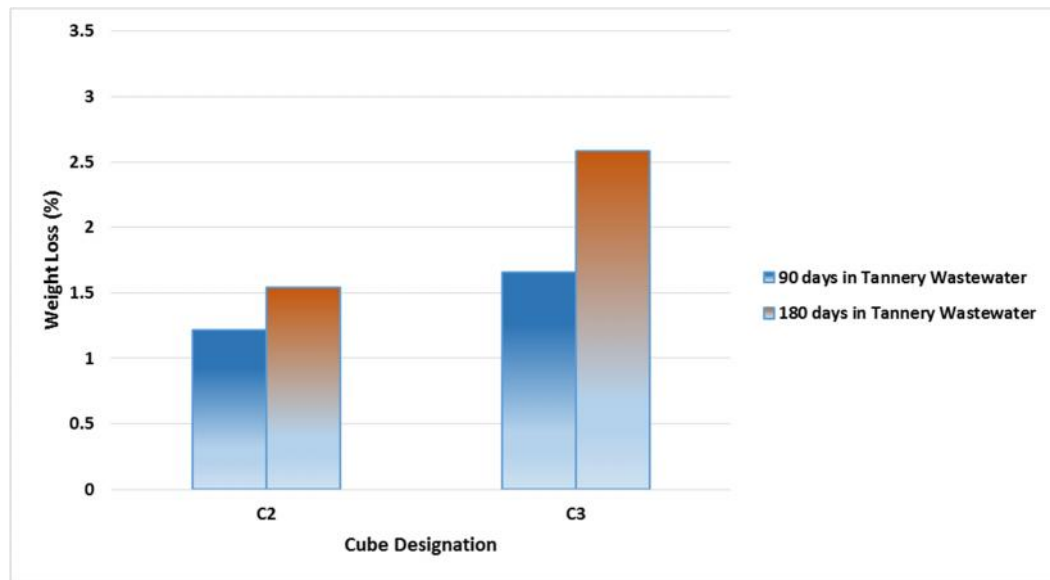


Figure 4.47: Weight loss % of only fly ash mixed cement mortar cubes submerged in tannery wastewater

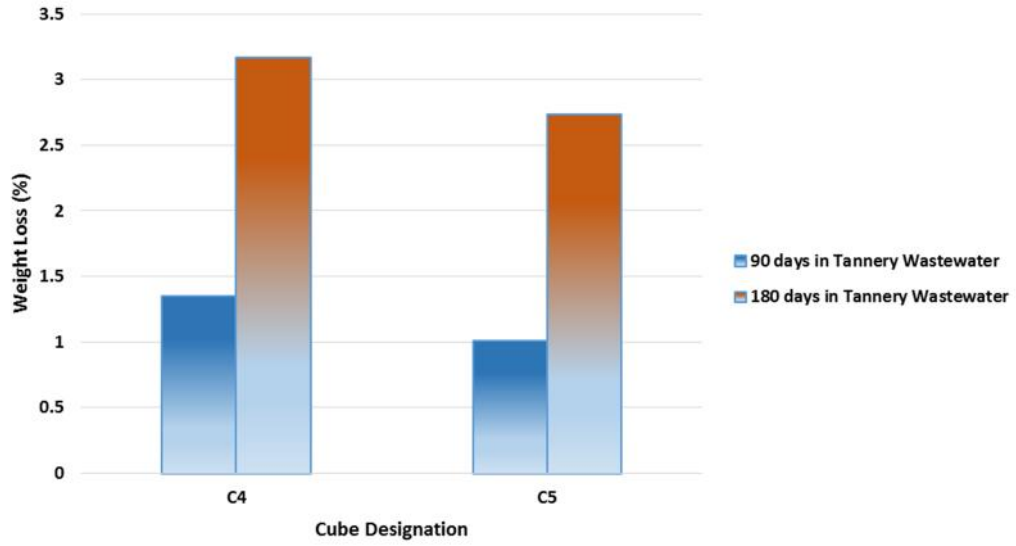


Figure 4.48: Weight loss % of only slag mixed cement mortar cubes submerged in tannery wastewater

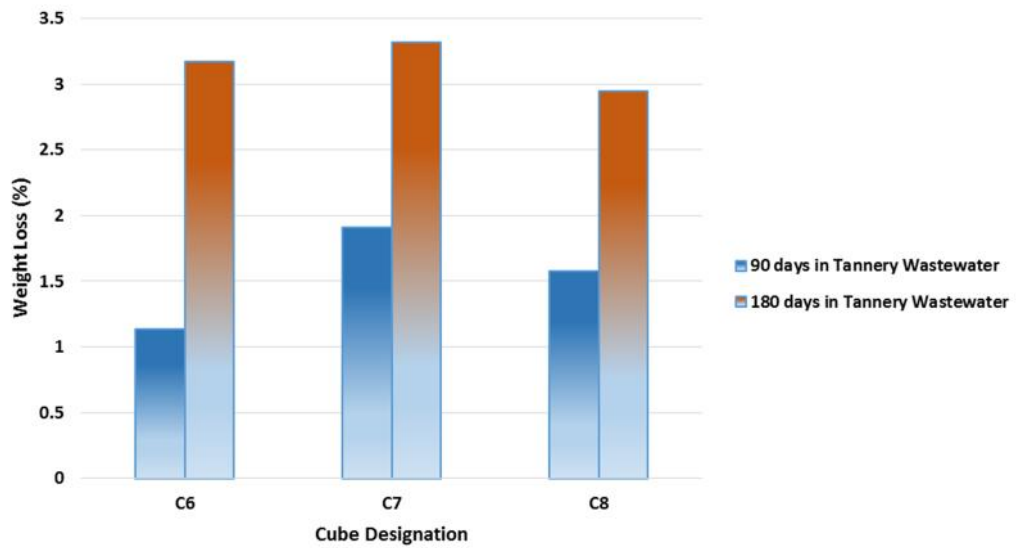


Figure 4.49: Weight loss % of both fly ash and slag mixed cement mortar cubes submerged in tannery wastewater

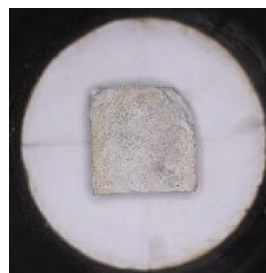
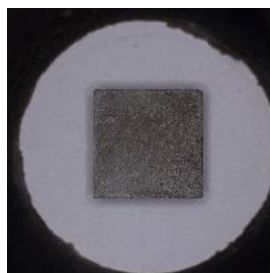
#### **4.8 Comparison of Images of Cube Surfaces**

Images of cube surfaces were taken to compare the conditions of mortar cubes before and after their submergence in tannery wastewater for 180 days. Images showed more or less symptoms of deterioration due to expansion, spalling and disintegration of cubes occurring from their reactions with tannery wastewater.

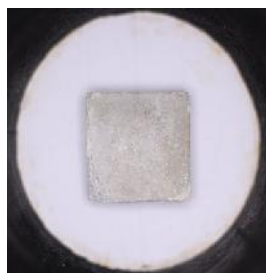
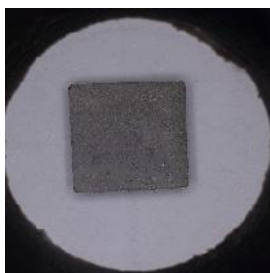
For C1 condition, it can be observed from Figure 4.50 that tannery wastewater caused significant surface area loss in OPC cube. The extent of deterioration is less in only fly ash blended cement cubes C2 & C3 than in only slag blended cement cubes, C4 & C5. For both fly ash and slag blended cement cubes (from C6 to C8), it can be observed that slight surface area loss and disintegration, occurred in all of them. Precipitation occurred but it was sporadic. Precipitations are formed on cube surface due to dissolved cations of tannery effluents such as Na, Ca, Cr, Pb, Cd and As (Chowdhury et al. 2013).

Cube Designation	Image before Submergence in tannery wastewater	Image after submergence in tannery wastewater for 180 days
------------------	--	--

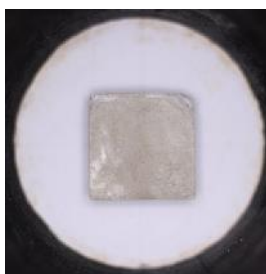
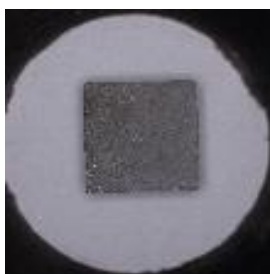
C1



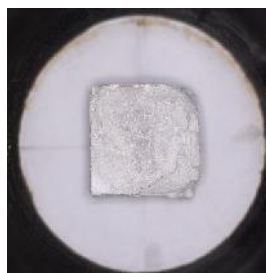
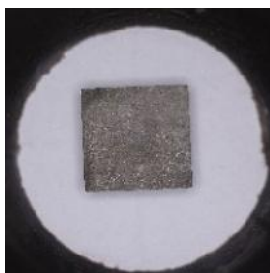
C2



C3



C4



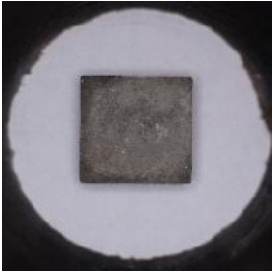
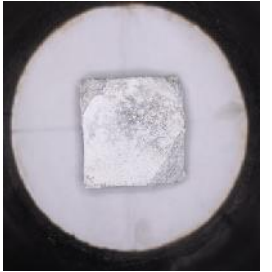
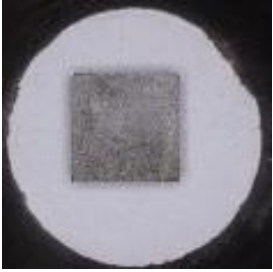
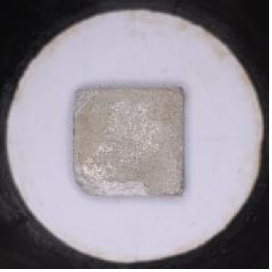
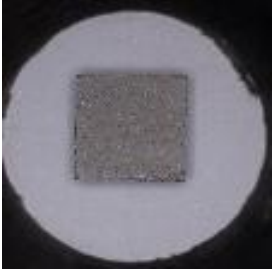
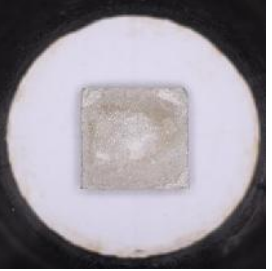
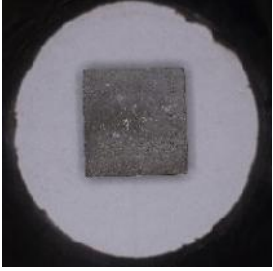
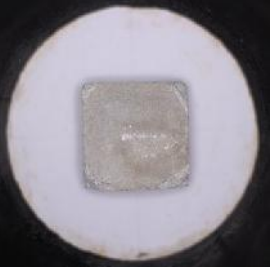
Cube Designation	Image before Submergence in tannery wastewater	Image after submergence in tannery wastewater for 180 days
C5		
C6		
C7		
C8		

Figure 4.50: Cube surface images before and after submergence in tannery wastewater for 180 days

#### 4.9 SEM Images

SEM images tend to explain micro-structure behavior of cement composites. SEM images were taken in different magnification level (500x and 1000x zoom) for cube samples of OPC (C1), fly ash blended (C2), slag blended (C5) and both fly ash and slag blended (C6) cubes, submerged in tannery wastewater condition for 180days. Formation of Ettringite, Calcium-Silica-Hydrate (C-S-H) and Portlandite (CH) were identified.

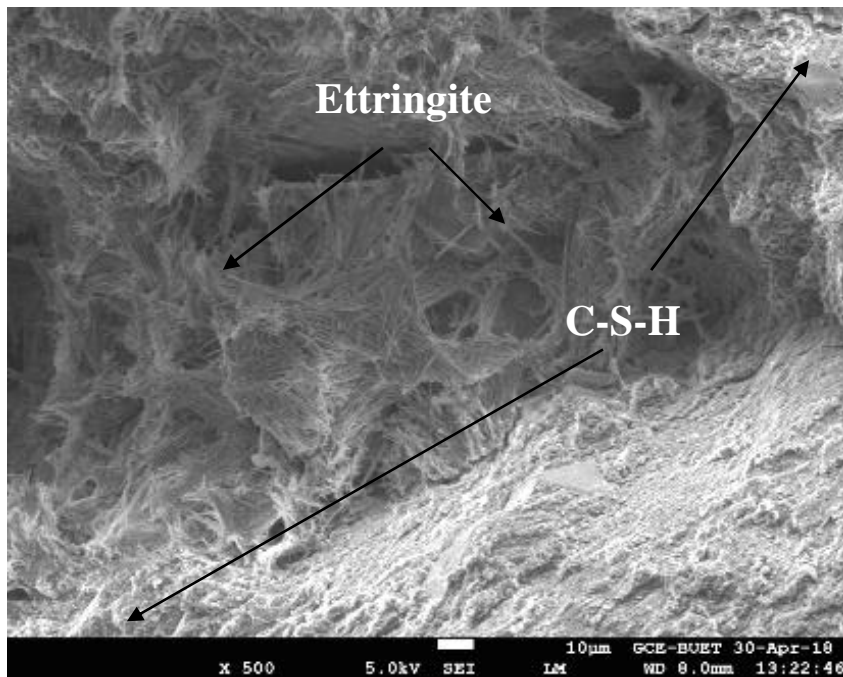


Figure 4.51: SEM image of C1 cubes submerged in tannery wastewater for 180 days (500x zoom)

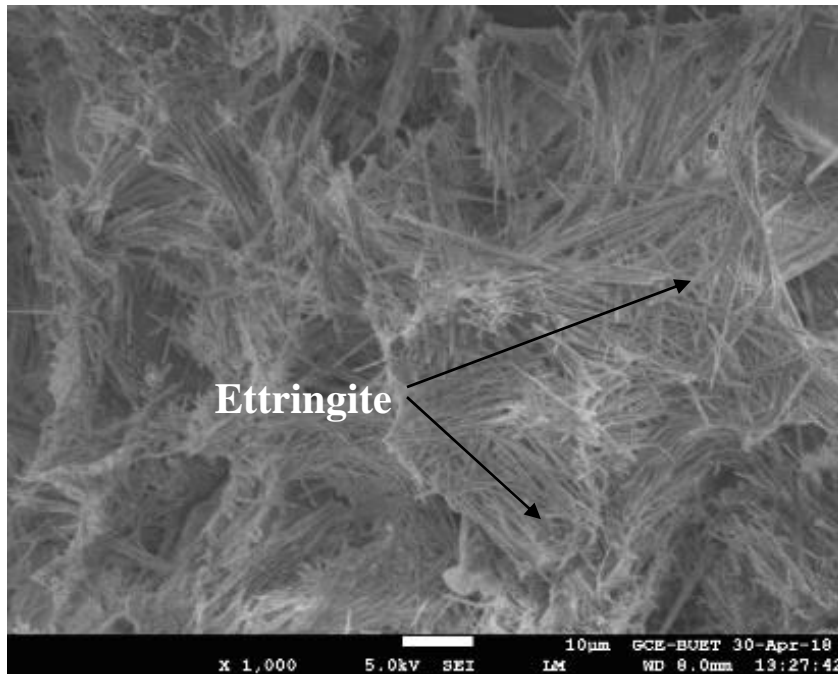


Figure 4.52: SEM image of C1 cubes submerged in tannery wastewater for 180 days (1000x zoom)

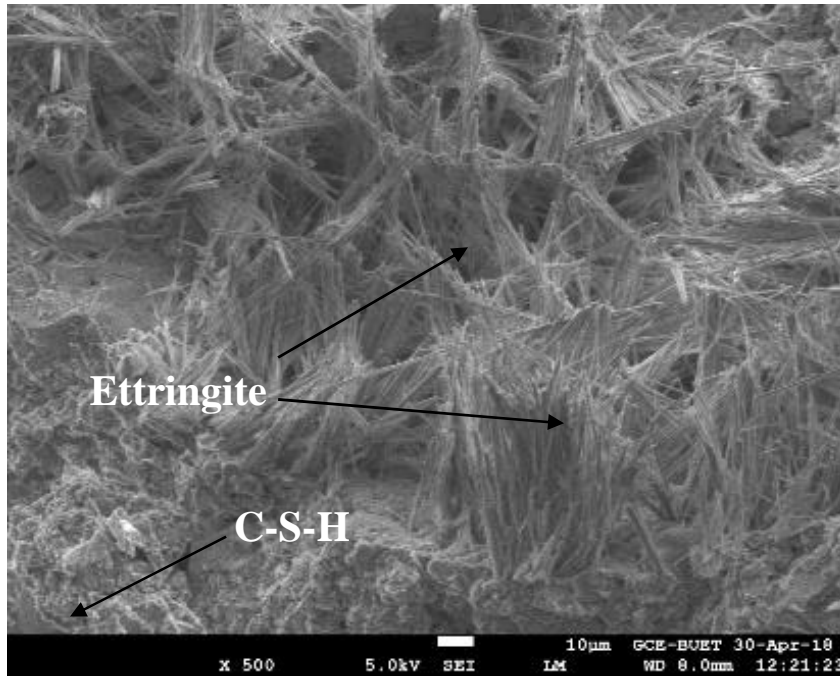


Figure 4.53: SEM image of C2 cubes submerged in tannery wastewater for 180 days (500x zoom)

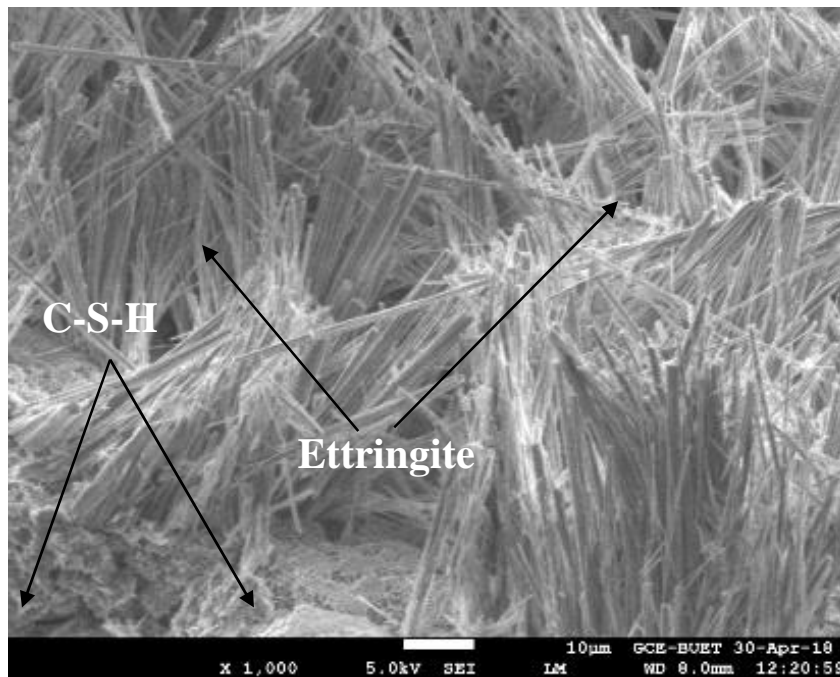


Figure 4.54: SEM image of C2 cubes submerged in tannery wastewater for 180 days (1000x zoom)



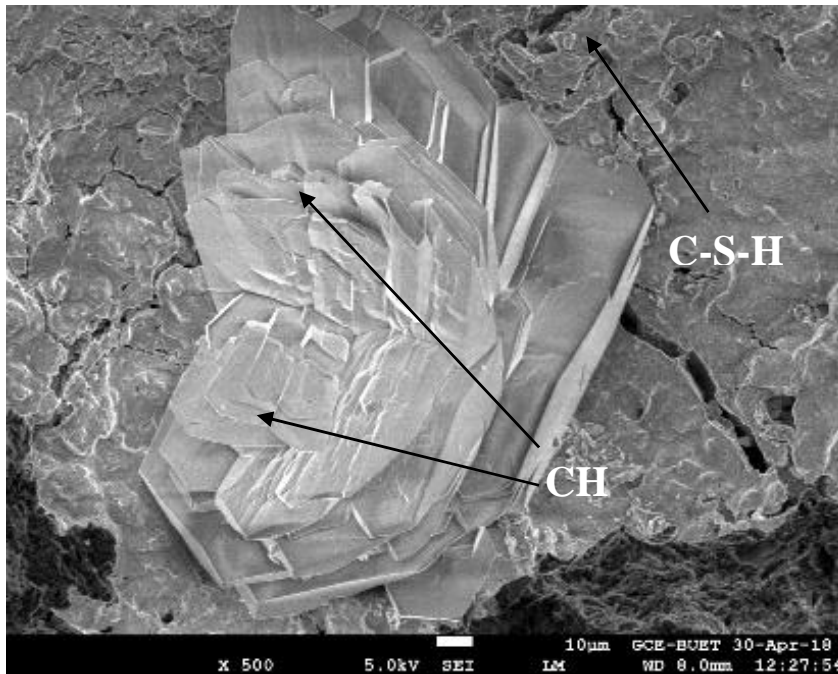


Figure 4.55: SEM image of C5 cubes submerged in tannery wastewater for 180 days (500x zoom)

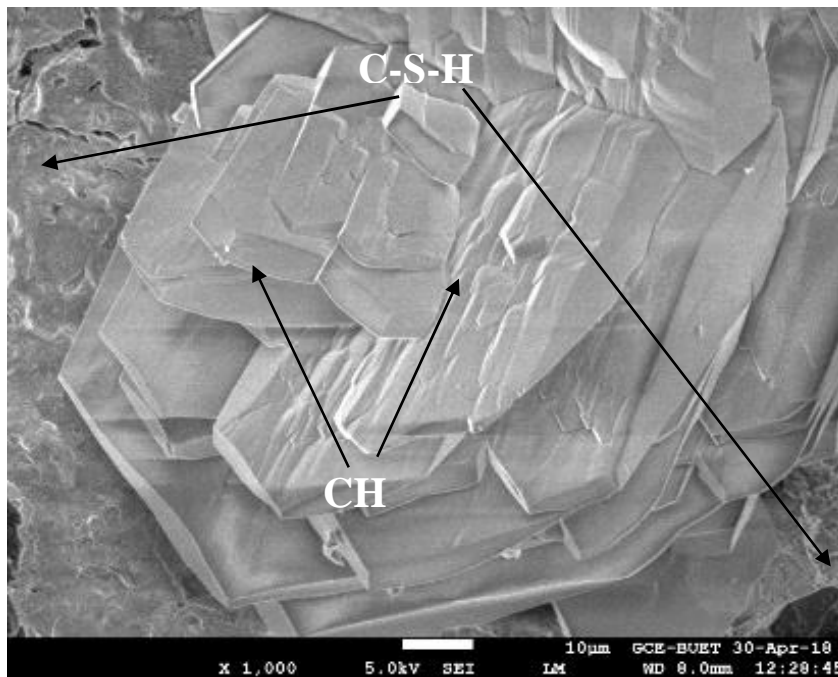


Figure 4.56: SEM image of C5 cubes submerged in tannery wastewater for 180 days (1000x zoom)

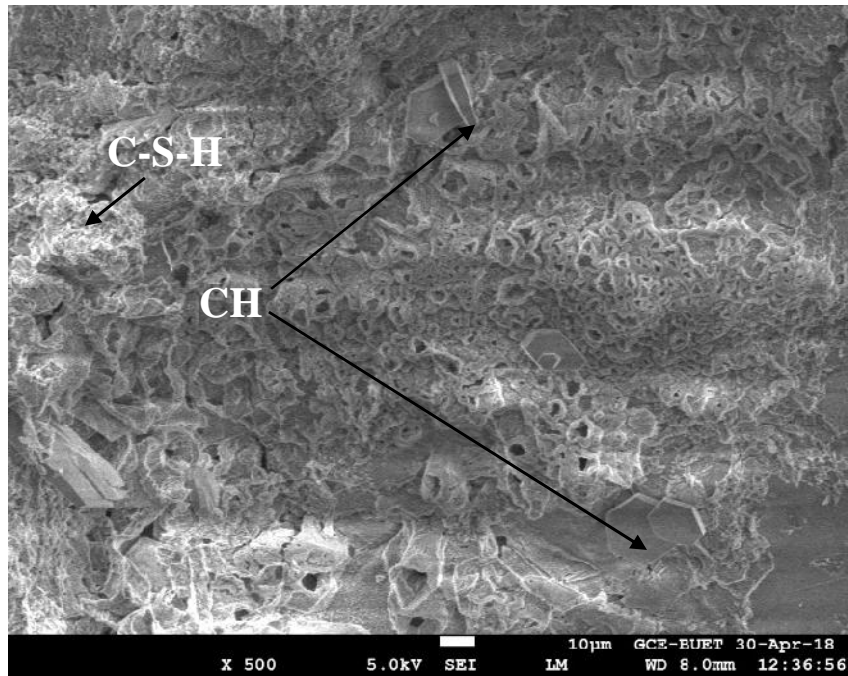


Figure 4.57: SEM image of C6 cubes submerged in tannery wastewater for 180 days (500x zoom)

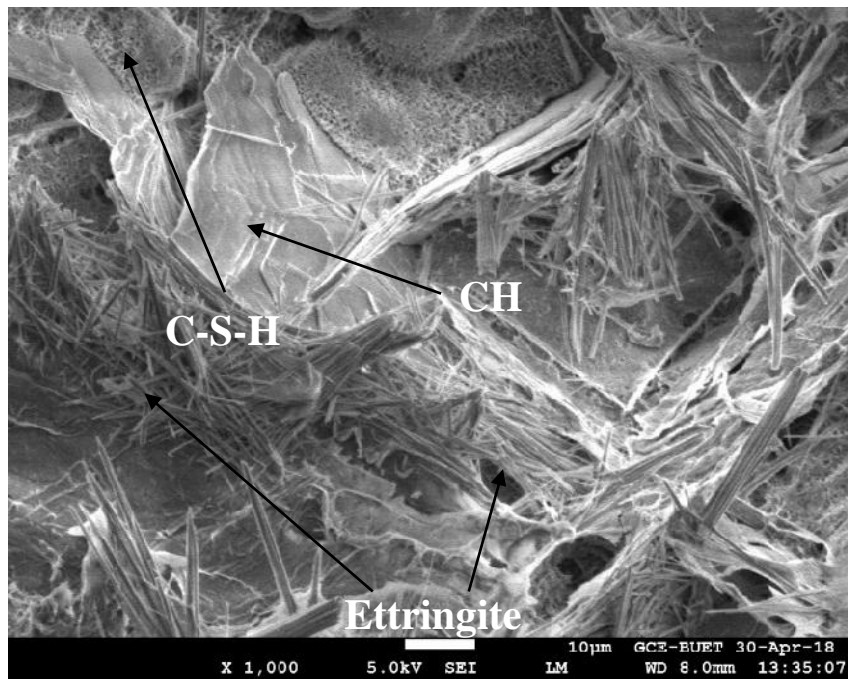
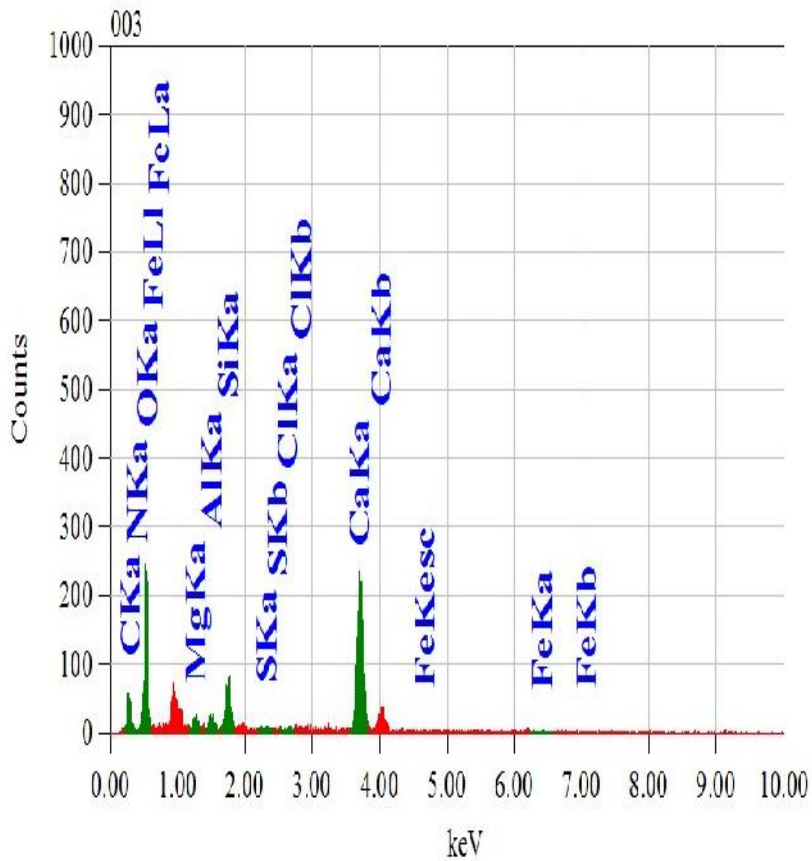


Figure 4.58: SEM image of C6 cubes submerged in tannery wastewater for 180 days (1000x zoom)

Needle like ettringite crystals are observed in cubes submerged in tannery wastewater from SEM images shown in Figures 4.51 to Figure 4.58. More ettringite formation is present in OPC (C1) image. Sulfate present in tannery wastewater reacts with monosulfate, transformed from exhausted portlandite and form ettringite. It can be observed that amount of C-S-H formation is relatively less in fly ash blended (C2) and both fly ash and slag blended cement mix (C6) compared to only slag blended cement mix (C5). Less amount of C-S-H leads to more damage in cubes which reflects compressive strength test results.

#### **4.10 Energy-Dispersive X-ray Spectroscopy (EDS) Analysis of Cube Samples**

Elemental analysis of cube samples was carried out through energy-dispersive X-ray spectroscopy (EDS/EDX). It is observed that presence of calcium is less in cubes submerged in tannery wastewater (Figure 4.61 to Figure 4.64) than cubes kept in normal condition (Figure 4.59 and Figure 4.60) as leaching of calcium happens when subjected to tannery wastewater. However, C2, C5 and C6 cubes have relatively more calcium than C1 cube which verify the hypothesis of increased strength and less damage in blended cement. About 42 % calcium is present in C1 cubes of normal condition while under tannery wastewater, C1 shows 8.13% calcium. On the other hand, C2, C5 and C6 show 14.46%, 24.96 % and 22.21% of calcium, respectively in tannery wastewater condition. The results are analogous to the findings of SEM images.



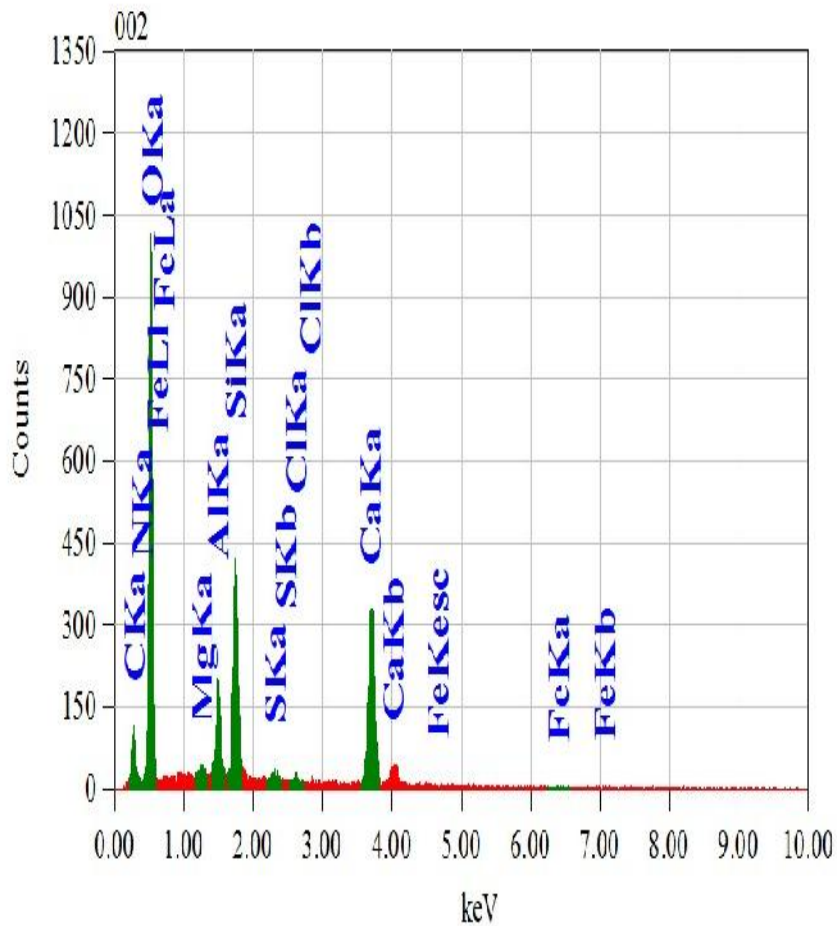
Acquisition Parameter  
 Instrument : 7600F  
 Acc. Voltage : 10.0 kV  
 Probe Current: 1.00000 nA  
 PHA mode : T3  
 Real Time : 30.11 sec  
 Live Time : 30.00 sec  
 Dead Time : 0 %  
 Counting Rate: 336 cps  
 Energy Range : 0 - 20 keV

ZAF Method Standardless Quantitative Analysis

Fitting Coefficient : 0.1838

Element	(keV)	Mass%	Sigma	Atom%	Compound	Mass%	Cation	K
C K	0.277	7.18	0.22	13.25				4.7668
N K								
O K	0.525	41.37	0.97	57.32				27.2909
Mg K	1.253	0.78	0.11	0.71				0.7950
Al K	1.486	0.91	0.12	0.75				1.0303
Si K	1.739	3.93	0.23	3.10				4.9694
S K	2.307	0.24	0.08	0.17				0.3224
Cl K	2.621	0.09	0.08	0.06				0.1245
Ca K	3.690	42.20	1.06	23.34				56.9029
Fe K	6.398	3.30	0.82	1.31				3.7979
Total		100.00		100.00				

Figure 4.59: EDS analysis of C1 cube in normal condition



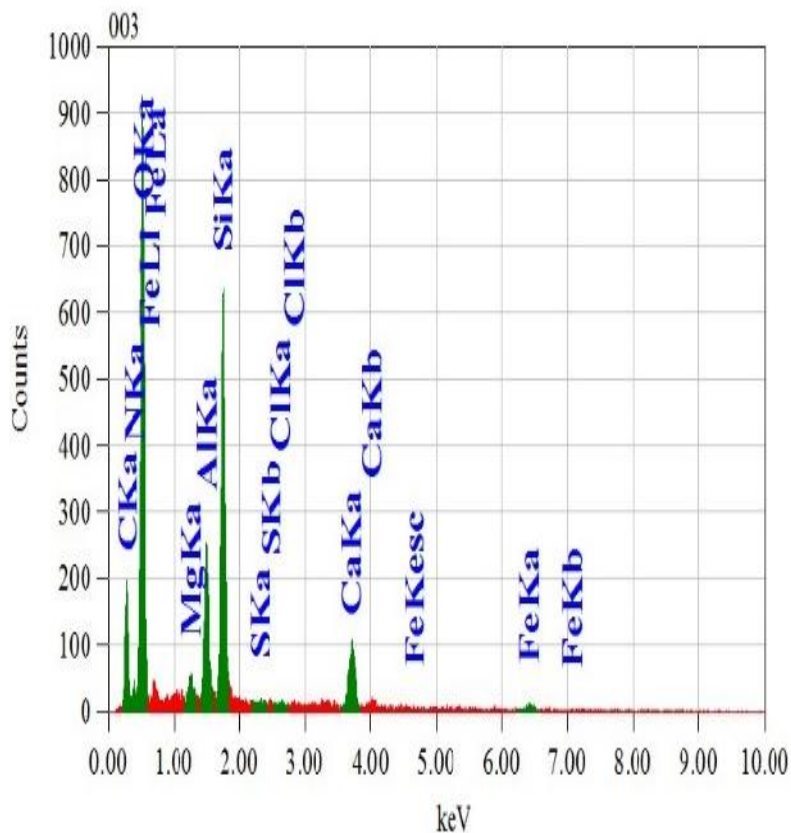
Acquisition Parameter  
 Instrument : 7600F  
 Acc. Voltage : 10.0 kV  
 Probe Current: 1.00000 nA  
 PHA mode : T3  
 Real Time : 30.20 sec  
 Live Time : 30.00 sec  
 Dead Time : 0 %  
 Counting Rate: 791 cps  
 Energy Range : 0 - 20 keV

ZAF Method Standardless Quantitative Analysis

Fitting Coefficient : 0.0807

Element	(keV)	Mass%	Sigma	Atom%	Compound	Mass%	Cation	K
C	0.277	7.01	0.15	11.56				3.7490
N								
O	0.525	53.42	0.61	66.14				45.5722
Mg	1.253	0.35	0.06	0.29				0.3681
Al	1.486	3.29	0.13	2.42				3.7638
Si	1.739	8.88	0.21	6.26				11.1011
S	2.307	0.52	0.06	0.32				0.6745
Cl	2.621	0.20	0.05	0.11				0.2697
Ca	3.690	25.56	0.54	12.63				33.6355
Fe	6.398	0.77	0.33	0.27				0.8660
Total		100.00		100.00				

Figure 4.60: EDS analysis of C6 cube in normal condition



Acquisition Parameter  
 Instrument : 7600F  
 Acc. Voltage : 10.0 kV  
 Probe Current: 1.00000 nA  
 PHA mode : T3  
 Real Time : 30.20 sec  
 Live Time : 30.00 sec  
 Dead Time : 0 %  
 Counting Rate: 749 cps  
 Energy Range : 0 - 20 keV

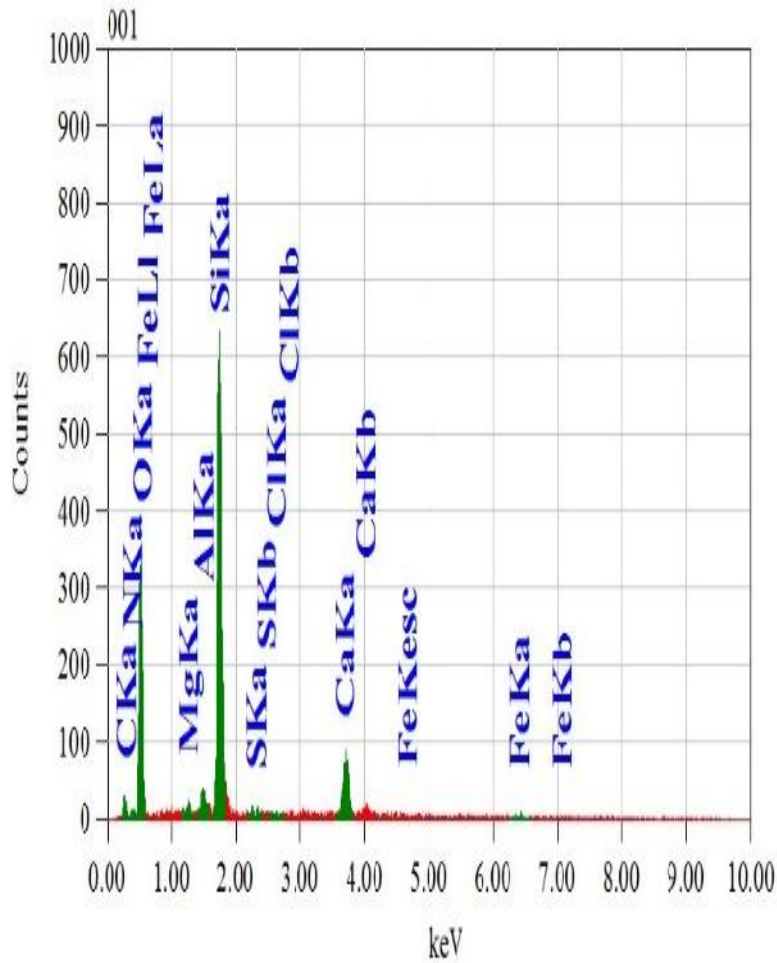
ZAF Method Standardless Quantitative Analysis

Fitting Coefficient : 0.0798

Element	(keV)	Mass%	Sigma	Atom%	Compound	Mass%	Cation	K
C K	0.277	16.73	0.27	24.95				7.5545
N K	0.392	4.15	0.26	5.31				3.9945
O K	0.525	45.61	0.55	51.07				46.0592
Mg K	1.253	0.72	0.07	0.53				0.7980
Al K	1.486	4.81	0.15	3.20				5.7657
Si K	1.739	15.39	0.29	9.81				19.7750
S K	2.307	0.15	0.05	0.08				0.1894
Cl K	2.621	0.18	0.06	0.09				0.2491
Ca K	3.690	8.13	0.33	3.63				10.8563
Fe K	6.398	4.13	0.62	1.32				4.7582
Total		100.00		100.00				

Figure 4.61: EDS analysis of C1 cube in tannery wastewater





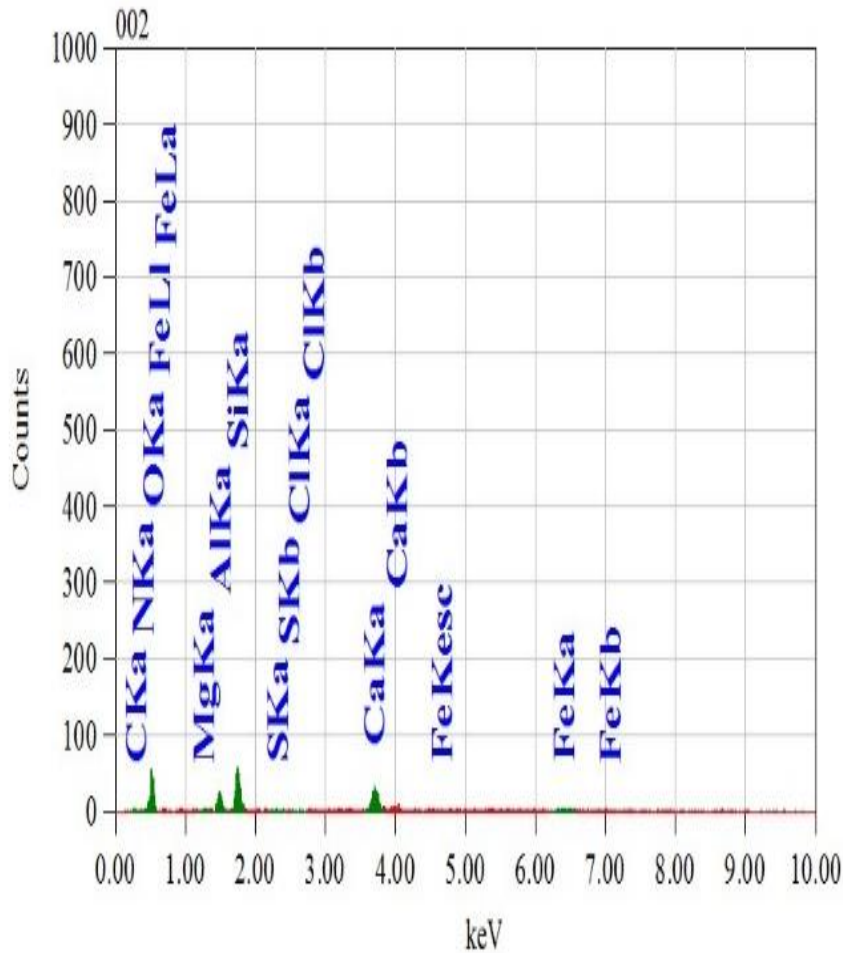
Acquisition Parameter  
 Instrument : 7600F  
 Acc. Voltage : 10.0 kV  
 Probe Current: 1.00000 nA  
 PHA mode : T3  
 Real Time : 30.12 sec  
 Live Time : 30.00 sec  
 Dead Time : 0 %  
 Counting Rate: 407 cps  
 Energy Range : 0 - 20 keV

ZAF Method Standardless Quantitative Analysis

Fitting Coefficient : 0.1050

Element	(keV)	Mass%	Sigma	Atom%	Compound	Mass%	Cation	K
C	0.277	5.65	0.27	9.78				1.7145
N	0.392	2.72	0.32	4.04				2.1698
O	0.525	40.17	0.80	52.24				34.4138
Mg	1.253	0.69	0.10	0.59				0.7058
Al	1.486	0.98	0.12	0.76				1.0910
Si	1.739	32.26	0.60	23.90				39.1357
S	2.307	0.15	0.08	0.10				0.1722
Cl	2.621	0.01	0.08	0.01				0.0137
Ca	3.690	14.46	0.65	7.51				17.5001
Fe	6.398	2.92	0.85	1.09				3.0834
Total		100.00		100.00				

Figure 4.62: EDS analysis of C2 cube in tannery wastewater



Acquisition Parameter  
 Instrument : 7600F  
 Acc. Voltage : 10.0 kV  
 Probe Current: 1.00000 nA  
 PHA mode : T3  
 Real Time : 30.08 sec  
 Live Time : 30.00 sec  
 Dead Time : 0 %  
 Counting Rate: 107 cps  
 Energy Range : 0 - 20 keV

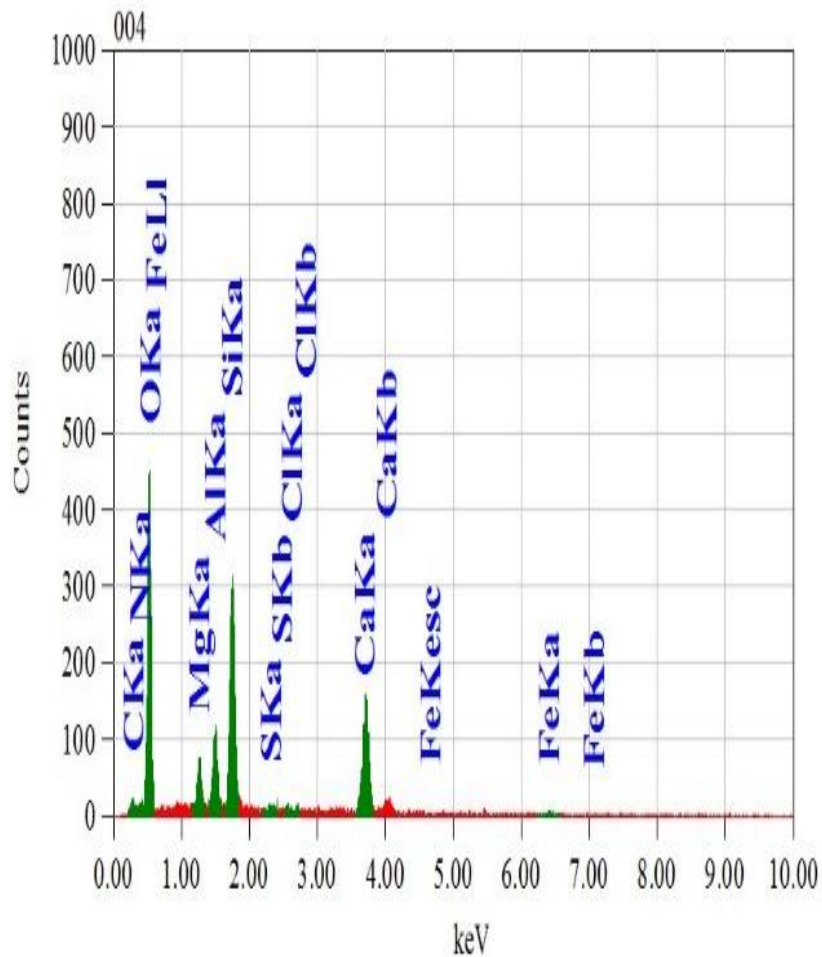
ZAF Method Standardless Quantitative Analysis

Fitting Coefficient : 0.2967

Element	(keV)	Mass%	Sigma	Atom%	Compound	Mass%	Cation	K
C	0.277	1.72	0.10	3.69				0.6474
N	0.392	0.56	0.43	1.02				0.4057
O	0.525	31.36	0.61	50.36				24.7370
Mg	1.253	0.53	0.15	0.56				0.4738
Al	1.486	5.67	0.32	5.40				5.7000
Si	1.739	14.54	0.57	13.30				15.9866
S	2.307	0.44	0.15	0.35				0.5076
Cl	2.621	0.14	0.15	0.10				0.1667
Ca	3.690	24.96	1.11	16.00				30.1834
Fe	6.398	20.09	2.65	9.24				21.1919
Total		100.00		100.00				

Figure 4.63: EDS analysis of C5 cube in tannery wastewater





Acquisition Parameter  
 Instrument : 7600F  
 Acc. Voltage : 10.0 kV  
 Probe Current: 1.00000 nA  
 PHA mode : T3  
 Real Time : 30.14 sec  
 Live Time : 30.00 sec  
 Dead Time : 0 %  
 Counting Rate: 437 cps  
 Energy Range : 0 - 20 keV

ZAF Method Standardless Quantitative Analysis

Fitting Coefficient : 0.1277

Element	(keV)	Mass%	Sigma	Atom%	Compound	Mass%	Cation	K
C K	0.277	2.98	0.16	5.15				1.2641
N K	0.392	2.12	0.30	3.14				1.7193
O K	0.525	48.58	0.84	62.90				41.5010
Mg K	1.253	2.65	0.16	2.26				2.6976
Al K	1.486	4.27	0.21	3.28				4.6692
Si K	1.739	14.65	0.40	10.80				17.4282
S K	2.307	0.25	0.08	0.16				0.3021
Cl K								
Ca K	3.690	22.10	0.75	11.42				27.8170
Fe K	6.398	2.39	0.76	0.89				2.6015
Total		100.00		100.00				

Figure 4.64: EDS analysis of C6 cube in tannery wastewater

#### **4.11 Concluding Remarks**

Various properties of cement and mortar such as compressive strength, expansion, weight loss as well as setting time, consistency and flowability of eight cement mix combinations were studied. To conclude, it can be stated that fly ash blended cement showed less expansion while slag blended cement showed higher strength. Slag provides better hydration due to its binding capacity and fly ash provides late hydration due to its pozzalonic activity. It is obvious that use of slag alone does not exhibit better long term permeability of composites. On the other hand, only fly ash addition reduces the strength of mortar. To limit both strength loss and expansion, combination of both fly ash and slag mixed cement can be suggested. However, only fly ash blended cement mortars have showed acceptable values of expansion which is why fly ash blended cement has been recommended in tannery wastewater.

## **Chapter 5**

### **CONCLUSIONS AND SUGGESTIONS**

#### **5.1 Conclusions**

The performance of supplementary cementitious materials like fly ash and slag on strength and durability properties of mortar exposed to tannery wastewater were investigated in this thesis. Mortar cubes with OPC and blended cement mix were prepared and submerged in simulated water prepared in laboratory containing dominant constituents of tannery wastewater. The results unraveled the differences in behavior of cement mixes with partial replacement of cement by fly ash and slag, individually and both combined. A tentative optimum replacement level of these supplementary materials is estimated and the major findings of the work are summarized below:

- i. Higher consistency values of 25.5% and 26% were detected in slag blended cement paste (C4 & C5) whereas a constant value of 25% was observed in OPC and other five blended cement pastes.
- ii. High values of setting time were observed in blended cement mortars compared to OPC.
- iii. Blended cement mortars showed improved value of flowability compared to OPC.
- iv. The strength loss in only slag mixed cement mortar under tannery wastewater was less than that of cement mortar with fly ash only. The loss of strength after 180 days submergence for slag blended C5 mortar was 55.2% while that for fly ash blended C2 mortar was 61.6%. While, strength loss value of C1 (OPC) and C6 (both fly ash and slag mixed combination) mortar were 63% and 62.2%, respectively.
- v. Weight loss in OPC cement mortar under tannery wastewater for 180 days was 5.47% while all blended cement mix mortars showed less weight loss. The highest loss in fly ash mixed mortars was 2.58% and slag mixed mortars was 3.17%. The weight loss value for mortar mixed with both supplementary materials (C6) was 3.17%.

- vi. The expansion in OPC mortar bars under tannery wastewater found to be 0.64% after 26 weeks which was much greater than that of other seven blended cement combinations. Only fly ash blended combinations showed almost no expansion while only slag blended combinations showed up to 0.47% expansion. When both fly ash and slag were present in cement, the corresponding values of expansion for mortar bars in tannery wastewater were 0.22%, 0.13% and 0.16% for C6, C7 and C8, respectively.
- vii. Among the seven blended combinations, slag mixed mortars showed higher strength while fly ash mixed ones showed less expansion and weight loss when submerged in tannery wastewater.
- viii. Deterioration was detected through surface images of cubes submerged in tannery wastewater. While only fly ash mixed cubes showed less damage than only slag mixed cubes, overall blended cement mortar cubes showed less surface degradation than OPC ones.
- ix. The SEM images demonstrate less C-S-H formation in fly ash mixed cement mortar. Sulfate in tannery wastewater reacts with monosulfate present in mortar and form ettringite leading to deterioration and loss of strength.
- x. The EDS data revealed a decline in the relative percentage of calcium by mass in all cement mortars submerged in tannery wastewater. However, the decrease in relative percentage of calcium was relatively greater in OPC than blended cement, endorsing the hypothesis that greater leaching of Portlandite occurred in OPC.
- xi. Considering expansion limit for cement mortar as per ACI 318-14, only fly ash blended cement has shown desired performance. As expansion is high priority issue, the optimum replacement level for fly ash in cement is recommended to be 30% for producing composite cement to be used in tannery waste water.

- xii. For slag blended cement (C4 to C8), expansion values are observed higher than ACI limit. Test should be conducted in mortar bars prepared from slag blended cement submerged in standard sulfate test solution as per ASTM C1012 for 18 months period to study their expansion in sulfate exposure.

Concrete prepared with such blended cement is environmentally friendly and demonstrates the attributes of high-performance concrete. About 10~15% reduction from cement industry can be estimated with 30~40% replacement level of cement with supplementary materials. This becomes one example of a construction material in harmony with the concept of sustainable development: lower environmental impact (reduced CO<sub>2</sub> emission), judicious use of resources such as energy conservation with use of by-products and in terms of durability, such blends are vastly superior to plain Portland cement concrete.

## **5.2 Suggestions for Future Study**

As it was mentioned in the introductory chapter, there are a lot of possibilities for further exploration which were out of the scope of this thesis. During the course of this research, there was always an urge to expand the scope of the study. Some suggestions are made with regard to future research work.

- i. The use of concrete samples as test specimens is recommended for better understanding of the overall strength of concrete structures prepared from blended cement, exposed to such extreme chemical conditions.
- ii. This research only looked into the adverse effect of aggressive constituents in tannery wastewater on the degradation of cement mortars. Issues such as concrete carbonation and chloride content in concrete could have significant effect on durability of reinforcements in the reinforced concrete structures. Further studies should be carried out to observe these concerns.
- iii. The author suggests that when further study is undertaken on this line of work, the readings should be continued to be taken for a longer time period preferably with more number of specimens for each test day in the hope of acquiring data which

produce more significant results. Expansion test should be conducted for 18 months duration to study expansion limits as per ACI 318-14.

- iv. Locally available admixtures could be used in some mortar samples prepared from blended cement mixes to compare their strength, expansion and weight loss with samples without admixtures.
- v. A comparative study could be conducted between performance of locally produced PCC mortar and the recommended blended cement mortar under different aggressive environmental conditions such as in dyeing industry, pharmaceutical industry, food and beverage industry, etc.

## References

ACI 318-14 (2014). Building Code Requirement for Structural Concrete. *American Concrete Institute*. Farmington Hills, MI, 2014.

Alaa, M. R., Hosam El-Din, H. S. and Amir, F.S. (2014). Effect of silica fume and slag on compressive strength and abrasion resistance of HVFA concrete. *Int. J. Concr. Struct. Mater.* 8(1): 69–81.

Alasali, M. M. and Malhotra, V. M. (1991). Role of Concrete Incorporating High Volumes of Fly Ash in Controlling Expansion Due to Alkali-Aggregate Reaction, *ACI Materials & Journal*, V 88, No. I, Mar.-Apr, pp. 159-165.

Alexander, M., Bertron, A. and Belie, N.D. (2012). *Performance of Cement Based Materials in Aggressive Aqueous Environments*, STAR 211-PAE, Springer, (Page 4, Chapter 1, Part I).

Al-Muti, S. A. and Ahmad, N. (2015). Bangladesh: Billion Dollar Leather Sector Poised for Growth after Environmental Reform, *The Asia Foundation*, Dhaka, Bangladesh.

ASTM C109 / C109M-13e1 (2013). Standard Test Method for Compressive Strength of Hydraulic Cement Mortars (Using 2-in. or [50-mm] Cube Specimens), *ASTM International*, West Conshohocken, PA.

ASTM C1012 / C1012M-15 (2015). Standard Test Method for Length Change of Hydraulic-Cement Mortars Exposed to a Sulfate Solution, *ASTM International*, West Conshohocken, PA.

ASTM C1437-07 (2007). Standard Test Method for Flow of Hydraulic Cement Mortar, *ASTM International*, West Conshohocken, PA.

ASTM C157 / C157M-08 (2008). Standard Test Method for Length Change of Hardened Hydraulic-Cement Mortar and Concrete, *ASTM International*, West Conshohocken, PA.

ASTM C187-98 (1998). Standard Test Method for Normal Consistency of Hydraulic Cement, *ASTM International*, West Conshohocken, PA.

ASTM C191-13 (2013). Standard Test Methods for Time of Setting of Hydraulic Cement by Vicat Needle, *ASTM International*, West Conshohocken, PA.

ASTM C230 / C230M-14 (2014). Standard Specification for Flow Table for Use in Tests of Hydraulic Cement, *ASTM International*, West Conshohocken, PA.

ASTM C305-14 (2014). Standard Practice for Mechanical Mixing of Hydraulic Cement Pastes and Mortars of Plastic Consistency, *ASTM International*, West Conshohocken, PA.

ASTM C490 / C490M-11e1 (2011). Standard Practice for Use of Apparatus for the Determination of Length Change of Hardened Cement Paste, Mortar, and Concrete, *ASTM International*, West Conshohocken, PA.

ASTM C778-13 (2013). Standard Specification for Standard Sand, *ASTM International*, West Conshohocken, PA.

Ates, E, Orhon, D. and Tunay. O. (1997). Characterization of tannery wastewaters for pretreatment selected case studies. *Water Sci Technol*; 36:217–23.



Bajza, A., Rousekova, I. and Vrana, O. (1986). Corrosion of hardened cement pastes by  $\text{NH}_4\text{NO}_3$  solutions, In: *8<sup>th</sup> International Congress on the Chemistry of Cement*, Rio, pp 99-103.

Baxi, C. and Patel, S.K. (1998). Concrete exposed to calcium ammonium nitrate. In: *Gjorv, O.E. Sakai*.

Berube, M. A., Duchesne, J. and Chouinard, D. (1995). Why the Accelerated Mortar Bar Method ASTM C 1260 is Reliable for Evaluating the Effectiveness of Supplementary Cement. *Cement, Concrete, and Aggregates*, V. 17, No. 1, pp. 26-34.

BGC Cement (2017). Slag or Fly ash – What’s the difference? Available at: <http://bgccement.com.au/2017/09/28/slag-or-flyash/> (Accessed on June 6, 2018).

Biczok, I. (1972). Concrete corrosion and concrete protection, *Akademiai Kiado*, Budapest.

Birbilis, N. and Cherry, B.W. (2004). Alternative methodology for on-site monitoring of corrosion and remediation of reinforced concrete, *Sci Technol*, 39 (4).

Bleszynski, R.F. and Thomas, M.D.A. (1998). Microstructural studies of alkali- silica reaction in fly ash concrete immersed in alkaline solutions, *Adv Cem Based Mater* 7, 66-78.

Bosnic, M., Buljan, J. and Daniels, R. P. (2000). Pollutants in tannery effluents, 9 august 2000, us/ras/92/120, *Regional Programme for Pollution Control in the Tanning Industry in South-East Asia*, United Nations Industrial Development Organization (UNIDO).

Brooks, J.J., Johari, M.A. and Mazloom. M (2000) Effect of admixtures on the setting time of high strength concrete, *Cement Concr. Compos.*, 22 (4), pp. 293-301.

Brundtland Commission (1987). Our common future technical report. World Commission on Environment and Development (WCED). Oxford: *Oxford University press*.

BS EN 197-1 (2011). Cement. Composition, specifications and conformity criteria for common cements.

Buck, A.D. and Mather, K. (1987). Methods for controlling effects of alkali-silica reaction in concrete, *Technical Report No. SL- 87 - 6*, US, Army Corps of Engineers, Waterways Experiment Station, Vicksburg.

CANMET (1997). High-Volume Fly Ash Concrete Using Canadian Fly Ashes, Phase II: Effectiveness of High-Volume of Fly Ash in Concrete to Control Alkali-Silica Reactions, *CEA Project No. 9017 G 804, prepared by CANMET for the Canadian Electrical Association*, Oct. 1997, 84 pp.

Carde. C, Francois. R. and Torrenti. J.M. (1996). Leaching of both calcium hydroxide and c-s-h from cement paste: modeling the mechanical behavior, *Cem, Concr, Res.*, 26(8), 1257-1268.

Carette, G.G. and Malhotra, V.M. (1984). Characterisation of Canadian fly ashes and their performance in concrete. in: *CANMET Technical Report MRP/MSL 8U-137*, Ottawa.

Chowdhury, M., Mostafa, M.G., Biswas, T.K. and Saha, A.K. (2013). Treatment of leather industrial effluents by filtration and coagulation processes. *Water Resources and Industry*, Volume 3, September 2013, Pages 11-22.

Chu, V. T. H. (2007). What-is-the-advantage-of-using-ggbs-asreplacement- of- cement-in-concrete. *A self learning manual – mastering different fields of civil engineering works*.

Damtoft, J. S., Lukasik, J., Hertford, D., Sorrentino, D. and M.Gartner, E. (2008). Sustainable development and climate change initiatives, *Cem. Concr. Res.*, 38, 115–127.

Dave, N., Misra, A. K., Srivastava, A. and Kaushik, S.K. (2016). Setting time and standard consistency of quaternary binders: The influence of cementitious material addition and mixing. *International Journal of Sustainable Built Environment*, Volume 6, Issue 1, June 2017, Pages 30-36, <https://doi.org/10.1016/j.ijsbe.2016.10.004>.

Demirboga, R. (2007). Thermal conductivity and compressive strength of concrete incorporation with mineral admixtures. *Build. Environ.*42, pp. 2467-2471.

Diamond, S. and Lopez -Flores, F. (1981). On the distinction in physical and chemical characteristics between lignite and bituminous fly ash, in: S. Diamond (Ed.), Effects of Fly ash Incorporation in Cement and Concrete, *Proceedings of the MRS Symposium N, Materials Research Society*, Boston, pp. 34-44.

Duchesne, J. and Berube, M.A. (1994). The effectiveness of supplementary cementing materials in suppressing expansion due to ASR. Another look at the reaction mechanisms. Part 1: Concrete expansion and Portlandite depletion. *Cement and Concrete Research*, 24: 73–82.

Dunstan, E.R. (1981). The effect of fly ash on concrete alkali-aggregate reaction, *Cem Concr Aggregates*, 3 (2), 101-104.

EHE-08 (2008). Ed. Instructions of Concrete Structures. *Ministry of Foment*, Spain.

Escadeillas, G/ (2012). *Performance of Cement Based Materials in Aggressive Aqueous Environments*, STAR 211-PAE, Springer, (pp. 117-122, Chapter 5, Part I).

Flatt, R.J. (2002). Salt Damage in Porous Materials: How High Supersaturation in Generated. *Journal of Crystal Growth*, 242:434-54.

Federation internationale de la Precontrainte (1988). Condensed silica fume in concrete. *Thomas Telford Ltd*, London.

Fly Ash Facts for Highway Engineers Booklet (2017). Chapter 3 - Fly Ash in Portland Cement Concrete. Available at:  
<https://www.fhwa.dot.gov/pavement/recycling/fach03.cfm>. (Accessed on June 8, 2018).

Frigione, G. and Zenone, F. (1992) Influence of gypsum content in Portland cement. *9<sup>th</sup> International Congress Chemistry of Cement*, New Delhi, IV: 60-86.

Gladstone Regional Council (2017). Odour and Corrosion Modelling Report. Available at:  
<http://www.gladstone.qld.gov.au/documents/1570002/44588629/G%203.2.5.1%20CH2M%20Australia%20Pty%20Ltd%20%28June%202017%29%20Odour%20and%20Corrosion%20Modelling%20Report.pdf> (Accessed 13 August, 2018).

Gollop, R.S. and Taylor, H.F.W. (1996). Microstructural and microanalytical studies of sulfate attack IV. Reactions of a slag cement paste with sodium and magnesium sulfate solutions. *Cement and Concrete Research* 26: 1013-1028.

Gonclaves, A. and Rodrigues, X. (1991). The resistance of cement to ammonium nitrate attack, In: *Proceedings of the 2<sup>nd</sup> International Conference on CANMET/ACI Durability of Concrete*, Montreal, Canada.

Gu, P., Beaudoin, J. J., Zhang, M. H. and Malhotra, V. M. (1998). Performance of Reinforcing Steel in Portland Cement and High-Volume Fly Ash Concrete, *MTL Division Report MTL 98-1 1 (OP&J)*, Natural Resources Canada, Ottawa, 1998, 19 pp.

Harrison, A. J. W. (2003). TecEco cement concretes—abatment, sequestration and waste utilization in the built environment. TecEco Pty. Ltd., Hobart, Tasmania, Australia. Available at: <http://www.tececo.com/files/conference%20papers/TecEcoTechnologyAbatementSequestrationandWasteUtilisation290105.pdf>. (Accessed on March 12, 2012).

Hooton, R.D. (2000). Canadian use of ground granulated blast-furnace slag as a supplementary cementing material for enhanced performance of concrete. *Can. J. Civ. Eng.* 27 (4), 754–760.

Hooton, R.D. and Emery, J.J. (1990). Sulfate resistance of a Canadian slag cement. *ACI Materials*, 87: 547–555.

Hughes, D.C (1985). Sulfate resistance of OPC/fly ash and SRPC pastes, pore structure and permeability, *Cement and Concrete Research* 15: 1003-1012.

Hvitved-Jacobsen, T., (2002) Sewer Processes – Microbial and Chemical Process Engineering of Sewer Networks. *CRC Press*, Boca Raton, Florida, USA.

Intergovernmental Panel on Climate Change (IPCC) (1997). *Revised 1996 IPCC Guidelines for National Greenhouse Gas Inventories*. Reference Manual (Revised). Vol 3. J.T. Houghton et al., IPCC/OECD/IEA, Paris, France.

Islam, B.I., Musa, A.E., Ibrahim, E.H., Sharafa, S.A.A. and Elfaki, B.M. (2014). Evaluation and Characterization of Tannery Wastewater. *Journal of Forest Products & Industries*; 3(3): 141-150.

Jahan. M.A.A, Akhtar. N, Khan. N.M.S, Roy. C.K, Islam. R and Nurunnabi (2014). Characterization of tannery wastewater and its treatment by aquatic macrophytes and algae. *Bangladesh Journal of Scientific and Industrial Research* 2014; 49(4): 233-242.

Khatib, J.M. and Hibbert, J.J. (2005). Selected Engineering properties of concrete incorporating slag and metakaolin. *Constr. Build. Mater. J.* 19 (2005), 460–472.

Khatri, R. P., Sirivivatnanon, V. and Gross, W. (1995). Effect of different supplementary cementitious materials on mechanical properties of high performance concrete. *Cement and Concrete Research*, Volume 25, Issue 1, Pages 209-220.

Klieger, P. and Gebler, S. (1987). Fly ash and concrete durability, *Concrete Durability, Katharine and Bryant Mather International Conference*, ACI SP- 100, vol. 1, American Concrete Institute, Detroit, 1043-1069.

Kondraivendhan, B. and Bhattacharjee, B. (2015). Flow behavior and strength for fly ash blended cement paste and mortar. *International Journal of Sustainable Built Environment* (2015) 4, 270–277, The Gulf Organisation for Research and Development. <http://dx.doi.org/10.1016/j.ijsbe.2015.09.0012212-6090/>.

Kolleck, J.J. and Lumly, J.D. (1990). Comparative sulfate resistance of SRPC and Portland slag cements. Durability of Building Materials and Components. *Proceedings of 5<sup>th</sup> International Conference*, Brighton UK, Ed. E & F N. Spon, paper 43.

Lea, F.M. (1965). The action of ammonium nitrate salts on concrete, *Magazine of Concrete Research* 17 (52):115-116.

Lee, C. (1989). Effects of alkalis in Class C fly ash on alkali-aggregate reaction, in: V.M. Malhotra (Ed.), *Proceedings of the 3rd International Conference on the Use of Fly Ash, Silica Fume, Slag and Natural Pozzolans in Concrete*, ACI SP- 114, vol. 1, American Concrete Institute, Detroit, pp. 417-430.

Mailvaganam, N.P., Bhagrath, R.S. and Shaw, K.L. (1983). Effects of admixture on Portland cement concretes incorporating blast furnace slag and fly ash, in *The 1st International Conference on the use of Fly Ash, Silica Fume, Slag, and other Mineral By-products in Concrete (CANMET/ACI)*: Proceedings, vol. 1. July 31–August 5, 19883, Montebello, Quebec. Canada: American Concrete Institute, ACI SP79, 519–537.

Maley, B. (2006). Deterioration of wastewater treatment and collection system assets: knowing where and how to look. Available at: [http://ftp.weat.org/Presentations/05-Sherman\\_Maley-Knowing%20Where%20and%20How%20to%20Look.pdf](http://ftp.weat.org/Presentations/05-Sherman_Maley-Knowing%20Where%20and%20How%20to%20Look.pdf) (Accessed on 14 August, 2018).

Manzur, T., Ehsan, K.M., Sultana, S.L. and Mahmud, S. (2016). Measurement of Surface Damage through Boundary Detection: An Approach to Assess Durability of Cementitious Composites under Tannery Wastewater: *Adv. Mater. Sci. Eng.*, Vol. 5368635, p. 13, DOI: 10.1155/2016/5368635.

Manzur, T., Sultana, S.L., Mahmud, S. Papry, S.A., Saha, S. and Choudhury, M.R. (2018). Performance of Cement Mortars under Tannery Wastewater. *KSCE (Korean Society of Civil Engineers) Journal Civil Engineering*.

Mapei (2011), *Technical Manual on the deterioration of concrete*, pp. 9-11. Available at: [http://www.mapei.com/public/GB/linedocument/Concrete\\_deterioration\\_-GB.pdf](http://www.mapei.com/public/GB/linedocument/Concrete_deterioration_-GB.pdf) (Accessed on 14 August, 2018)

Marland, G., Boden, T.A., Griffin, R.C., Huang, S.F., Kanciruk, P. and Nelson, T.R. (1989). Estimates of CO<sub>2</sub> Emissions from Fossil Fuel Burning and Cement Manufacturing, *Based on the United Nationals Energy Statistics and the U.S. Bureau of Mines Cement Manufacturing Data. Report No. #ORNL/CDIAC-25*, Carbon Dioxide Information Analysis Centre, Oak Ridge National Laboratory, Oak Ridge, Tennessee, USA.

Mehta, P.K. (1988). Sulfate resistance of blended cements. Proceedings of the International Workshop on the use of fly ash, silica fume and other siliceous materials in concrete. *Concrete 88 Ed. W.G Ryan, Sydney, 337-351*.

Mehta, P. K. (1986). Effect of fly ash composition on sulphate resistance of cement, *ACI Materials J* 83 (6) (1986) 994–1000.

Menendez, E. (1999). Electron microscopy: A tool to study the degradation process in field concrete like sulfate attack and ettringite formation. *7<sup>th</sup> Euroseminar on Microscopy Applied to Building Materials*. Ed. Pietersen HS, Larb Ja, Jansson HHA, 171-180.

Menendez, E. (2010). Analisis del hormigon en estructuras afectados por reaccion arido-alkali, ataque por sulfatos y ciclos de hielo-deshielo (Concrete analysis in structures affected by alkali-silica reaction, sulphate attack and freezing-thawing cycles) Ed, *IECA*, Madrid.



Menendez, E., Matschei, T. and Glasser, F.P. (2012). pp. 67-68, Part 1, Chapter 2, *Performance of cement based materials in aggressive aqueous environments*, STAR 211-PAE, Springer.

Mohr, A. (1925). Uber die Einwirkung von Ammoniumsalzlosungen auf Beton. *Der Bauingenieur* 6(8):284-293 (in German).

Naik, T.R., Singh, S.S. and Ramme, B.W. (2001). Time of setting influenced by inclusion of fly ash and chemical admixtures, in *The 7th International Conference on Fly Ash, Silica Fume, Slag and Natural Pozzolans in Concrete (CANMET/ACI): Proceedings*, vol. 1. Ed. by V.M. Malhotra. July 22–27, 2001, Madras, India, 393–413.

Nirmalkumar, K. and Sivakumar, V. (2008), A study on the durability impact of concrete by using recycled waste water, *Journal Of industrial pollution control* 24 (1)(2008) pp 1-8.

Odler, T. (1984). A discussion of the paper “Mechanism of sulfate attack on Portland cement and concrete-another look” by P.K. Mehta. *Cement and Concrete Research* 14: 147-148.

Parker, C. D. (1945a) The Corrosion of Concrete .1. The Isolation of a Species of Bacterium Associated with the Corrosion of Concrete Exposed to Atmospheres Containing Hydrogen Sulphide. *Australian Journal of Experimental Biology and Medical Science*, 23(2), 81-90.

Parker C. D. (1945b). The Corrosion of Concrete 2. The Function of Thiobacillus-Concretivorus (Nov-Spec) in the Corrosion of Concrete Exposed to Atmospheres

Containing Hydrogen Sulphide. *Australian Journal of Experimental Biology and Medical Science*, 23(2), 91-98.

Poulsen, E. and Mejlbro, L. (2006). Diffusion of Chloride in Concrete- *Theory and Application*, Taylor and Francis, London.

Perlot, C., Verdier, J. and Carcasses, M. (2006). Influence of cement type on transport properties and chemical degradation: Application to nuclear waste storage. *Materials and Structures* 39 (5): 511-523.

Perlot, C., Bourbon, X., Carcasses, M. and Ballivy, G. (2007). The adaptation of an experimental protocol to the durability of cement engineered barriers for nuclear waste storage. *Magazine of Concrete Research* 59 (5): 311-322.

Peterson, O. (1984). Chemical attack of strong chloride solutions on concrete. Does experience confirm that different chloride salts may influence concrete in different ways? (*Report TVBM*; Vol. 3020). Division of Building Materials, LTH, Lund University.

Prusinski, J.J, Carrasquillo, R.L. (1995). Using medium to-high volume fly ash blended cements to improve the sulfate resistance of high-lime fly ash concrete. *Proceedings of the Fifth International Conference on Natural Pozzolans in Concrete*, Milwaukee, ACI SP-153: 43-65.

QCL Group Technical Note, (1999). *Sulphate Attack and Chloride Ion Penetration: Their Role in Concrete Durability*.page-2.

Ramasami, T., Rajamani, S. and Raghavarao, J. (1994). Pollution control in leather industry: Emerging technological options, *International symposium on surface and colloidal science and its relevance to soil pollution*, madras.

Raupach. M. and Schiessl, P. (1997). Monitoring system for the penetration of chlorides, Carbonation and the corrosion risk for the reinforcement: *Construction of Building Materials*, II (4) (1997), pp. 207–214.

Sagris, T. and Abbott, J. (2015). *An analysis of industrial water use in Bangladesh with a focus on the leather and textile industries*, Washington DC, USA.

Saha, S., and Papry, S.A. (2016). Assessment of Cement Mortar Degradation when Exposed to Tannery Wastewater, *B.Sc Thesis*, Department of Civil Engineering, Bangladesh University of Engineering and Technology, Dhaka, Bangladesh.

Saeed, A. and Shah, A. (2007). Effects of granulated blast furnace slag on the alkali aggregates reactions of various types of concrete. *32nd Conference on Our World in Concrete & Structures*. August 28–29, Singapore.

Samad, S. and Shah, A. (2017). Role of binary cement including Supplementary Cementitious Material (SCM), in production of environmentally sustainable concrete. Review Article, *International Journal of Sustainable Built Environment* 6, 663–674.

Samad, S., Shah, A. and Limbachiya, M.C. (2017). Strength development characteristics of concrete produced with blended cement using ground granulated blast furnace slag (GGBS) under various curing conditions. Vol. 42, No. 7, July 2017, pp. 1203–1213, *Indian Academy of Sciences*, DOI 10.1007/s12046-017-0667-z.

SCA. (2003). Compressive and flexural strength: slag cement in concrete: Slag Cement Association No 14. Available at: [www.slagcement.org](http://www.slagcement.org) (Accessed on September 20, 2009).

Scherer, G. (1999). Crystallization in pores. *Cement and Concrete Research* 29 (8): 1347-1358.

Schecher, W., and McAvoy, D. (2001). *MINEQL+: A Chemical Equilibrium Modeling System (Version 4.5)*.

Schneider, U and Chen, S.W (2005). Deterioration of high-performance concrete subjected to attack by the combination of ammonium nitrate solution and flexure stress, *Cement and Concrete Research* 35 (9): 1705-1713.

Shehata, M.H., Thomas, M.D.A. and Bleszynski, R.F. (1999). The effect of fly ash composition on the chemistry of pore solution, *Cem Concr Res* 29, 1915- 1920.

Shehata, M. H. and Thomas, M. D. A. (2000). The effect of fly ash composition on the expansion of concrete due to alkali-silica reaction. *Cement and Concrete Research*, ISSN: 0008-8846, Vol: 30, Issue: 7, Page: 1063-1072.

Snelson, D. Wild, S. and Farrel, M. O. (2011). Setting times of portland cement – metakaolin-fly ash blends. *Taylor & Francis*, 17 (2011), pp. 55-62.

Soroushian, P. and Alhozimy. A. (1992). Correlation between fly ash effects on permeability and sulfate resistance of concrete. *9<sup>th</sup> International Congress Chemistry of Cement*, New Delhi, V:196-202.

Soutsos, M.N., Millard, S.G., Bungey, J.H., Jones, N., Tickell, R.G. and Gradwell, J. (2004). Using recycled demolition waste in concrete building blocks. *Proceedings – Institution of Civil Engineers Engineering Sustainability* 157 (3), 139–148.

Srrolczyk, Heinz. G. (1968), "Chemical Reactions of Strong Chloride-Solutions with Concrete." *Proceedings of The Fifth International on the Chemistry of Cement*, Tokyo, *Supplementary Paper* 111-31, 274-280.

Stark, J. and Bollmann, K. (1999). Delayed ettringite formation in concrete. *Proceedings of Nordic Concrete Research Meetings Island*. Bauhaus- University, Weimar, Germany, 4–28.

Statista, The Statistic Portal (2018). World and U.S. Cement Production 2010-2017. Available at <https://www.statista.com/statistics/219343/cement-production-worldwide/> (Accessed on 15 April, 2018).

Stephens, J.B and Carrasquillo, R. L. (2000). Evaluating performance-based test and specifications for sulfate resistance in concrete. *Texas Dept of Transportation Report* No 0-1706-3.

Struble, L. and Godfrey, J. (2004). How sustainable is concrete. In: *Proceedings of the International Workshop on Sustainable Development and Concrete Technology* Beijing, China, May 20–21, 2004. Centre for Transportation Research and Education, Iowa State University Ames, Iowa, USA, pp. 201–211.

Swam, R. N. (1999). Role of slag in the development of durable and sustainable high strength concretes. *Proceedings of International Symposium on concrete technology for sustainable development in the 21st Century*. Hyderabad, pp. 186–121.

The Concrete Centre, (2010). Concrete Industry Sustainability Performance Report, Surrey, UK. [online], Available at <http://www.sustainableconcrete.org.uk/> (Accessed on 15 Feb, 2011).

Thomas, M.D.A. (1996). Review of the effect of fly ash and slag on alkali-aggregate reaction in concrete, Building Research Establishment Report, BR314, *Construction Research Communications*, Watford, UK, pp, 117.

Thomas, M.D.A. (1996). Field studies of fly ash concrete structures containing reactive aggregates, *Mag Concr Res*, 48 (177) 265-279.

Thomas, M.D.A. (1998). The role of calcium on alkali-silica reaction, Materials Science of Concrete, *The Sidney Diamond Symposium*, American Ceramics Society, Westerville, OH, 325- 335.

Thomas, M.D.A. and Innis, F.A. (1998). Effect of slag on expansion due to alkali-aggregate reaction in concrete, *ACI Mater J*, 95 (6), 716-724.

Thomas, M.D.A. and Matthews, J.D. (1996). Chloride penetration and reinforcement corrosion in marine-exposed fly ash concretes, *Proceedings 3d CANMET/ACI International Conference on Concrete in a Marine Environment*, V.M. Malhotra (Ed.), ACI SP-163, American Concrete Institute, Detroit, pp. 317–338.

Thomas, M.D.A., Shehata, M.H. and Shashiprakash, S.G. (1999). The use of fly ash in concrete: classification by composition, *Cement, Concrete, and Aggregates*, 21 (2).

Tikalsky, P.J. and Carrasquillo, R.L. (1992). Influence of fly ash on the sulfate resistance of concrete, *ACI Materials J*. 89 (1) 69–75.

Tunay, O., Kabdasli, I., Orhon, D. and Ates, E. (1995). Characterization and pollution profile of leather tanning industry in Turkey. *Water Sci Technol*; 32:1–9.

Ueli, M.A., Elsener, B., Larsen, C.K. and Vennesland, O. (2011). Chloride induced reinforcement corrosion – electrochemical monitoring of initiation stage and chloride threshold values, *Corros Sci*, 53 (2011), pp. 1451–1464.

United Kingdom Quality Ash Association (2010). Embodied CO<sub>2</sub> of UK cement, additions and cementitious material. Technical data sheet 8.3, MPA; UK Quality Ash Association. Available at <http://www.ukqaa.org.uk> (Accessed on October 4, 2012).

Ukraincik, V., Bjegovic, D. and Djurekovic, A. (1978). Concrete corrosion in a nitrogen fertilizer plant. In: *Proceedings of the First International Conference on the Durability of Building Materials and Components*, Ottawa, Canada, 397-409.

U.S. EPA. (1986). *Guidelines for the health risk assessment of chemical mixtures* (PDF) EPA/630/R-98/002.

Von Fay, K.F. and Pierce, J.S. (1989). Sulfate resistance of concretes with various fly ashes, *ASTM Standardization News*, 32–37.

Wanga, K., Nelsena, D. E. and Nixon, W.A. (2006). Damaging effects of deicing chemicals on concrete materials, *Cement and Concrete Composites* Vol. 28(2), pp 173-188. doi:10.1016/j.cemconcomp.2005.07.006.

Worrell, E., Price, L., Martin, N., Hendriks, C. and Meida, L. O. (2001). Carbon dioxide emissions from the global cement industry, *Annu. Rev. Energy Environ.*, 26, 303–329.

X-Ray Fluorescence (XRF) (2017). Available at: <https://www.xos.com/XRF> (Accessed on June 27, 2018).

Yazici, H. (2007). The effect of curing conditions on compressive strength of ultra high strength concrete with high volume mineral admixtures. *Build. Environ.*, 42 (2007), pp. 2083-2089.

Yazici, H., Yigiter, H., Karabulut, A.S. and Baradan, B. (2008). Utilization of fly ash and ground granulated blast furnace slag as an alternative silica source in reactive powder concrete, *Fuel*, 87 (2008), pp. 2401-2407.

Yongsiri, C., Vollertsen, J., Rasmussen, M. and Hvitved-Jacobsen, T. (2004a). Air-Water Transfer of Hydrogen Sulfide: An Approach for Application in Sewer Networks. *Water Environment Research*, 76(81), 81 – 88.

Yongsiri, C., Vollertsen, J. and T. Hvitved-Jacobsen (2004b). Effect of Temperature on Air-Water Transfer of Hydrogen sulfide. *Journal of Environmental Engineering*, 130(1), 104 – 109.